Investigations on an Iron Transport Pathway

Paul Bilton

PhD Thesis

The University of Edinburgh

2007

Acknowledgements

First of all, I would like to thank Prof Peter J Sadler and Dr Dominic J Campopiano for giving me the opportunity to do a PhD in this very interesting research field. Their support and stream of ideas kept me focused and continually motivated.

I would like to thank Dr Dave Clarke, Mr Robert Smith and Dr Jim Creanor for help with mass spectrometry and peptide mass fingerprinting; Dr Martin Wear for guidance on surface plasmon resonance; and Dr Lorna Eades for help with ICP-OES. I would also like to thank Dr Helen Palmer for allowing me to purify *N. gonorrhoeae* genomic DNA at the Scottish National Gonorrhoeae Research Laboratory. I also have to thank members of the two groups – PJS group and Lab 229 – that I was very much a part of: with special mention to Dr Ross Stevenson, Dr Anna Peacock and Mrs Beverley Yard. All of their suggestions about various aspects of my work were invaluable and their friendships made it a pleasure to go to work each day. Neil Diamond and Bon Scott also provided much needed inspiration throughout my PhD!

At Imperial College, London, I am especially indebted to Dr Simon Newstead, whose invaluable advice and guidance was fundamental to the success of much of the work presented here. Similarly, I wish to thank Prof So Iwata for his collaboration and for allowing me to visit and use his facilities at Imperial College. I also thank Dr Ian Harvey at the Daresbury SRS for performing EXAFS.

I would like to thank the EPSRC for funding.

Last, but by no means least, I would like to thank my family and my wife, Claire, for her continued support and love, and for providing me with my beautiful daughter, Poppy, whom made writing-up this thesis such a joy.

Abstract

The emergence of multi-resistant strains of bacteria is a critical health problem worldwide. Antimicrobial-resistant infections are essentially untreatable and have begun to occur as epidemics around the globe. The need for new targets for chemotherapeutic agents, and the development of new chemotherapeutic agents themselves, is now a greater need than ever. In this study, an iron-uptake ATP-binding cassette (ABC) transporter, FbpABC, from the Gram-negative human pathogen *Neisseria gonorrhoeae* has been investigated. The periplasmic binding protein, FbpA, has been mutated to facilitate investigation of complex formation with the two other components of the transporter, FbpB and FbpC.

FbpBC was PCR-amplified from *N. gonorrhoeae* genomic DNA, co-expressed in *E. coli* cells, and its purification optimised. FbpA residues R48 and V272 have been mutated to allow covalent modification with a linker molecule to allow attachment to a sensor surface and used as bait to detect the purified FbpBC complex, using surface plasmon resonance. This is the first report of the purification of FbpB, and the first demonstration of FbpABC association *in vitro*. A radioactive iron-uptake assay revealed that *E. coli* cells expressing the *N. gonorrhoeae FbpABC* operon take-up more iron than control cells.

The *FbpC* gene was cloned using recombinant DNA technology and over-expressed in *E. coli* to perform biochemical characterisation of the enzyme. The expression and purification of selenomethionine-labelled FbpC allowed determination of the X-ray crystal structure of FbpC at Imperial College, London. Crystals of FbpC diffracted to a resolution of 2.7 Å, and the structure was solved

with ATP and calcium bound in the active site, at the interface between two FbpC monomers. The structure also revealed a novel C-terminal fold for a nucleotide binding domain from an ABC transporter.

Metal-free *apo*-FbpA was reloaded with ruthenium(III) and osmium(III) salts and characterised by various techniques. Chromatography and ICP-OES analysis of Ru- and Os-FbpA showed that there were two main species formed with each metal. Both species have four metal atoms bound and differ in that one species may be capped by a single phosphate anion, and the other by two phosphate anions. EXAFS was also performed on the ruthenium bound species.

Abbreviations

Aa	Amino acid(s)
ABC transporter	ATP binding cassette transporter
ADP	Adenosine 5'-diphosphate
ATP	Adenosine 5'-triphosphate
ATPase	ATP hydrolysing enzyme
BCA	Bicinchoninic acid
Bp	Base pair(s)
CM	Cytoplasmic membrane
CTAB	Cetyl trimethylammonium bromide
CV	Column volumes
DDM	n-dodecyl-β-D-maltopyranoside
DDT	Dithiothreitol
DNTP(s)	Deoxy nucleotide triphosphate(s)
EDTA	Ethylenediaminetetracetic acid
ESI-MS	Electrospray ionization mass spectrometry
FbpA	Ferric-ion binding protein A
FbpB	Ferric-ion binding protein B
FbpC	Ferric-ion binding protein C
FT-ICR	Fourier transform ion cyclotron resonance

Fur	Ferric uptake regulator
g	Gravity (centrifugal force)
HEPES	N-(2-Hydroxyethyl)piperazine-N′-(2-ethanesulfonic acid)
IAF	5-iodoacetamidofluoroscein
IPTG	Isopropyl-1-thio-β-D-galactopyranoside
kbp	Kilo base pairs
keV	Kilo electron volts
kDa	Kilo daltons
LB	Luria Bertani
LC-MS	Liquid chromatography mass spectrometry
M-PEO_2-B	Maleimide-polyethyleneoxide$_2$-biotin
MALDI	Matrix-associated laser desorption ionization
MDG	M9 salts/aspartic acid/glucose media
NBD	Nucleotide binding domain
OM	Outer membrane
ORF	Open reading frame
PAGE	Polyacrylamide gel electrophoresis
PBP	Periplasmic binding protein
PBS	Phosphate buffered saline
PCR	Polymerase chain reaction

P_i	Inorganic phosphate
Rpm	Revolutions per minute
RT-PCR	Reverse transcriptase PCR
SeMet	Selenomethionine
SDS	Sodium dodecylsulfate
SPR	Surface plasmon resonance
TB	Terrific broth
TbpA	Transferrin binding protein A
TbpB	Transferrin binding protein B
TCEP	Tris carboxyethylphosphine
Tf	Transferrin
TMD	Transmembrane domian
ToF	Time of flight
Tris	Tris [hydroxymethyl] aminomethane
UV-Vis	Ultraviolet-visible spectroscopy

Table of Contents

List of Figures

Chapter 1: Metals in Medicine

Chapter 2: ATP Binding Cassette (ABC) Transporters

Chapter 3: Materials and Methods

Chapter 4: Results and Discussion: FbpA

Chapter 5: Results and Discussion: FbpABC.

List of Tables

Chapter 1: Metals in Medicine

Chapter 2: ATP Binding Cassette (ABC) Transporters

Chapter 3: Materials and Methods

Chapter 4: Results and Discussion: FbpA

Chapter 5: Results and Discussion: FbpABC.

Chapter 1: Metals in Biology

1.1 Metals in Biological Systems

It is currently estimated that over 50% of all proteins will turn out to be metalloproteins dependent on the metal for structure and/or function (1). Molecules containing metal ions are involved in many different functions in biological systems. They are involved in electron transfer, metal storage, oxygen binding, enzymatic catalysis, structural stability and can be involved in signal transduction (2).

Metal ions have been used in various drugs for the treatment of many diseases. Platinum anticancer, bismuth antiulcer, and gold antiarthritic drugs are just some of the metal-ion-containing drugs that have been developed. The study of metal ions and their chemistry in life has thus become a major area in bioinorganic research (3).

Iron is an essential element, as it serves as a co-factor in fundamental metabolic processes, such as nucleotide biosynthesis and energy production. Iron is a key player in the electron transport pathway that is essential for respiration in both eukaryotes and prokaryotes, and as such is an essential requirement for Gram-negative pathogens that infect mammals. Indeed, the acquisition of iron is possibly the major determinant as to whether a microorganism can maintain itself within a host. The process of iron acquisition is recognised as a key step in the development of any pathogen within a host, as without iron the host defence mechanisms would effectively eliminate infection or the pathogen would simply die of nutrient starvation (4).

However, in mammals, iron is not freely available and is kept tightly associated with proteins such as haemoglobin, the iron storage protein ferritin (up to

4 500 Fe^{3+} ions per ferritin molecule), and the metal transport protein family of transferrins. Gram-negative bacteria have evolved several mechanisms to thrive in this iron-depleted environment. Such is the importance of iron acquisition for a pathogen, that it is a key target for the development of new chemotherapeutic agents (4). It follows that the study and understanding of the mechanisms that bacteria utilise to acquire iron are crucially important for the development of such novel agents.

1.2 Mechanisms of Iron Uptake in Gram-negative Bacteria

1.2.1 Availability of Iron

Iron is usually found in the environment as insoluble ferric oxo-hydroxide (rust) and the solubility of iron at physiological pH is very low (10^{-18} M). In the body, free iron is efficiently scavenged by various proteins in the blood stream and tissues (5). It thus follows that pathogens are limited in their capacity to multiply *in vivo* because of the "iron sequestering" defence mechanism of the infected host. Pathogenic bacteria multiply in a host, which implies that they have developed ways of overcoming these defence mechanisms (4). These mechanisms and the proteins involved are summarised in **Table 1.1**.

Table 1.1. Mechanism of iron uptake by some species of Gram-negative bacteria. Although the *Neisseria* spp do not secrete siderophores, they do express outer membrane siderophore receptors that permit uptake of exogenous siderophores from the environment (6).

Iron source	Bacteria	Protein	Function
Transferrin Lactoferrin	*Haemophilus influenzae*	LbpAB	Lf outer membrane receptor
		TbpAB	Tf outer membrane receptor
		HitABC	Fe^{3+} ABC transport system
	Neisseria spp.	LbpAB	Lf outer membrane receptor
		TbpAB	Tf outer membrane receptor
		FbpABC	Fe^{3+} ABC transport system
Lactoferrin	*Yersinia enterocolitica*	Yfu	Fe^{3+} ABC transport system
	Actinobacillus pleuropneumoniae	Afu	Fe^{3+} ABC transport system
	Helicobacter pylori		ABC transport system
Haem Haemoglobin Haemopexin	*Escherichia coli O157*	ChuA	haem outer membrane receptor
	Neisseria spp.	HmbR	haem/Hb outer membrane receptor
		HpuAB	haem/Hb outer membrane receptor
	Serratia marcescens	SfuABC	Fe^{3+} ABC transport system
	Shigella dysenteriae	ShuA	haem outer membrane receptor
	Vibrio cholerae		
	Yersinia enterocolitica	HemPRSTUV	
	Yersinia pestis	YbtP,Q	haem/Hb outer membrane receptor
	Neisseria gonorrhoeae	HpuAB	haem/Hb outer membrane receptor
	Neisseria meningitidis	HmbR	haem/Hb outer membrane receptor
	Pseudomonas aeruginosa	PhuR	haem ABC transport system
		PhuSTUVW	haem receptor, hemophore, ABC transporter for HasA export
		HasRADEF	
	Haemophilus influenzae		
Siderophores	*Azotobacter vinelandii* *Bacillus subtilis*	FhuBCDG	ferrichrome transport
	Bordetella pertussis	BfeA	ferrienterobactin outer membrane receptor
		BfrABC	siderophore outer membrane receptor
	Camphyobacter coli	FauA	alcaligin outer membrane receptor
		CeuBCDE	ABC ferrienterobactin transport
	Erwinia chrysanthemi	Fct	chrysobactin outer membrane receptor
		CbrABCD	achromobactin ABC transporter
	Escherichia coli	FecABCDE	ferric citrate transport
		FepABCDG	ferrienterobactin transport
		FhuABCDE	ferrichrome , rhodoturulate and coprogen transport
		Cir	dihydroxybenzylserine outer membrane receptor
		Fiu	dihydroxybenzylserine outer membrane receptor
	Morgenella morganii	IutA	aerobactin outer membrane receptor
		RumAB	rhizoferrin transport

(Continued over the page)

Table 1.1 (continued).

Iron source	Bacteria	Protein	Function
Siderophores (continued)	*Neisseria* *Pseudomonas aeruginosa*	FrpB	siderophore outer membrane receptor
		FptA	ferric pyochelin outer membrane receptor
		FpvA	ferric pyoverdine outer membrane receptor
		FiuA	ferrioxamine outer membrane receptor
		PfeA (E?), PirA	ferric enterobactin outer membrane receptor
		PiuA,PfuA,UfrA	unknown outer membrane receptor
	Pseudomonas putida	PupAB	Pseuobactin
	Rhizobia	FhuA	siderophore uptake
	Vibrio		vibriobactin outer membrane receptor
	Vibrio cholerae	ViuA	ferric anguibactin transport
	Vibrio anguillarium	FatDCBA	
	Yersinia enterocolotica	FyuA	yersiniabactin outer membrane receptor
		FoxA	ferrioxamine B outer membrane receptor
		FcuA	ferrichrome outer membrane receptor
Reduced iron	*Escherichia coli*	FeoAB	Fe^{2+} transport
	Pseudomonas aeruginosa	FeoAB	Fe^{2+} transport
	Streptococcus spp.		

Uptake of iron in Gram-negative bacteria is globally regulated by the Fur (ferric uptake regulator) protein, which responds to cellular levels of iron (7,8). The Fur protein represses genes that transcribe proteins involved in high affinity iron transport under iron-replete conditions, and also controls genes required for virulence (9). The model of Fur function speculates that the binding of ferrous (Fe^{2+}) iron, causes Fur to bind to its specific DNA sequence target within the promotor of the regulated gene with high affinity to repress transcription. During iron starvation, iron dissociates from Fur, causing the protein to lose its affinity for DNA, triggering derepression of gene transcription. Strong evidence for this direct iron-Fur association has recently been published and several crystal structures have also been

reported (10,11). All the proteins described in the following sections that are involved with the high affinity transport of iron are regulated by the Fur system.

1.2.2 Siderophore-Mediated Iron Acquisition

Siderophores are defined as low molecular mass compounds (<1000 Da) that are produced by many, but not all, microorganisms (4). They are excreted into the environment in response to iron starvation and have a very high specificity and affinity towards Fe^{3+} ions. Siderophores can remove iron from molecules such as ferritin, transferrin and lactoferrin, and can also solubilise the metal from insoluble ferric salts, including ferric oxo-hydroxide. Over 500 different siderophores have been identified that are produced by bacteria, yeast and fungi (4,5). Examples of siderophores from Gram-negative and Gram-positive bacteria are shown in **Figure 1.1**.

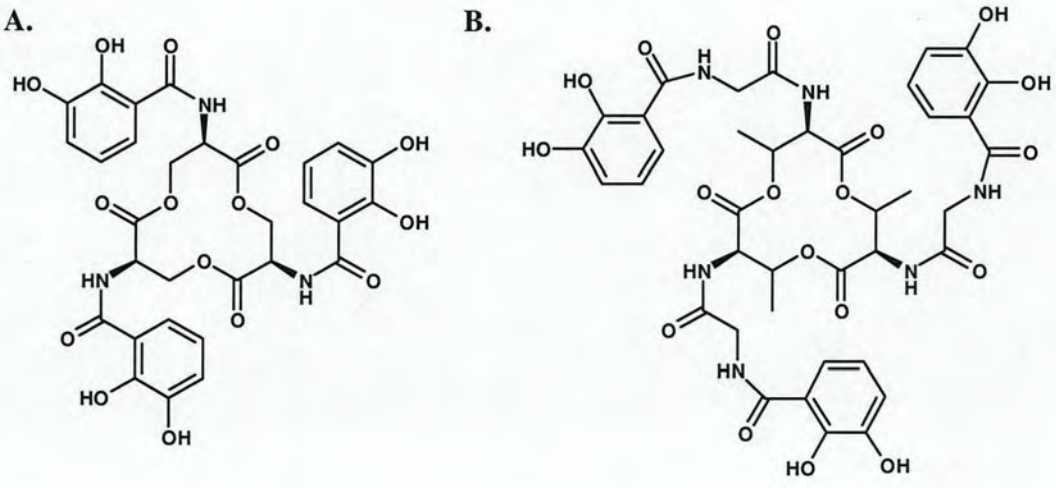

Figure 1.1. Structures of two bacterial siderophores. **A**, Enterobactin from the Gram-negative bacterium *Salmonella typhimurium*. **B**, Corynebactin from the Gram-positive bacteria *Corynebacterium glutanicum* and *Bacillus subtilis*. Note that both siderophores, although from very different species of bacteria, contain a central trilactone ring and three catecholate binding moieties (12).

After acquiring iron, the ferri-siderophore complex is internalised via specific receptor proteins in the outer membrane (OM) in a process that is driven by the cytoplasmic membrane (CM) potential (proton motive force) and mediated by the energy transducing TonB-ExbB-ExbD system (13). The ferri-siderophore is shuttled across the periplasmic space from the OM receptors by periplasmic binding proteins to the CM and is then presented to an ATP-binding cassette (ABC) transporter that, in turn, delivers the ferri-siderophore to the cytoplasm at the expense of ATP. Here the complexes are thought to dissociate via reduction of Fe^{3+} to Fe^{2+} and the siderophore is recycled (5).

1.2.2.1 Siderophore Receptors

All known OM siderophore receptors are structurally related. They have a monomeric β-barrel domain consisting of a 22-β-antiparallel stranded transmembrane tube (which forms the pore), a globular 'plug' or 'cork' domain of about 160 residues residing in the periplasmic end of the pore and an NH_2-terminal extension. Part of the 'plug' domain protrudes to the exterior and contributes part of the ligand-binding site, with other important residues being located in loops or in the barrel walls (13,14).

Crystal structures have been determined for the siderophore receptors FepA (ferric enterobactin receptor), FecA (ferric citrate receptor) and FhuA (ferrichrome receptor) (14-16). The structures of these receptors are presented in **Figure 1.2**.

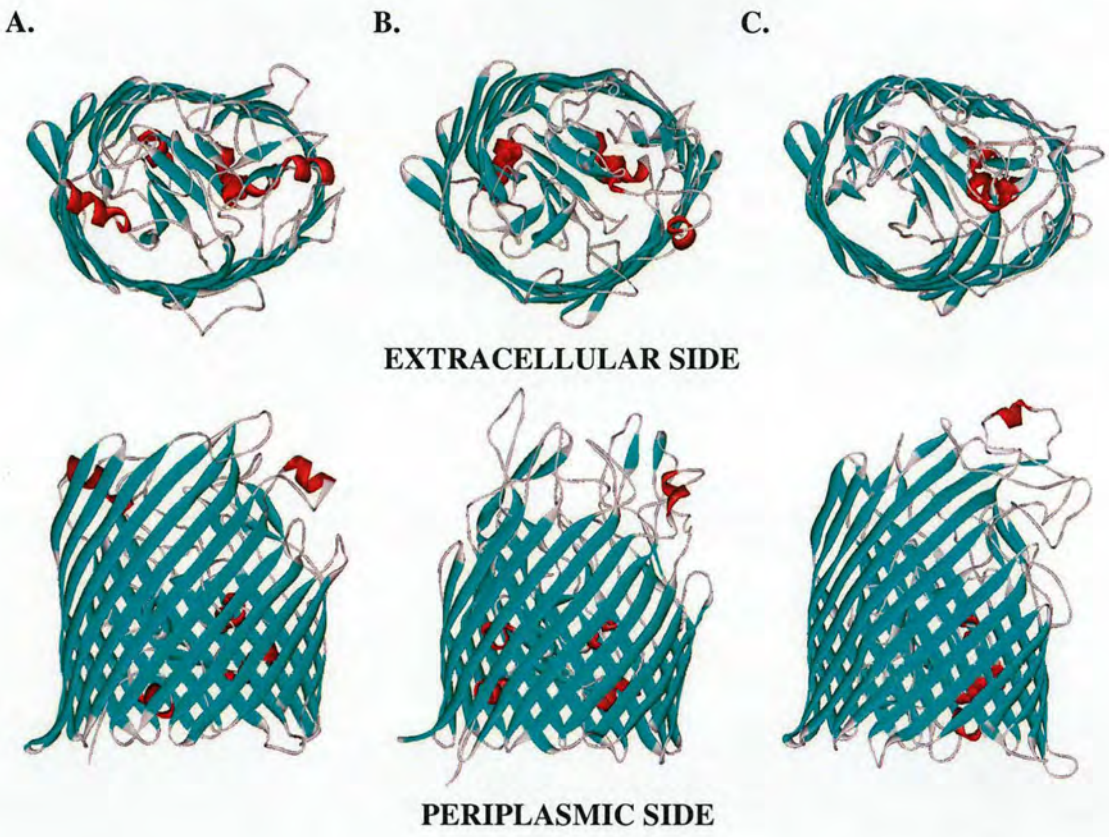

Figure 1.2. Crystal structures of the siderophore receptors: A, FecA (PMD: 1KMP); B, FepA (PMD: 1FEP) and; C, FhuA (PMD: 1BY5). All three receptors share the characteristic β barrel fold containing a central cork domain that facilitates ligand transfer (14-16). The top panel shows the receptor from the extracellular side and the bottom panel shows a side-on projection.

1.2.2.2 TonB-ExbB-ExbD Complex

TonB-ExbB-ExbD is a protein complex situated in the CM (17,18). TonB (239 amino acid residues) is periplasmic and anchored to the CM by its hydrophobic N-terminal domain, whereas ExbB and ExbD are integral CM proteins. Cross-linking studies have suggested that, *in vivo*, the ratio of TonB:ExbB:ExbD subunits in the complex is 1:7:2 (5). The intermediate domain of TonB contains Pro-Glu and Pro-Lys repeats, and the C-terminal domain is composed of a β-sheet and two α-

helices (19). To date, the only structural information known about TonB is for the small C-terminal domain, and recently the structure of TonB complexed to FhuA (an outer membrane siderophore receptor) was solved and revealed a 1:1 stoichiometry (20-22). This structure highlighted that the C-terminal domain of TonB makes extensive contacts with the N-terminal domain 'TonB box' region of FhuA, as well as other regions of the cork domain of the protein. This report suggested that these contacts with the cork domain of FhuA may mediate conformational disruption of the internal cork, allowing passage of the siderophore into the periplasm (21).

TonB forms a complex in the inner membrane with ExbB and ExbD, two membrane proteins that potentially act as proton translocators. ExbB is homologous to the protein MotA, and ExbD has a similar topology as MotB, both of which are proposed to exploit the proton gradient to drive the bacterial flagellum. ExbB has been proposed to modulate the conformation of TonB, as well as mediate its recycling, but what these structural changes might be remains unknown. Cross-linking studies have suggested the regions through which TonB might interact with its partners in the inner membrane: contact with ExbB is mediated by the signal anchor, whereas the residues responsible for the interaction with ExbD are unknown (23).

Although the binding of the ferri-siderophore to the OM receptor is energy independent, transport through the receptor pore requires energy. This energy is derived from the electrochemical charge gradient of the CM and is delivered by the energy transducing TonB complex. This process requires the TonB complex to be in

direct contact with the OM receptors. A transport mechanism has been postulated as described below (14).

Stage 1: the siderophore is adsorbed from the medium with low affinity via hydrophobic residues residing in the upper part of the external pocket of the unliganded receptor.

Stage 2: the siderophore is transferred to its high-affinity binding site comprising residues on the plug domain and on the walls of the barrel domain. The interactions with the latter residues cause the plug domain to move downward leading to the unwinding and repositioning of the switch helix and the 'TonB box'.

Stage 3: multiple extracellular loops of the receptor change their relative conformation and position which closes the external pocket of the barrel disrupting the low-affinity binding site and shielding the high-affinity binding site from the solvent.

Stage 4: conformational changes of the plug and barrel domain are required for transport through the receptor pore. These changes are mediated by physical interactions between TonB and the 'TonB box'. Formation of a complex with TonB results in the transfer of energy to the receptor, which in turn promotes ligand transport.

Recent research proposes a supplemental role for TonB: the protein may also coordinate the periplasmic binding protein components of iron transport systems to directly orchestrate transport events between the OM and CM (21). As such, TonB would act as a periplasm-spanning scaffold that "oversees" the process of substrate transfer between members of an iron transfer system (21).

1.2.3 Iron Acquisition from Haem and Haemoproteins

Haem is the most abundant source of iron in the body and thus bacteria have developed two basic mechanisms for the removal of iron from haem (24). Some bacteria have an absolute requirement for haem or its precursor protoporphyrin IX. Extracellular pathogens liberate haem or haemoglobin with haemolysins and proteases (5).

The first, and commonest, of the two mechanisms is that Gram-negative bacteria can acquire iron directly from haem, or haem complexes, binding to specific OM receptors. The haem is transported across the OM in a TonB-ExbB-ExbD dependent fashion. Not surprisingly, these TonB-dependent OM receptors are related to those involved in siderophore uptake. Periplasmic binding proteins then chaperone the haem complex to the CM where it is transported into the cytoplasm. Once inside the cytoplasm, the haem can either be incorporated directly into enzymes or the iron removed by degradation of the porphyrin ring (25).

The other mechanism for acquiring iron from haem is via proteins collectively called haemophores (25). These are secreted soluble extracellular proteins that acquire iron from haem containing host proteins such as haemopexin (a scavenging protein that has the strongest affinity for haem of any known protein) and haemoglobin. Gram-negative bacteria produce HasA (Haem-acquiring system) and HxuA (Haem-haemopexin binding protein), which, like siderophores, mediate the delivery of haem to specific OM receptors (26). Again, these OM receptors (HasR) transport the haem-haemophore complex into the periplasm via a TonB-ExbB-ExbD-dependent system (4). Shuttling across the periplasmic space does not appear to

require any periplasmic binding protein but transport across the CM could involve an ABC permease (5).

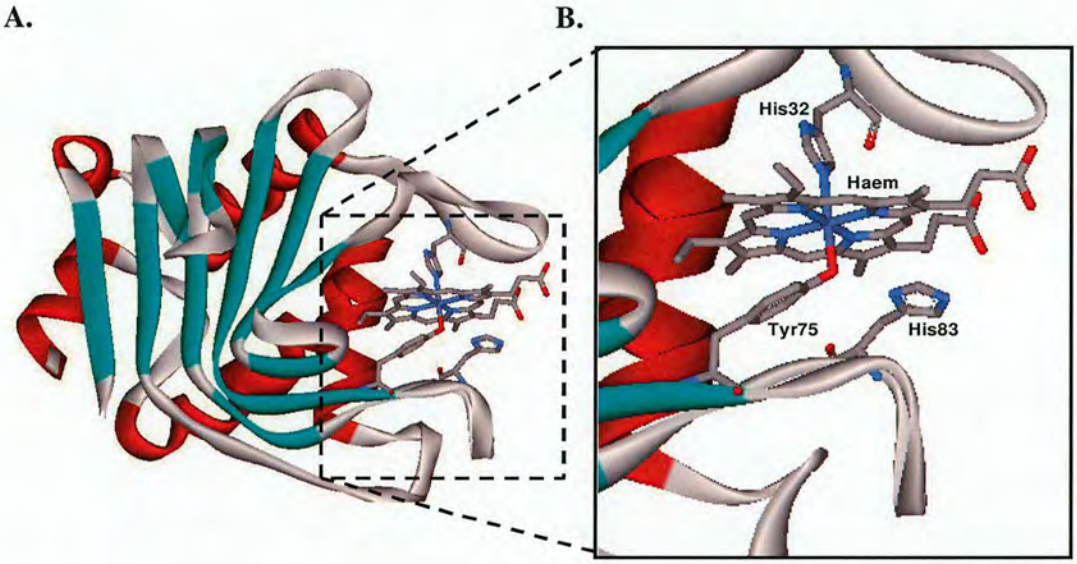

Figure 1.3. Structure of HasA (PDB: 1DK0) haem binding protein. A, complete structure of HasA; B, detail of Has A binding site showing residues involved in haem binding. His83 is presumed to be involved in haem capture and release (26).

1.2.4 Iron Acquisition from Transferrin

1.2.4.1 Transferrin

Transferrins are a superfamily of iron binding proteins that can be divided into three major classes: serum transferrins, lactoferrins and ovotransferrins (formerly called conalbumin) (27). These proteins are known to be at least as ancient as the insect phylogenic family (28). All transferrins are ~80 kDa monomeric glycoproteins that bind two ferric ions (and two CO_3^{2-} as synergistic anions) per molecule with high affinity and share significant sequence homology. Serum transferrins (serotransferrins) transport iron in serum and deliver iron to cells via receptor-mediated endocytosis (29). Lactoferrins (lactotransferrins) are found in extracellular

fluids and in polymorphonuclear lymphocytes. Lactotransferrins are known to have antimicrobial and antifungal properties. Ovotransferrins are found in avian egg white and are identical to serotransferrins except for their attached carbohydrates (30).

The general structure of the transferrin superfamily is two lobes (which represent the C- and N –terminal halves of the protein) with each lobe divided into two domains (**Figure 1.4**). Two high affinity Fe^{3+} binding sites are located in deep clefts between each domain. The iron-binding protein ligands are characteristically two tyrosines, a histidine and an aspartate residue. A distorted octahedral coordination is completed by a bidentate carbonate synergistic anion. The aspartate residue is not solely involved in iron binding but also forms hydrogen bonds with other residues in the polypeptide chain when iron is bound, thus stabilising the lobe in a closed conformation. When iron is absent, the lobe is in an open conformation with no such hydrogen-bonding taking place (31). Human transferrin can bind various metals under physiological conditions and more than 35 have been identified to date (32,33). This has been particularly valuable for the study of the metal-binding properties of this protein (34).

Many important human pathogens are capable of acquiring iron directly from transferrin and lactoferrin (35,36). Non-siderophore secreting pathogens such as *Neisseria gonorrhoeae*, *Neisseria meningitides*, *Haemophilus influenzae* and *Moraxella catarrhalis* have developed this mechanism for iron acquisition. To do this they have evolved an outer membrane receptor for transferrin, called the

transferrin-binding proteins, TbpA and TbpB (or LbpA and LbpB), to capture and remove iron from transferrin (36).

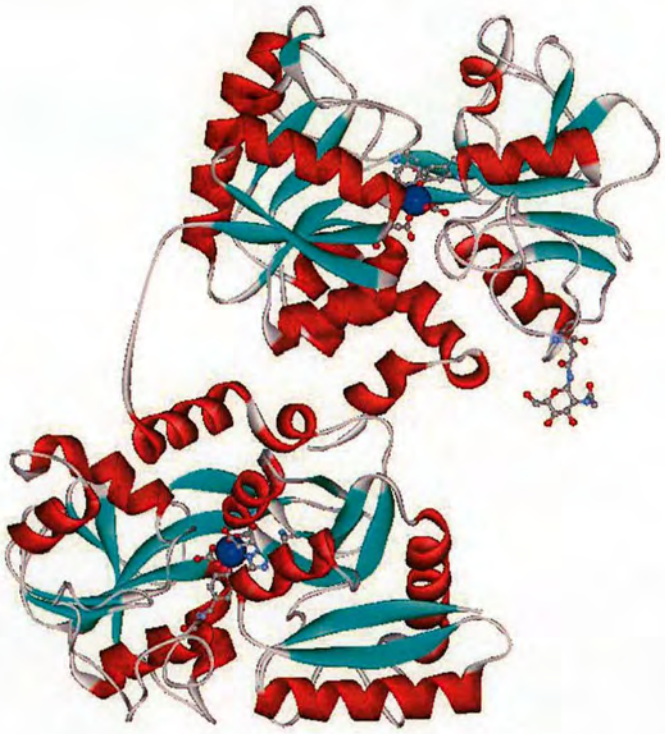

Figure 1.4. Crystal structure of the di-ferric form of porcine serum transferrin (PDB: 1H76). Residues involved in iron (blue) binding are represented in ball-and-stick, as is *N*-acetyl glucosamine (*N*AG) that is covalently linked to N497 (37).

1.2.4.2 Transferrin Binding Proteins

The OM receptor molecules that bind and extract iron from the transferrin family are the so-called transferrin (or lactoferrin) binding proteins (Tbp or Lbp). These receptor complexes consist of two components: an integral porin-like OM protein TbpA (100 kDa) and an extracellular OM anchored TbpB (65-90 kDa). TbpA is proposed to serve as a channel for the transport of iron across the OM and shows sequence similarity to FepA and FhuA: both proteins form an antiparallel β-barrel

and TbpA is proposed to have similar structure (15). Both TbpA and TbpB can independently bind their ligand, human serum transferrin (38).

Currently two isotypes of TbpB have been identified: isotype I form of the protein has a molecular mass of ~68 kDa, whereas the larger isotype II form has a molecular mass of ~80-90 kDa (39). It remains unclear what role each isoform plays *in vivo*.

The process of iron transport across the OM requires energy that is derived from the electrochemical charge gradient of the CM and is delivered by the energy transducing TonB-ExbB-ExbD complex in a similar fashion to the siderophore and haem iron acquisition mechanisms (4). A schematic of this transferrin acquisition pathway arrangement is provided in **Figure 1.5**.

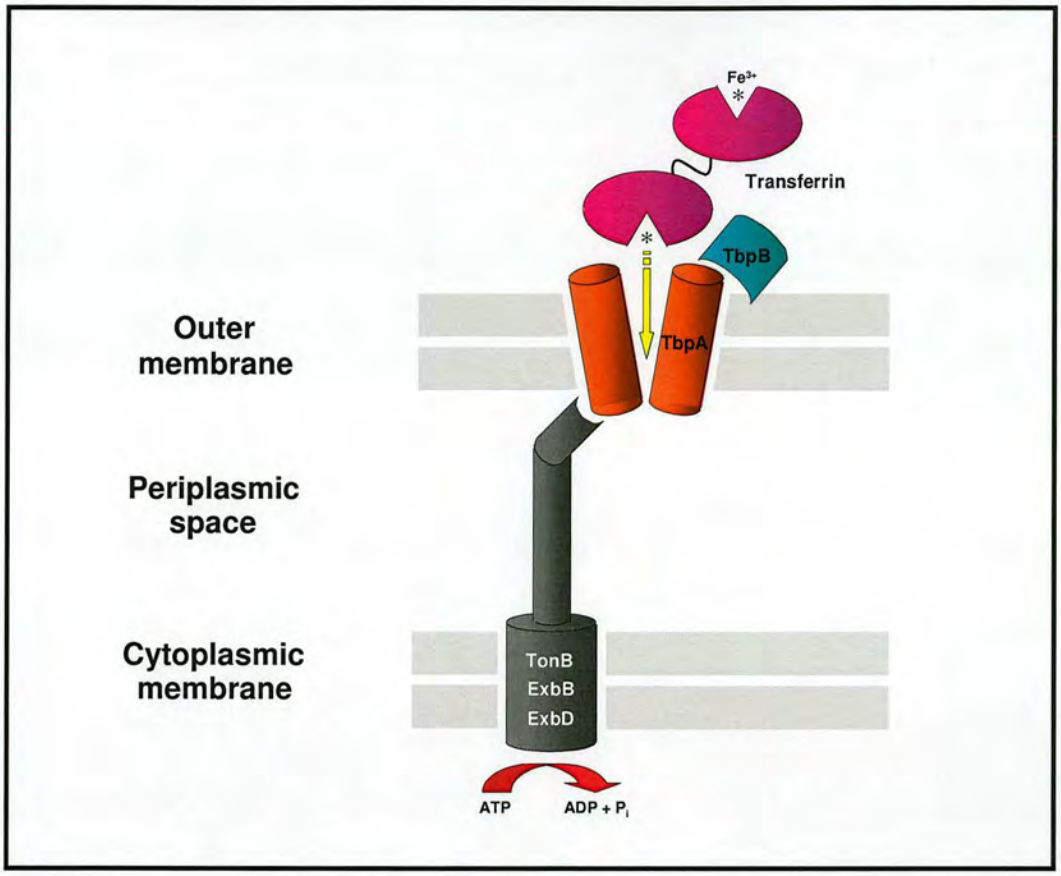

Figure 1.5. Schematic representation of mechanism of transferrin binding by transferrin binding proteins A and B. Energy for iron transport is supplied via the a TonB-ExbB-ExbD energy transducing complex. Based on (40).

1.2.5 The *Neisseriaceae*

The *Neisseria* genus consists of aerobic, non-spore-forming Gram-negative coccobacilli, which inhabit the mucous membranes of many animals (including humans) (41). These non-motile microbes require a moist environment and warm temperatures (37°C) to achieve optimum growth. *Neisseria* infections are identified by the means of the oxidase test, for which all members test strongly positive. Additionally, *Neisseria* grow well on chocolate agar containing antibiotics that inhibit growth of other Gram-negative bacteria, Gram-positive bacteria, and moulds.

The two most clinically-significant members of the genus *Neisseria* are *N. gonorrhoeae* and *N. meningitides* (41,42).

1.2.5.1 *Neisseria gonorrhoeae*

Infection by the diplococcoid bacterium *N. gonorrhoeae* is referred to as gonococcal infection (or gonorrhoea). The organism is an obligate human pathogen and does not infect other mammalian species. There are four types of *N. gonorrhoeae* (T1, T2, T3, and T4) that are classified by their fimbriae; these are extracellular proteinaceous appendages used to adhere to each other and to host cells. Without these fimbriae the bacteria are avirulent, and the four types display different levels of clinical virulence. The bacteria also produce cytotoxic substances, such as LPS endotoxin, that damage ciliated epithelial cells found in fallopian tubes and stimulate the immune system. However, to counter the host immune responses, *N. gonorrhoeae* produces an extracellular protease that cleaves a proline-threonine bond in immunoglobulin IgA (the major antibody in mucosal tissues) causing loss of antibody activity (43,44). The organism is identified clinically by growth on Thayer-Martin or chocolate agar, being strongly oxidase positive and by the abilty to metabolise glucose (but not maltose) (45).

Gonorrhoea (infection) is transmitted between humans through intimate contact of the mucous membrane, and the organism can be carried by both sexes for many years without any sign or symptoms. In infected males, the disease is characterised by a urethral discharge of pus and can eventually result in other complications such as prostatitis and periurethral abscess. Females with a gonorrhoea infection exhibit vaginal discharge, abdominal pain, and abnormal non-

menstrual bleeding. Ironically, the widespread use of birth control devices such as the pill has actually increased the number of gonococcal infections in the United States, as the use of the pill can lower the glycogen concentration of the vaginal membrane. This environmental change inhibits the growth of acid-producing bacteria, such as *Lactobacillus*, which are the natural flora of the vagina. This change leads to the vaginal pH being less acidic, allowing a variety of pathogenic organisms (including *N. gonorrhoeae*) to thrive there. As with most other sexually transmitted diseases, gonorrhoea is prevalent in young adult and homosexual populations (46). *N. gonorrhoeae* is sensitive to wide range of environmental conditions such as ultraviolet radiation, drying, and antibiotics; the current regime of treatment is with the third generation cephalosporins, such as ceftriaxone. However, the range of antibiotics that are clinically effective against the organism is limited, and at present, the third generation cephalosporins are the only antibiotics that are an effective treatment of the disease. Should the organism become resistant to these drugs there will no longer be an effective clinical treatment for gonorrhoea infection (41).

The bio-availability of iron is a fundamental requirement for *N. gonorrhoeae*; there being no natural reservoir in the environment, the infection is perpetuated asymptomatically at low levels in the general population.

1.2.6 Iron Uptake in *Neisseriaceae*

Iron is an essential requirement for pathogenic *Neisseria* species to maintain virulence, and they acquire it by utilising several of the above mechanisms. Although *Neisseria spp* do not produce their own siderophores, their growth can be supported by the addition of exogenous siderophores, thus suggesting that they may possess a pathway for utilising iron bound siderophores that have been excreted by other microbes (47). Genome analysis of meningococcal and gonococcal species reveals at least three open reading frames that share sequence homology with known siderophore receptors, further suggesting that *Neisseria spp* may have a battery of siderophore receptors to utilise siderophores secreted by other organisms (47).

Pathogenic *Neisseria* are capable of sequestering iron from haemoglobin, haptoglobin-haemoglobin and haem, but not from haem-haemopexin or haem-albumin. There are two kinds of receptor for haem in *Neiserria* species: HmbR, and HpuA and HpuB. HmbR is an 89.5 kDa outer membrane protein that binds and acquires iron from haem and haemoglobin. HpuA is an 85 kDa outer membrane protein, and HpuB is a 34.8 kDa lipoprotein that forms a complex that binds and removes iron from haemoglobin and haptoglobin-haemoglobin. The levels of haem and haem-containing proteins in mucosal surfaces are low, but are obviously much higher in other body compartments (47,48).

The *Neisseriaceae* can acquire iron from transferrin (and lactoferrin) via Tbps (and Lbps) expressed in the outer membrane (49). Although iron levels are thought to be low, transferrin appears to be a vital source of iron in mucosal surfaces, as Tbp-deficient mutants are avirulent compared with the wild-type organism (50). This

certainly indicates that transferrin levels in genitourinary mucosa are of a sufficient level to be able to support growth of the organism in this environment. However, given the amount of transferrin in the serum and other body compartments, the Tbps are probably also important during the invasive phases of infection, and are always detected in clinical isolates. Lactoferrin (which is also present in mucosal surfaces) can also be utilised for the acquisition of iron, but how essential its requirement is for infection is unclear. It has been demonstrated that an Lbp-deficient strain, but not its Tbp-deficient derivative is virulent in a human infection model, and that the Lbp genes are deficient from a significant number of clinical isolates (47,50). Iron that is acquired from this source is then passed to an ATP Binding Cassette (ABC) transporter system (FbpABC) that facilitates transport of the iron across the periplasmic space and through the cytoplasmic membrane into the cytoplasm (51). The exact details of this process remain mostly undescribed.

1.3 Chapter 1 References

1. Thomson, A. J., and Gray, H. B. (1998) *Curr. Opin. Chem. Biol.* **2**, 155-158
2. Shriver, D. F., and Atkins, P. W. (1999) *Inorganic Chemistry* (Third, Ed.), Oxford
3. Broderick, J. B., and Coucouvanis, D. (2003) *Curr. Opin. Chem. Biol.* **7**, 157-159
4. Ratledge, C., and Dover, L. G. (2000) *Annu. Rev. Microbiol.* **54**, 881-941.
5. Andrews, S. C., Robinson, A. K., and Rodriguez-Quinones, F. (2003) *FEMS Microbiol. Rev.* **27**, 215-237
6. Clarke, T. E., Tari, L. W., and Vogel, H. J. (2001) *Curr. Top. Med. Chem.* **1**, 7-30
7. Friedman, Y. E., and O'Brian, M. R. (2004) *J. Biol. Chem.* **279**, 32100-5
8. Stojiljkovic, I., Baumler, A. J., and Hantke, K. (1994) *J. Mol. Biol.* **236**, 531-545
9. Sebastian, S., Agarwal, S., Murphy, J. R., and Genco, C. A. (2002) *J. Bacteriol.* **184**, 3965-3974
10. Pecqueur, L., D'Autreaux, B., Dupuy, J., Nicolet, Y., Jacquamet, L., Brutscher, B., Michaud-Soret, I., and Bersch, B. (2006) *J. Biol. Chem.* **281**, 21286-21295
11. Pohl, E., Haller, J. C., Mijovilovich, A., Meyer-Klaucke, W., Garman, E., and Vasil, M. L. (2003) *Mol. Microbiol.* **47**, 903-915
12. Dertz, E. A., Stintzi, A., and Raymond, K. N. (2006) *J. Biol. Inorg. Chem.* **11**, 1087-1097
13. Ferguson, A. D., and Deisenhofer, J. (2004) *Cell.* **116**, 15-24

14. Ferguson, A. D., Chakraborty, R., Smith, B. S., Esser, L., van der Helm, D., and Deisenhofer, J. (2002) *Science.* **295**, 1715-1719

15. Buchanan, S. K., Smith, B. S., Venkatramani, L., Xia, D., Esser, L., Palnitkar, M., Chakraborty, R., van der Helm, D., and Deisenhofer, J. (1999) *Nat. Struct. Biol.* **6**, 56-63

16. Locher, K. P., Rees, B., Koebnik, R., Mitschler, A., Moulinier, L., Rosenbusch, J. P., and Moras, D. (1998) *Cell* **95**, 771-778

17. Bayer, P., and Harjes, S. (2001) *Trends Biochem. Sci.* **26**, 472

18. Traub, I., Gaisser, S., and Braun, V. (1993) *Mol. Microbiol.* **8**, 409-423

19. Carter, D. M., Gagnon, J. N., Damlaj, M., Mandava, S., Makowski, L., Rodi, D. J., Pawelek, P. D., and Coulton, J. W. (2006) *J. Mol. Biol.* **357**, 236-251

20. Kodding, J., Killig, F., Polzer, P., Howard, S. P., Diederichs, K., and Welte, W. (2005) *J. Biol. Chem.* **280**, 3022-3028

21. Carter, D. M., Miousse, I. R., Gagnon, J. N., Martinez, E., Clements, A., Lee, J., Hancock, M. A., Gagnon, H., Pawelek, P. D., and Coulton, J. W. (2006) *J. Biol. Chem.* **281**, 35413-35424

22. Pawelek, P. D., Croteau, N., Ng-Thow-Hing, C., Khursigara, C. M., Moiseeva, N., Allaire, M., and Coulton, J. W. (2006) *Science* **312**, 1399-1402

23. Chang, C., Mooser, A., Pluckthun, A., and Wlodawer, A. (2001) *J. Biol. Chem.* **276**, 27535-27540

24. Stojiljkovic, I., and Perkins-Balding, D. (2002) *DNA Cell Biol.* **21**, 281-295

25. Sebastian, S., and Genco, C. A. (1999) *Infect. Immun.* **67**, 3141-3145

26. Arnoux, P., Haser, R., Izadi, N., Lecroisey, A., Delepierre, M., Wandersman, C., and Czjzek, M. (1999) *Nat. Struct. Biol.* **6**, 516-520

27. Welch, S. (1992) *Transferrin: The Iron Carrier* (S, W., Ed.), 1 CRC Press, Florida

28. Gasdaska, J. R., Law, J. H., Bender, C. J., and Aisen, P. (1996) *J. Inorg. Biochem.* **64**, 247-258

29. Jandl, J. H., Inman, J. K., Simmons, R. L., and Allen, D. W. (1959) *J. Clin. Invest.* **38**, 161-185

30. Thibodeau, S. N., Lee, D. C., and Palmiter, R. D. (1978) *J. Biol. Chem.* **253**, 3771-3774

31. Grossmann, J. G., Neu, M., Evans, R. W., Lindley, P. F., Appel, H., and Hasnain, S. S. (1993) *J. Mol. Biol.* **229**, 585-590

32. Zhong, W., Parkinson, J. A., Guo, M., and Sadler, P. J. (2002) *J. Biol. Inorg. Chem.* **7**, 589-599

33. Sun, H., Li, H., and Sadler, P. J. (1999) *Chem. Rev.* **99**, 2817-2842

34. Sigel, A., and Sigel, H. (1998) *Metal Ions in Biological Systems*, v35, Marcel Dekker, New York

35. Desai, P. J., Garges, E., and Genco, C. A. (2000) *J. Bacteriol.* **182**, 5586-5591

36. Genco, C. A., and Desai, P. J. (1996) *Trends Microbiol.* **4**, 179-184

37. Hall, D. R., Hadden, J. M., Leonard, G. A., Bailey, S., Neu, M., Winn, M., and Lindley, P. F. (2002) *Acta Crystallogr. D Biol. Crystallogr.* **58**, 70-80

38. Krell, T., Renauld-Mongenie, G., Nicolai, M. C., Fraysse, S., Chevalier, M., Berard, Y., Oakhill, J., Evans, R. W., Gorringe, A., and Lissolo, L. (2003) *J. Biol. Chem.* **278**, 14712-14722.

39. Rokbi, B., Mazarin, V., Maitre-Wilmotte, G., and Quentin-Millet, M. J. (1993) *FEMS Microbiol. Lett.* **110**, 51-57

40. Bruns, C. M., Anderson, D. S., Vaughan, K. G., Williams, P. A., Nowalk, A. J., McRee, D. E., and Mietzner, T. A. (2001) *Biochemistry.* **40**, 15631-15637

41. http://textbookofbacteriology.net/neisseria.html.

42. http://medic.med.uth.tmc.edu/path/00001510.htm.

43. http://www.cehs.siu.edu/fix/medmicro/neiss.htm.

44. Chintalacharuvu, K. R., Chuang, P. D., Dragoman, A., Fernandez, C. Z., Qiu, J., Plaut, A. G., Trinh, K. R., Gala, F. A., and Morrison, S. L. (2003) *Infect. Immun.* **71**, 2563-2570

45. http://www.cdc.gov/std/Gonorrhea/lab/default.htm.

46. Murray, P. R., Rosenthal, K. S., Kobayashi, G. S., and Pfaller, M. A. (1998) *Medical Microbiology*, 3rd Ed., Mosby, St. Louis

47. Schryvers, A. B., and Stojiljkovic, I. (1999) *Mol. Microbiol.* **32**, 1117-1123

48. Perkins-Balding, D., Ratliff-Griffin, M., and Stojiljkovic, I. (2004) *Microbiol. Mol. Biol. Rev.* **68**, 154-171

49. Cornelissen, C. N. (2003) *Front. Biosci.* **8**, d836-847

50. Cornelissen, C. N., Kelley, M., Hobbs, M. M., Anderson, J. E., Cannon, J. G., Cohen, M. S., and Sparling, P. F. (1998) *Mol. Microbiol.* **27**, 611-616

51. Gomez, J. A., Criado, M. T., and Ferreiros, C. M. (1998) *Res. Microbiol.* **149**, 381-387

Chapter 2: ATP Binding Cassette (ABC) Transporters

2.1 ATP-Binding Cassette (ABC) Transporters

ATP-Binding Cassette (ABC) transport systems are a ubiquitous ligand-transporting motif present found in mammals, bacteria and fungi (1). The vectorial transport of molecules across lipid bilayers is central to cell physiology, including the uptake of nutrients, elimination of waste products, protein secretion, energy generation and movement of signalling molecules (2). ABC transporters facilitate the unidirectional translocation of these chemically diverse substrates across cell or organelle membranes and constitute one of the largest superfamily of proteins known (3). In *E. coli*, genes encoding ABC transport systems occupy almost 5% of the genome, and in humans, mutations in ABC transporter genes are responsible for many genetic disorders, including cystic fibrosis (lung and gut systems; CFTR gene), Tangier disease (cardiovascular system; *ABC1* gene on chromosome 9q31) and Stargardt disease (eye; ABCR gene on chromosome 1q21-p13) (2,4). Other ABC transporters can confer resistance to drugs such as antibiotic, antifungal and anticancer compounds (2).

ABC transporters share a common architecture and basic mechanism of action: two nucleotide-binding domains (NBDs) that bind and hydrolyse ATP, and energise unidirectional substrate transport, which occurs through a translocation pathway provided by two trans-membrane spanning domains (TMDs) (2). It has been shown that all ABC transporters share highly conserved motifs that are essential for binding and hydrolysis of ATP, and that they have similar structures. By contrast, the membrane-spanning domains share very little sequence homology unless the substrates are chemically related. Thus, a common engine is attached to a

specialized translocation pathway in all ABC transporters. The bacterial ABC transporters that function to import ligands to the cytoplasm also have an extra soluble domain that resides in the periplasmic space and is thought to be responsible for the transport of its ligand from the outer membrane to the cytoplasmic membrane and presents the ligand for translocation.

Most eukaryotic ABC transporters that have been characterized thus far are usually composed of a TMD and NBD that are fused into a single polypeptide and mediate the export of substrate from the cytoplasm, out of the cell or into organelles (5,6). The exceptions are the ABC transporters that transport substrate from the mitochondrial matrix, which is the equivalent to the cytoplasm of the original symbiot. This can lead to a general designation of "ABC exporters" when referring to eukaryotic ABC transporters.

The bacterial "ABC importers", on the other hand, are generally composed of separate subunits, and consist of; a soluble periplasmic binding protein (PBP) that delivers the substrate to the TMD for translocation; the membrane spanning domain that forms the translocation pathway; and the NBD that hydrolyses ATP to energise the translocation of the substrate across the cytoplasmic membrane. The TMD and NBD form dimers in the lipid bilayer and cytoplasm, respectively, in the active transport complex. The prokaryotic ABC exporter systems show more structural homology (though not necessarily sequence homology) to the eukaryotic ABC exporters: they consist of a TMD and NBD that are fused into a single polypeptide and mediate the export of substrate from the cytoplasm (7,8). Indeed, the lipid flippase MsbA from *E. coli* is more closely related to the mammalian P-

glycoproteins (multidrug resistance ABC transporters) than any other bacterial ABC transporter by sequence homology (8). Again, the active transporter requires the formation of a dimer in the membrane. Although these proteins belong to the same superfamily, ABC transporters cannot replace each other in different ligand transport systems (9).

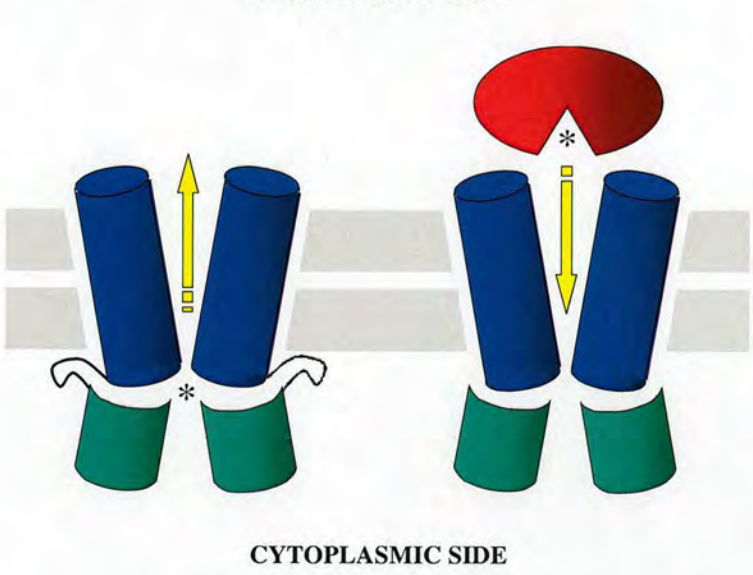

Figure 2.1. Schematic representation of the two main types of ABC transporter found in eukaryotes and prokaryotes. The ABC exporters (**left**) have a transmembrane domain (blue) that is fused (black coil) to a nucleotide binding domain (green). The active transporter is formed by dimer formation of two like subunits It is presumed there is a substrate binding site on the cytoplasmic face of the TMD dimer (*). The ABC importers (**right**) have separate TMD and NBD that associate as a tetramer: two TMDs and two NBDs. The import systems may or may not have a dedicated periplasmic binding protein (red) that transports and presents the ligand (*) to the TMD/NBD complex for translocation. The cytoplasmic membrane is represented in grey. Direction of transport is represented by the yellow arrows.

There has been biochemical characterisation of many ABC transporters that are involved in varied roles such as osmotic regulation (OpuA), uptake of macromolecules (AlgSM1M2), amino acids (GlnPQ), and multidrug resistance (LmrCD, Sav1866) (7,10-13). However, to date, there have only been a limited number of high-resolution structural studies of bacterial ABC importers. The

vitamin B_{12} transporter, BtuCD from *E. coli*, remains the only (high-resolution) structure of a TMD and NBD complex to have been published, and along with the X-ray crystal structure of the PBP in this system, BtuF, means that the $BtuFC_2D_2$ complex remains the only visual representation of a complete bacterial ABC importer published to date (1). However, the crystal structure of the NBD and TMD from another metal-chelate-type transporter called *HI1470/1* from *H. influenzae* has recently been published, but the structure of the PBP from this system has not been determined, and the exact nature of the substrate was not described (14). The structures of this newly exhibited transporter and the BtuCD share a striking similarity, and are proposed to be functionally very closely related. In contrast to the situation with the TMD, the structures of many PBPs from other ABC transporter systems have been elucidated, as have several of the NBD. The following sections are a general review of each of the components of the bacterial ABC importers.

2.1.1 The Periplasmic Binding Domain

Gram-negative periplasmic binding proteins (PBPs) are members of a widely distributed protein superfamily (15). PBPs have been identified that bind a diverse range of ligands, including lipids, metal ions, amino acids, peptides and carbohydrates. These proteins on the whole share little sequence homology with other members of the family, but do retain a similar fold and overall structure: two globular domains connected by a hinge region, with the ligand binding site situated at the interface between the two domains. These proteins have been characterised into two structural classes defined by the number and arrangement of β-strands in each domain of the protein: class I proteins contain six β-strands (order 213456),

class II PBPs contain five β-strands (order 21354) (16). However, this classification system can breakdown when considering members of the metal-binding PBPs, as the β-strand content can vary in each domain, and the hinge region is often composed of β-strand in this particular family of PBPs. The proteins exhibit large conformational changes upon binding of their ligand, being "open" in the *apo* (ligand-free) form, and "closed" in the *holo* (ligand-bound) form. These conformational changes upon ligand binding have led researchers to refer to these proteins as "venus fly-trap" and "Pacman" proteins, due to the relatively large rotational motion around the hinge region (17). Over 100 PBP structures have been determined by X-ray crystallography from a wide variety of sources, including *E. coli*, pathogenic and thermophillic bacteria (16).

The adaptability of this large superfamily is likely to have arisen from the positioning of the binding site at the interface between the domains and from the large ligand-mediated conformational change. In this arrangement, the ligand environment resembles that of a protein interior, but the binding residues are positioned on the surface of their domains. These conditions not only allow the desirable physiochemical characteristics arising from the placement of ligands in a solvent-excluding environment, but also combine the adaptability of evolving sites on protein surfaces (16).

2.1.1.1 Iron Binding Periplasmic Binding Proteins

The importance of the acquistition and proper control of intracellular levels of this essential, but potentially toxic, metal ion has driven bacteria to evolve safe methods of iron transport and storage. Ferric iron-binding proteins have been identified in

many Gram-negative organisms, and several have had their crystal structures determined by X-ray crystallography (**Table 2.1**). They all share a very similar tertiary structure but can vary widely, not only in their amino acid sequence, but also in the residues involved in complexation of the bound ferric ion (18). However, these proteins are defined by the presence of a sequential di-tyrosyl motif that is intrinsically involved in coordination of the ferric ion. In addition to the protein ligands, there may also be a synergistic anion present that completes the coordination of the metal ion. These variations have led at least two groups to classify the iron binding PBPs according to their substrate binding residues and/or amino acid sequences, and the presence or absence of a synergistic anion (19,20).

Table 2.1. The iron-binding periplasmic binding proteins from Gram-negative bacteria whose X-ray crystal structures are known. NTA: nitrilotriacetate, EDTA: Ethylenediaminetetracetic acid.

Organism	PDB Code	Resolution (Å)	Mutant	Description
H. influenzae	1MRP (21)	1.60	-	*Holo* – Fe and PO_4
	1QWO (22)	1.90	N175L	*Holo* – Fe_4 and PO_4
	1QVS (22)	2.10	H9A	*Holo* – Fe_3 and PO_4
	1NNF (23)	1.14	H9Q	*Holo* – Fe and EDTA
	1D9V (24)	1.75	-	*Apo* – PO_4
M. haemolytica	1Q3S (25)	1.20	-	*Apo* – 2 x formate
	1SIO (26)	1.35	-	*Holo* – Fe and CO_3
	1SI1 (26)	1.45	-	*Holo* – Fe
C. jejuni	1Y4T (19)	1.80	-	*Holo* – Fe
Y. enterolytica	1XVX (20)	1.53	-	*Holo* – Fe
S. marscesens	1XVY (20)	1.74	-	*Apo* – citrate
B. pertussis	1Y9U (19)	1.39	-	*Apo*
N. gonorrhoeae	1D9Y (27)	2.20	-	*Holo* – Fe and PO_4
	1O7T (28)	1.65	-	Hf_3, Hf_5, and PO_4
	1R1N (29)	1.74	-	*Holo* and *apo* – Fe_3, Fe and NTA
	1XC1 (30)	1.51	-	Zr_3

FbpA (the iron-binding PBP from *N. gonorrhoeae*) is categorised as a Class I iron binding PBP; it binds a single ferric-ion with two (sequential) tyrosine residues, a histidine and a glutamic acid residue, with a monodentate phosphate synergistic anion. Pseudo-octahedral coordination of the metal-ion is completed by a water molecule. Examples of the other classes are: Class II; *Mannheimia haemalytica* FbpA that coordinates a ferric ion with three tyrosine residues and a bidentate carbonate anion: Class III; *Yersinia enterolitica* YfuA that coordinates ferric ion via two tyrosine residues, a histidine, aspartic acid and glutamic acid residues (no synergistic anion): Class 4; *Campylobacter jejuni* FbpA which coordinates its ferric ion through four tyrosine residues and a histidine residue (no synergistic anion). It should be noted that the two classification systems are mutually exclusive, as YfuA is classified, somewhat confusingly, as Class 2 in one system and Class III in the other.

Much work has been published on the ability of these iron-binding sites to bind other metal ions with variable affinity. The crystal structures of oxo-Fe_3, oxo-Hf_3 & Hf_5 clusters, oxo-Zr_3 and a Fe-NTA (nitriloacetate) complex bound to nFbpA have been published (28,30,31). The fact that FbpA can bind metal clusters possibly suggests another mechanism for iron uptake: some of these PBPs may be able to interact directly with the extracellular environment. This suggestion has been supported by work that has shown that anti-FbpA antibodies bind to the surface of whole cells expressing the iron-binding PBPs from a least two different species (32-34).

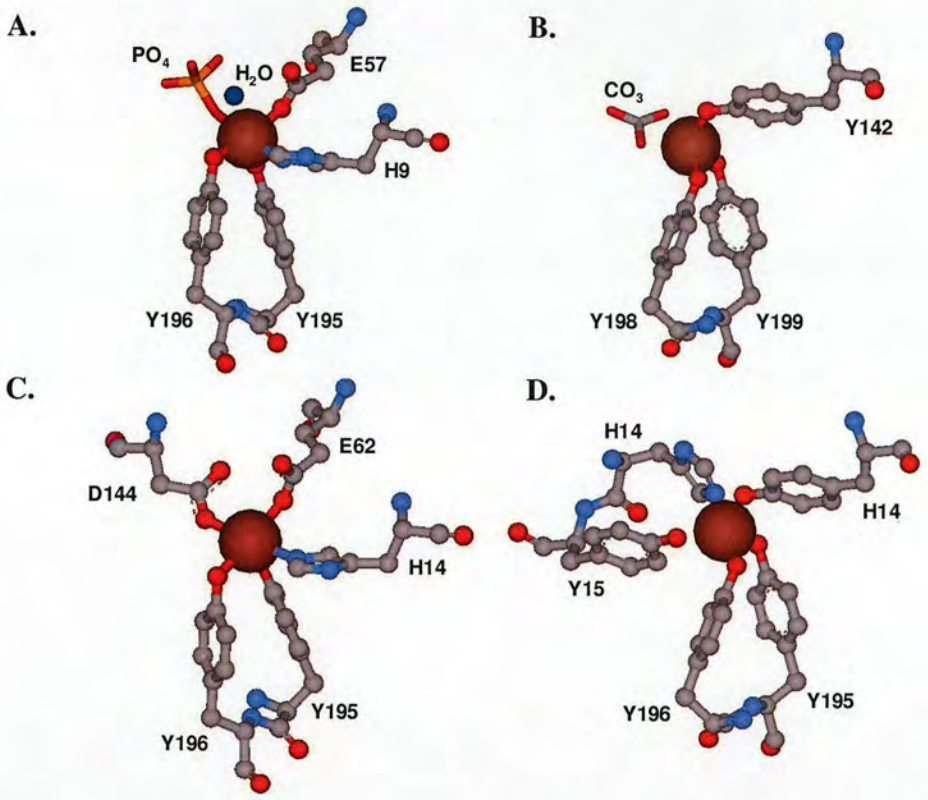

Figure 2.2. Representation of different classes of iron binding sites in the iron-binding periplasmic binding proteins (PBP). A, class 1 binding site of FbpA from *N. gonorrhoeae* (PDB: 1D9Y); **B**, class 2 binding site of FbpA from *M. haemolytica* (PDB: 1SI1); **C**, class 3 binding site of YfuA from *Y. enterolytica* (PDB: 1XVX); **D**, class 4 binding site of FbpA from *C. jejuni* (PDB: 1Y4T) (19,20,26). Iron is shown in brown.

2.1.2 The Transmembrane Domain

To date the transmembrane domains (TMD) of the ABC transporters have been largely ignored in the literature and the only extensive investigations performed on these proteins have been the few crystallographic studies, whilst their biochemistry remains broadly undescribed. This is probably in no short measure due to the difficulty of expressing and purifying such membrane proteins. The membrane-spanning domains of ABC transporters share very little sequence homology unless the substrates are chemically related. However, it is likely that all ABC transporters

share the common motif of forming the translocation pathway for their ligand between the interface of two TMD subunits (by homo- or hetero-dimer formation). The TMD of ABC transporters vary not only in amino acid sequence, but also in the number of transmembrane helices that form the translocation pathway: MsbA (a bacterial lipid transporter) contains 12 transmembrane helices (6 helices per subunit), whereas the FhuD protein is predicted to have up to 20 such helices (8). However, it should be noted that recently the published MsbA structure has been retracted due to an error in the structural software program used to determine the topology of the molecule, and thus a revised structure is currently awaited (35).

Five crystal structures of full-length bacterial ABC transporters (i.e. structures of the TMD) have been reported, and of these structures two are known for bacterial importers; the vitamin B_{12} transporter from *E. coli*: BtuC and an ABC transporter from *H. influenzae* called *HI1470* for which the substrate is not known (1,14). Recently the 2.4 Å crystal structure of the TMD and NBD of another bacterial ABC transporter (*HI1470/1*) whose substrate is unknown was published. The authors reported that the transporter is involved in "metal-chelate"-type transport, such as haem and vitamin B_{12}, but the PBP associated with the transporter was not described (14,36).

2.1.2.1 The Vitamin B_{12} Transmembrane Domain: BtuC

The 3.2 Å crystal structure of BtuC was reported by Locher and co-workers in 2002 (1). These researchers succeeded in cloning, co-expressing, co-purifying and co-crystallising the transmembrane (BtuC) and nucleotide-binding domains (BtuD) of this ABC transporter. The structure of BtuF (the periplasmic binding protein of

this transporter) has also been determined, making BtuFCD the only complete crystal structure known for a bacterial importer.

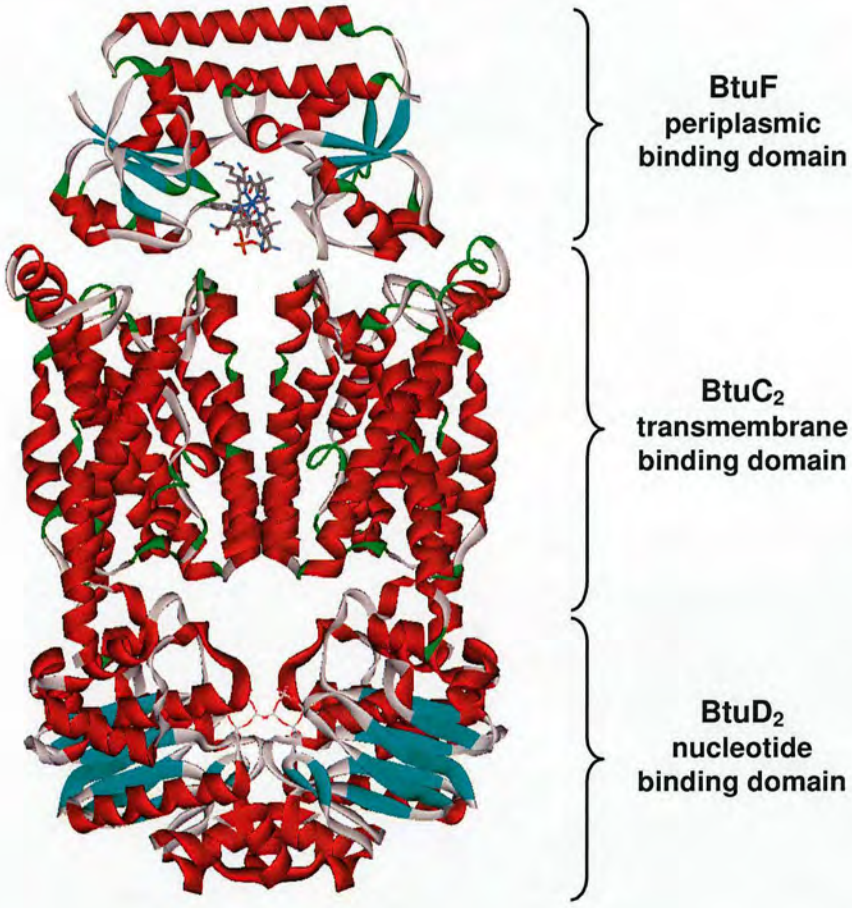

Figure 2.3. Crystal structures of the vitamin B_{12} ATP transporter BtuFCD from *E. coli* (PDB: 1N4A and 1L7V). This structure remains the only full-length bacterial import ABC transporter to be solved (1,37). Vitamin B_{12} shown in stick representation.

The structure reveals that BtuC forms a homodimer that traverses the membrane, and that each of the two subunits traverses the membrane ten times: thus, the active transporter is formed by twenty transmembrane helices. The interface between the two BtuC subunits is formed by the antiparallel packing of two pairs of helices that create a large cavity that opens to the periplasmic space. This cavity is of sufficient size as to accommodate the corrin ring of vitamin B_{12}, but there is no

continuous pathway across the membrane due to the presence of two loops of amino acid residues inside the cytoplasmic opening of the tranporter that are proposed to act as a gate. It has been suggested that a single translocation pathway formed by the interface of a membrane-spanning dimer is likely to be a common feature of ABC-transporters.

The bulk of the interface between $BtuC_2$ (TMD dimer) and $BtuD_2$ (NBD dimer) is formed by two short helical stretches connected by a sharp bend on the cytoplasmic surface of BtuC making extensive contacts with BtuD. A small number of contacts are also made between the cytoplasmic loops of the transmembrane-spanning helices and the N-terminus of BtuC (1).

2.1.3 The Nucleotide Binding Domain

The nucleotide binding domain (NBD) of ABC transporters, unlike the TMD, are highly conserved throughout the family, and whether from prokaryotic or eukaryotic origin, and irrespective of substrate, share extensive amino acid sequence and several characteristic motifs. Studies of bacterial ABC transporters first showed that the NBDs bind and hydrolyse ATP, and that ATP hydrolysis is required for transport. At least 15 structures of NBDs from bacterial transporters have been published, and they all show a similar architecture, in which the conserved amino acid motifs contribute to the nucleotide-binding pocket.

2.1.3.1 Conserved Motifs

The Walker A (G--G-GK(S/T)T, also known as the P loop) and Walker B (L-DEP) motifs are highly conserved within the ABC transporter family and hydrogen-bond

extensively with the bound nucleotide. The Walker B sequence also contributes the catalytic base (E) involved in hydrolysis of the bound ATP. The ABC signature motif (LSGG--QRV), the D-loop (-LD-), the H loop ((S/T)H(D/E), also called the switch region) and Q loop (Q, also called the lid region) are distinctive to ABC transporter NBDs, and although they are involved in the coordination of the nucleotide or nucleophilic water, their precise role in the catalytic mechanism is less clear (2).

2.1.3.2 Mechanism of Transport

Several models have been formatted that describe the mechanism of transport for the ABC transporters, but there is still much debate as to which proposed mechanism (if any) is correct. Studies performed on the mammalian multidrug resistance P-glycoprotein (P-gp) ABC transporter defined the biochemistry of the ATPase cycle and proposed an alternating catalytic sites model (6). In this model, one molecule of ATP is first bound to one NBD domain and is hydrolysed, and then the other NBD binds a second molecule of ATP. The substrate is translocated during the ATP hydrolysis step and binding of the second molecule of ATP holds the NBD dimer in a "ready" state to accept another substrate molecule; as such, this mechanism keeps the transporter in a permanently "primed" position to immediately transport a substrate molecule as soon as one binds. Several related models have since been proposed for the bacterial histidine and maltose transporters (4,38). Again, these models generally assume that ATP hydrolysis provides the principal energy input ("powerstroke") for transport and that the two NBDs operate alternately and are coupled to distinct steps in the transport cycle.

Some recent observations, however, have caused researchers to readdress the underlying tenets of the proposed mechanisms. Firstly, biochemical data have suggested that it is ATP binding (not hydrolysis) that provides the power stroke for transport. Secondly, the finding that for some ABC transporters (the ABCC family) the two NBDs are non-equivalent in their ability to hydrolyse ATP and, thirdly, structural data have revealed that the ATP binding site is situated at the interface of the NBD dimer, suggesting that the two domains act in concert during a single power stroke step rather than influencing distinct steps in the transport cycle (39). This dynamic communication and synergistic approach between the NBDs in the active dimer has spawned a newly-proposed mechanism known as the ATP-switch model (2).

2.1.3.3 The ATP-switch Model

This mechanism requires repeated communication, in both directions, between the NBDs and TMDs in the form of noncovalent conformational changes. The model gets its name from the switch between two conformations of the NBDs: a closed dimer formation upon the binding of two ATP molecules at the dimer interface, to an open dimer facilitated by ATP hydrolysis and release of P_i and ADP. The ATP switch model is summarized in **Figure 2.4**. The kinetics of this "switching" process are enhanced by the cooperativity between the two nucleotide-binding pockets and can also be tightly regulated by signals from the TMDs (40). Switching between the open and closed configurations induces conformational changes in the TMDs that are necessary to faciltate vectorial transport of the substrate across the membrane (2,40). The mechanism can be summarised as follows:

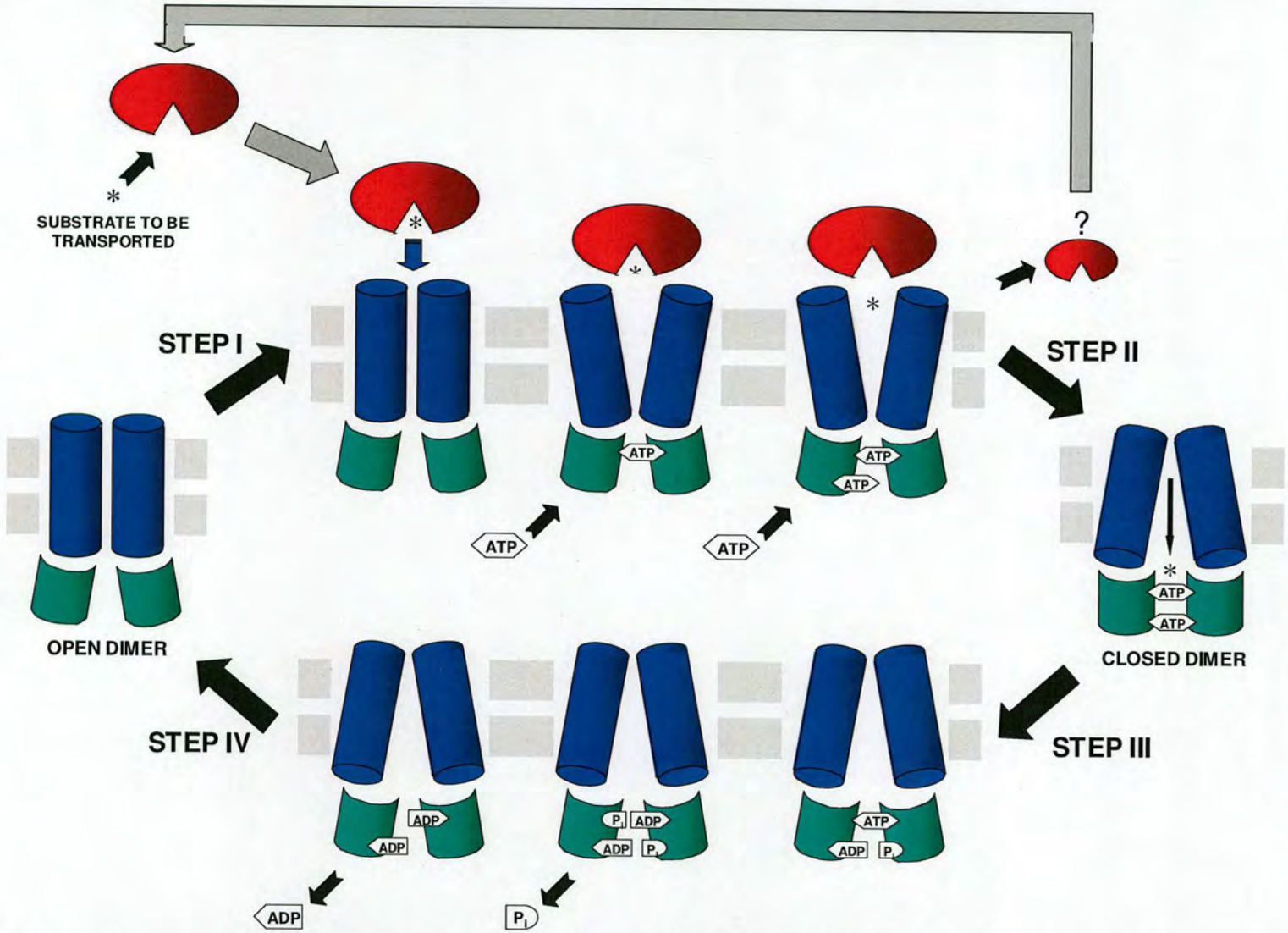

Figure 2.4. Schematic representation of the ATP switch model of TP hydrolysis by the nucleotide binding domain of ABC transporters. TMD shown in blue, NBD shown in green, PBP shown in red, substrate to be transported is represented by *. **Step I**, PBP complexes with TMD/NBD in CM, causing ATP to bind at NBD dimer interface. **Step II**, closed dimer formation produces power stroke for substrate translocation. **Step III**, ATP is hydrolysed and ADP and P_i (inorganic phosphate) dissociate from NBD. **Step IV**, TMD/NBD return to open dimer conformation, ready to accept another PBP/substrate molecule complex (2). CM is shown in grey. Based on (2).

Step I. *Binding of substrate to the TMDs initiates the transport cycle by facilitating ATP-dependent closed dimer formation.* For the bacterial ABC import transporter this must be via the docking of a PBP-substrate complex to the periplasmic face of the TMDs. Although there is no direct experimental evidence, it is expected that binding of the PBP-substrate complex to the TMDs induces a conformational change in the NBDs, mediated via changes in the TMDs. These conformational changes allow the binding of two ATP molecules to the NBDs.

Step II. *Binding of ATP induces closed dimer formation, the power stroke for transport.* Upon binding of ATP to the NBDs, it is predicted that closed dimer formation transmits a signal to the PBP, inducing it to release the ligand into the chamber of the transporter. There are then two possible routes for ligand translocation: either the substrate binds to a site on the TMDs that is re-oriented during a subsequent step in the cycle so as to expose this site to the cytoplasm, or, more probably, the TMDs are analogous to that of a pore of an ion channel. In this refinement of the model, the pore merely restricts passage of the substrate but does not require the reorientation of a binding site on the TMDs.

Evidence that it is this step that provides the energy input for translocation is supported by the experimental observation that the maltose transporter still releases maltose into the cytoplasm in a vanadate-trapped transition state (2).

Step III. *ATP is hydrolysed.* The hydrolysis of ATP seems to initiate the resetting of the transporter to its basal, open-dimer conformation by destabilizing the NBD closed dimer. This may also serve to induce a conformational change in the TMDs to open the channel into the cytoplasm and block the periplasmic opening of

the TMDs. There may also be dissociation of the *apo*-PBP from the TMDs at this point.

The trigger for ATP hydrolysis is still unknown. Release of the substrate into the TMDs may induce a conformational change that is transmitted to the NBDs, or it may be that ATP hydrolysis is autocatalytic – a consequence of the geometry of ATP with respect to the specific hydrolytic residues introduced by the closed-dimer configuration. This is supported by the evidence that mutation of the catalytic base in the Walker B sequence allows crystal structures to be obtained in which ATP is bound to the active sites of the NBDs.

Step IV. *Release of P_i and ADP.* P_i and ADP are released, restoring the transport complex to its basal state. Hydrolysis of ATP destabilizes the closed dimer by introducing electrostatic repulsion between ADP and the residues in the Walker A motif of one NBD and P_i coordinated to the signature motif of the other NBD. This leads to a conformational change that returns the NBDs to an open conformation, releasing P_i and ADP in the process. There is some evidence to suggest that ADP remains bound in the open configuration of some transporters and that binding of a new substrate imbues conformation changes that cause ADP to dissociate, allowing ATP to bind, and thus, beginning the cycle over again.

2.1.4 NBDs from Three Bacterial ABC Transporters

There have been many crystal structures of bacterial NBDs deposited in the RCSB Protein Data Bank (PDB). The best studied of these are MalK, HisP and BtuD from the maltose, histidine and vitamin B_{12} bacterial ABC transporters, respectively (4,41,42). There follows a brief description of the structures in the PDB.

MalK: Six crystal structures of MalK have been deposited in the PDB since 2003 (PDB codes: 1Q1E, 2ANO, 2AWN, 1G29, 1Q12, 1Q1B): five of the *E. coli* protein and one from the thermophilic organism *Thermococcus litoralis*. Three structures are of the nucleotide-free forms of the protein (including T.l.MalK), two are of the ADP-Mg bound form and one is of the ATP-bound form (4,42).

HisP: There is one structure of the histidine ABC transporter NBD from *Salmonella typhimurium* (PDB code: 1B0U). The structure was determined with ATP bound at the dimer interface (41).

BtuD: There is one structure of the vitamin B_{12} ABC transporter from *E. coli* (PDB code: 1L7V). Interestingly, the researchers managed to co-crystallise the transmembrane domain (BtuC) with the NBD (BtuD). The BtuD structure was crystallised with ortho-vanadate (a non-hydrolysable ATP analogue) bound in the active site (1).

Sequence alignment of the polypeptide chains of all three of these proteins reveals a high consensus identity (64.8%), but low sequence identity (6.7%), and all three proteins adopt a similar fold, suggesting they are descended from a common "ATPase" ancestor that diverged into specific substrate translocation systems over the course of millions of years. The MalK structures differ markedly from the HisP

and BtuD structures in that MalK contains a ~100 amino acid extension at its C-terminus. This so called regulatory domain shares structural identity to the C-terminal aminoacyl-tRNA-binding domains of bacterial elongation factors EF-Tu, the C-terminal barrel domain of bacterial methionyl-tRNA formyltransferase and other proteins of the so-called OB-fold. These domains function as binding modules for aminoacyl-tRNA, carbohydrates and DNA, and the existence of the C-terminal domain in T.l.MalK indicates that the NBD domain of this ABC-transporter may be involved in regulatory circuits. Indirect evidence for a similar fold is shared by other members of the bacterial ABC-type ATPase domains, which also possess an extension of ~110 residues at the C-terminus of their ATPase domain. This strongly suggests that many of these proteins have a dual function within the bacteria cell; not only do they provide the energy input for vectorial transport of a substrate across the inner membrane, but may also be involved in signal transduction within the cytoplasm. However, it should be noted that not all NBDs of the ABC transporters possess such a C-terminal extension: BtuD from the *E. coli* vitamin B_{12} transporter does not have such a domain. When this C-terminus extension is excluded from these sequence alignments, the consensus identity rises to 81.9% and sequence identity increases to 10.1%. Consensus and sequence analysis is summarized in **Figure 2.5**.

When the secondary structure is mapped onto the amino acid sequence of all four proteins, it reveals that they all contain conserved secondary structure for much of the protein: the exception to this is MalK, which contains the extended C-terminal domain (**Figure 2.6**). However, all four proteins do contain the critical conserved motifs that define the ABC transporter NBD family: the Walker A (P loop), Walker

B, Q loop (or lid), H loop (or swith), D loop and ABC signature motifs (**Figure 2.7**). When all four proteins are modelled it reveals that the NBD adopt a similar fold (**Figure 2.8**).

Biochemical studies on the $MalFGK_2$, $BtuFC_2D_2$ and $HisJQMP_2$ systems have shown that the functional complexes can be reconstituted *in vitro* (43-45). The functional complexes were incorporated into proteoliposomes and uptake assays performed using radiolabelled substrate. The $BtuFC_2D_2$ (vitamin B_{12} transporter) study revealed that BtuD (NBD) incorporated into proteoliposomes had a high basal rate of ATP hydrolysis that was stimulated when BtuF (PBP) and substrate (^{57}Co-vitamin B_{12}) was added. However, this research also highlighted that when the transporter was solubilsed in different detergents, the rate of ATP hydrolysis varied widely (43).

The $HisJQMP_2$ (histidine) transporter was reconstituted into proteoliposomes by dialysis and revealed that substrate (L-[H^3]histidine) transport was entirely dependent upon the presence of ATP and liganded HisJ (PBP), and was sensitive to pH, temperature and salt concentration changes. These researchers found that the transport of radiolabelled substrate was inhibited by ADP and high concentrations of histidine inside the proteoliposomes, suggesting that the membrane-bound HisQMP complex contained a substrate-binding site. This is strong evidence that the membrane complexes of other ABC transporters may also contain a similar substrate binding site (41). Similar experiments using the reconstituted $MalFGK_2$ complex yielded analogous results (45).

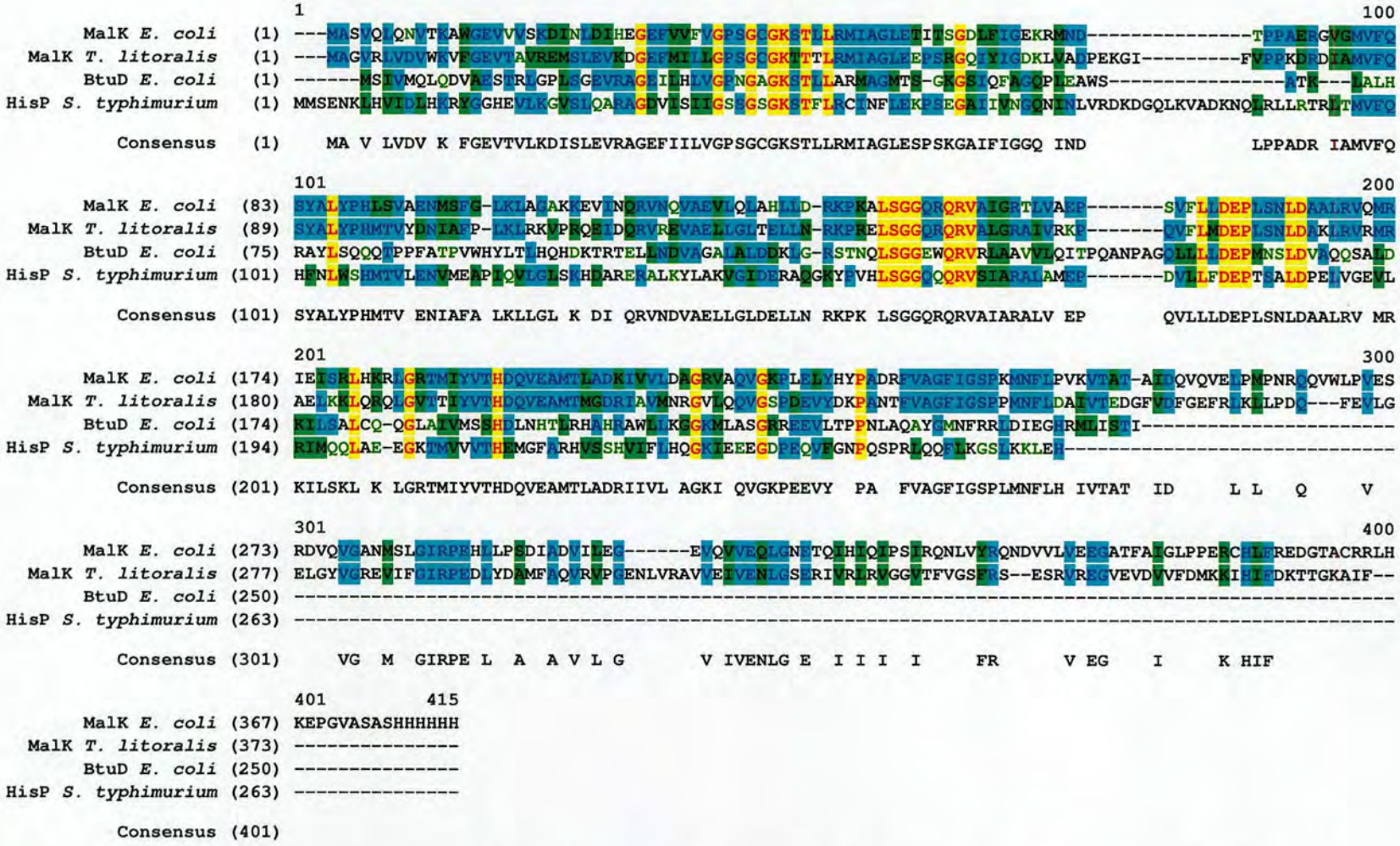

Figure 2.5. Sequence alignment and consensus of MalK from *E. coli* and *T. litoralis*, BtuD from *E.coli* and HisP from *S. typhimurium*. X - Identical residues, X - conservative residues, X - block of similar, X - weakly similar, and X - non-similar. Note the C-terminal extension on both MalK sequences.

Figure 2.6. Sequence alignment showing secondary structure of MalK from *E. coli* and *T. litoralis*, BtuD from *E.coli* and HisP from *S. typhimurium*. X – β strand, X – α helix, X – not known.

Figure 2.7. Sequence alignment showing conserved motifs in MalK from *E. coli* and *T. litoralis*, BtuD from *E.coli* and HisP from *S. typhimurium*. All four sequences contain the essential ABC motifs that define this family of proteins.

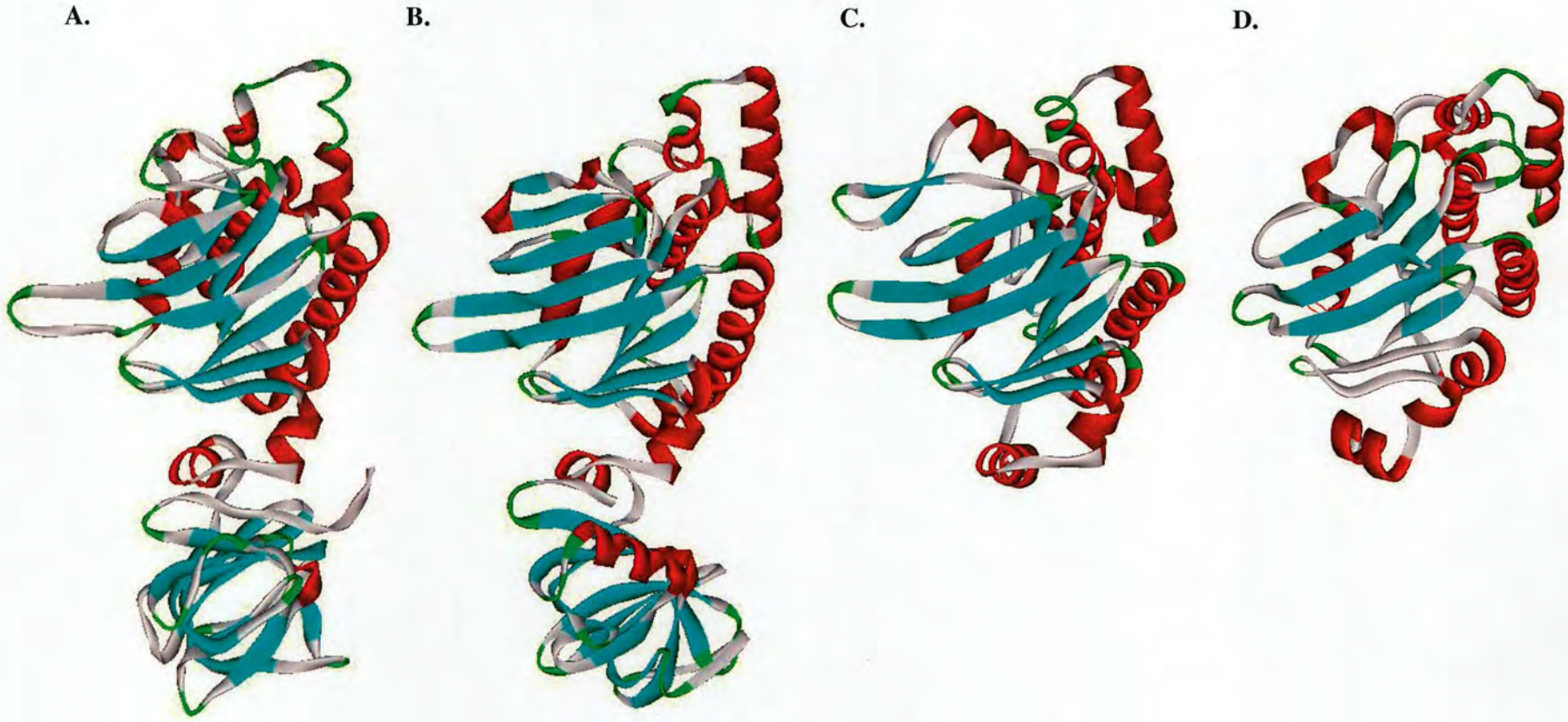

Figure 2.8. Representation of the crystal structures of MalK, BtuC and HisP (monomers). **A**, MalK (PDB: 1Q1B) from *T. litoralis*; **B**, MalK (PDB: 1G29) from *E. coli*; **C**, HisP (PDB: 1B0U) from *S. typhimurium*; **D**, BtuC (PDB: 1L7V) from *E. coli*. Note the conserved fold in the NBD for all four proteins and the C-terminal regulatory domain present only in the MalK structures.

2.2 The Iron Uptake ABC Transporter from *N. gonorrhoeae*: FbpABC

2.2.1 The *FbpABC* Operon

The FbpABC proteins are encoded on a three-gene operon in the genomic DNA of *Neiserria gonorrhoeae* called *FbpABC* (46). This operon encodes a member of the ABC transporter family that is involved in the specific uptake of iron into the cytoplasm. *FbpA* is a 993 bp gene that encodes an iron-binding periplasmic binding protein that, in its mature form, is a 309 amino acid long globular protein with a mass of 33.6 kDa. *FbpB* is a 1527 bp gene that is predicted to encode a cytoplasmic transmembrane protein 511 amino acids long, with a calculated mass of 56.3 kDa. *FbpC* is a 1056 bp gene that that is predicted to encode a nucleotide binding protein that is 309 amino acids in length, with a predicted mass of 37.9 kDa (**Figure 2.9** and **Appendix 1**).

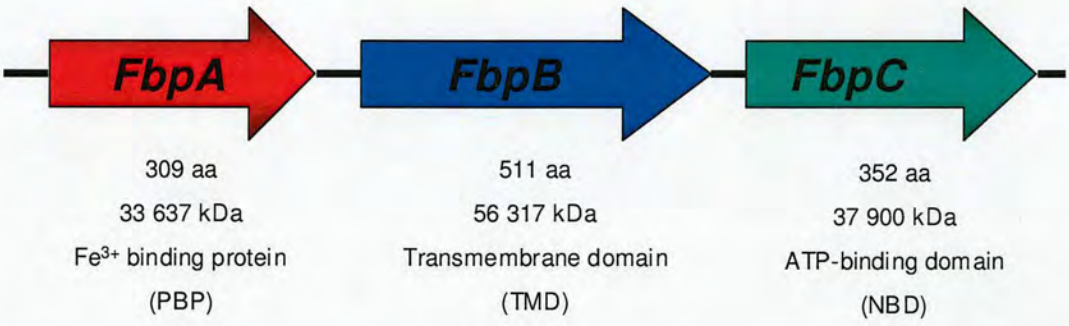

Figure 2.9. Schematic representation of the *FbpABC* iron-uptake operon from the Gram-negative human pathogen *Neisseria gonorrhoeae*.

FbpABC is proposed to facilitate the transfer of iron from the transferrin binding protein in the outer membrane, across the periplasm and into the cytoplasm (**Figure 2.10**).

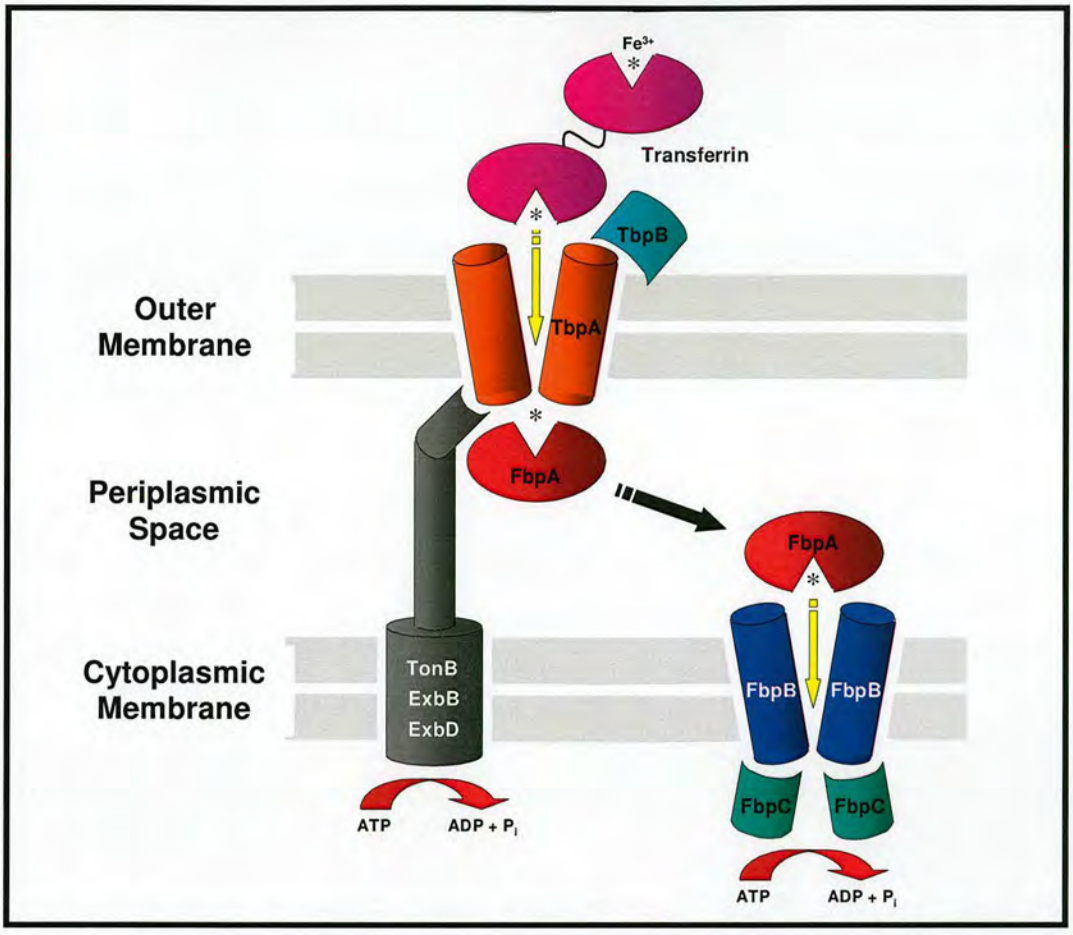

Figure 2.10. The proposed mechanism for iron transfer into the cytoplasm. The exact mechanism of iron transport across the outer membrane, periplasmic space and cytoplasmic membrane remains undescribed. Based on (21).

The gene cluster in *N. meningitidis* was identified as an operon using RT-PCR amplification transcription assays, and thus the same can be assumed for *N. gonorrhoeae* (47). Expression of the operon is tightly regulated by the ferric uptake regulator (Fur; see above), and the gene encoding FbpA is separated from the downstream two genes by a putative stem-loop structure that suggests there is rho-independent transcriptional regulation (48-50). This is a protein (rho) independent mechanism for terminating transcription of DNA and is characterized by a dGdC rich sequence followed by a short dT connecting sequence to a pallindromic dCdG

sequence complementary to the first. The motif is terminated by a longer dT sequence at the 3' end. The effect is that base-pairing is observed within the nascent RNA chain between the two dGdC regions that form a stem loop structure. The base pairing is so strong that the sequence "zippers" down to the RNA-DNA structure in the transcription bubble of the RNA polymerase/DNA helix complex. As the RNA-RNA helices are more stable than RNA-DNA helices, some of the RNA-DNA base pairing in the bubble is disrupted. The remaining base pairs, being A-U pairs, are not strong enough to maintain the RNA-DNA association and the RNA product is released, terminating transcription (**Figure 2.11**). This has the overall effect of upregulating the FbpA gene expression with respect to the FbpB and FbpC genes by several orders of magnitude. Work by other researchers supports this finding and shows that the ratio of *FbpA* to *FbpABC* mRNA (as determined by quantatitive RT-PCR) is 10- to 20-fold greater in *N. meningitidis* grown in iron limiting conditions (47). This is indeed what is observed when *N. gonorrhoeae* is cultured under iron limiting conditions – FbpA is the most upregulated protein in the cell, an observation that highlights the importance of iron acquisition to this species (51).

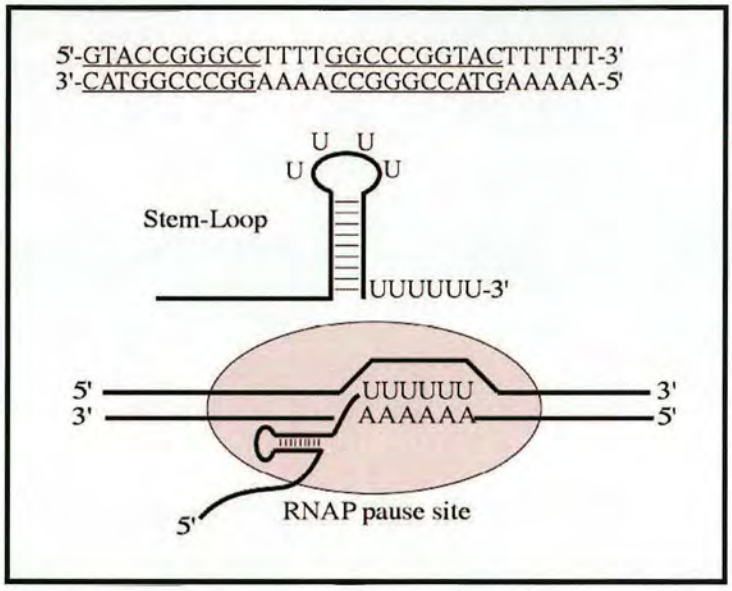

Figure 2.11. Schematic representation of *rho*-independent transcription termination. A general *rho*-independent termination DNA sequence is shown at the top. This sequence forms a stem-loop structure when the nascent RNA chain is formed that "zippers down" into the transcription bubble and disrupts the A-U pairing in the bubble causing the release of the RNA product, thus terminating transcription. RNAP: RNA Polymerase (52).

The *FbpABC* gene cluster in *Neisseria spp.* is homologous to iron import transporters found in many Gram-negative pathogens. FbpABC pathways have been identified in *Haemophilus influenzae*, *Mannheimia haemolytica*, *Campylobacter jejuni* and *Actinobacillus pleuropneumoniae* (19,20,50). Functional homologues of FbpABC have also been found in *Serratia marscesens* and *Yersina spp* (19).

2.2.2 Ferric-Binding Protein A: FbpA

The *FbpA* gene (933 bp) was identified in 1990 and the encoded protein was first purified two years later (53,54). Since that time much work has been published on this protein. It is this protein that is proposed to receive the iron acquired from transferrin via the transferrin-binding protein complex in the outer membrane (34). Exactly how and in which form the iron is transported across the outer membrane

and then transferred to FbpA remains unclear, although several researchers have studied the kinetics of iron binding and release to elucidate this process (55-60).

FbpA is transcribed as a pre-protein that contains a 23 amino acid signal (or leader) peptide (**Figure 2.12**) at its N-terminus that directs the protein for translocation into the periplasm, presumably via a SecA-dependent pathway. SecA mediates the translocation of the nascent protein chain by targeting it to a translocation channel composed of SecYEG in the cytoplasmic membrane. During the process of translocation the signal peptide is cleaved by a signal peptidase (LepB) located on the periplasmic side of the cytoplasmic membrane (61). The mature FbpA protein is a 309-amino-acid, 33.6 kDa globular protein with an isoelectric point (pI) of 9.35, making the protein cationic at physiological pH. FbpA has been referred to as a "bacterial transferrin" due to the possession of an iron-binding site that is almost identical to that found in human serum transferrin. The FbpA protein contributes four ligands to coordinate a single ferric-iron ion with high affinity: tyrosinate oxygen ligands from Tyr195 and Tyr196, an imidazole nitrogen ligand from His9, and a carboxylate ligand from Glu57. Two additional oxygen ligands are provided by a phosphate synergistic anion and water to complete almost perfect octahedral coordination of the ferric ion (**Figure 2.12**). Upon iron binding there is a rotational conformational movement around the hinge region. **Figure 2.13** shows the binding sites of the *apo* and *holo* forms of FbpA. It can be observed that, although the *apo* form of the protein does not have iron bound (by definition), it does have a phosphate ion associated with the two tyrosine residues in the binding site. This "pre-prepared" binding site could possibly act to accept an incoming iron ion, allowing the other protein ligands (H9 and E57) to swing into the binding site, thus

completing coordination of the ion. Upon iron binding a ligand-metal charge transfer (LMCT) band is observed at 481 nm by UV-visible spectroscopy, although this can vary depending on the iron-binding environment (59). No such LMCT is observed in the *apo* form of the protein. Similarly, the binding site of transferrin contains two tyrosines and a histidine residue coordinated to the iron, however, the fourth coordinating protein ligand is an aspartate residue instead of glutamate. There is also a single bidentate carbonate synergistic anion in transferrin making up the two remaining coordinating oxygen ligands (**Figure 2.12**). Although the sites are similar, the residues involved in binding come from different parts of the polypeptide chain, suggesting that FbpA and transferrin are descended from a common iron-binding ancestor.

A.

```
  1  MKTSIRYALL AAALTAATPA LADITVYNGQ HKEAAQAVAD AFTRATGIKV
 51  KLNSAKGDQL AGQIKEEGSR SPADVFYSEQ IPALATLSAA NLLEPLPAST
101  INETRGKGVP VAAKKDWVAL SGRSRVVVYD TRKLSEKDLE KSVLNYATPK
151  WKNRIGYVPT SGAFLEQIVA IVKLKGEAAA LKWLKGLKEY GKPYAKNSVA
201  LQAVENGEID AALINNYYWH AFAREKGVQN VHTRLNFVRH RDPGALVTYS
251  GAAVLKSSQN KDEAKKFVAF LAGKEGQRAL TAVRAEYPLN PHVVSTFNLE
301  PIAKLEAPQV SATTVSEKEH ATRLLEQAGM K
```

B.

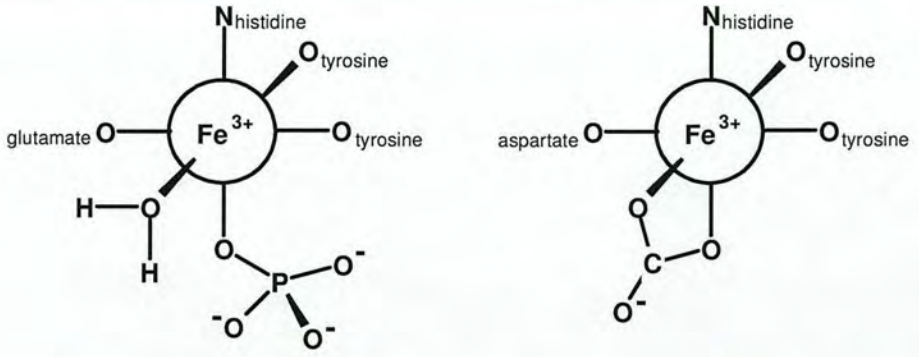

C.

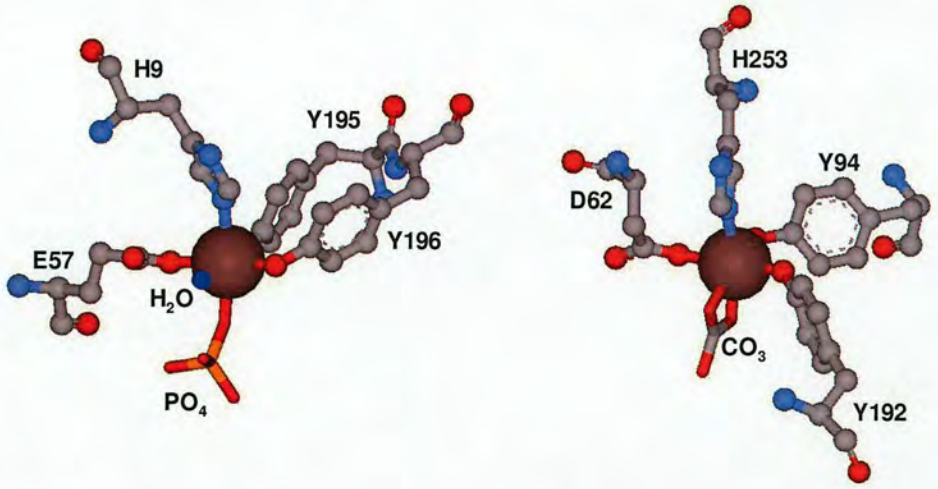

Figure 2.12. A, Amino acid sequence of FbpA. The signal peptide shown in red, mature protein sequence shown in black, iron-binding residues shown in blue. Note that FbpA contains no cysteine residues **B, Diagram showing arrangement of residues involved in iron binding in FbpA (left) and transferrin (right).** Note the similarity between the arrangements of binding residues. **C, Modelled iron-binding sites of FbpA (PDB: 1D9Y) and the N-lobe of (porcine) transferrin (PDB: 1H76) showing iron-binding residues.** Note that, although the residues are identical or similar, they arise from different parts of the polypeptide chain. Iron is shown in brown.

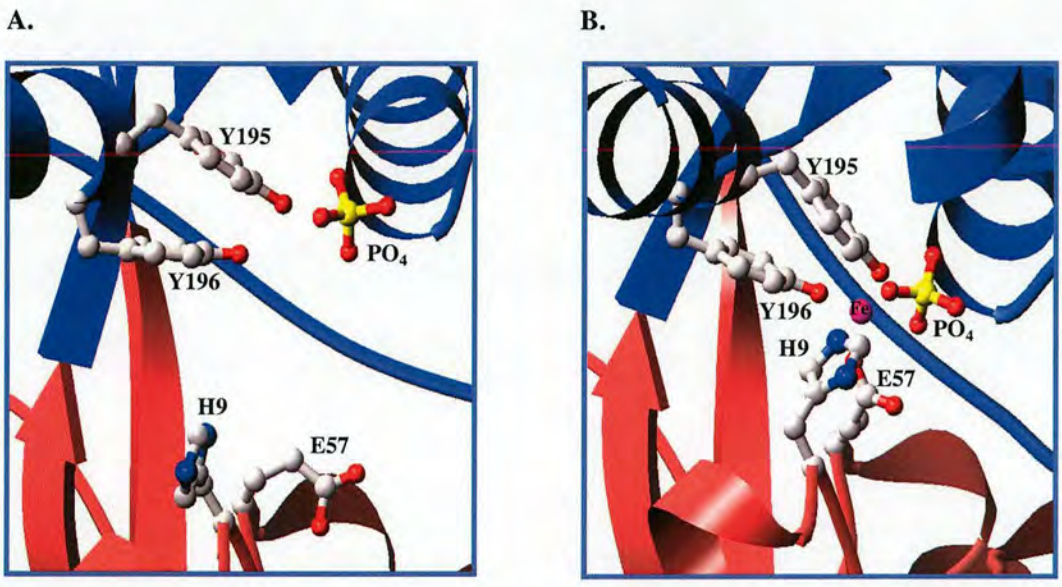

Figure 2.13. Structure of the *apo*-Fbp (A) and *holo*-FbpA (B) binding sites with protein ligands labelled (62). There is ~14° rotation around the hinge region between the two conformations. A phosphate ion is bound in the binding site of the *apo* form of the protein and is proposed to "prime" the site for iron binding. Upon iron binding the other two protein ligands swing into the binding site, completing pseudo-octohedral coordination of the iron ion. The exact mechanism of iron binding and release is still not fully understood.

Like transferrin, the promiscuity and flexibility of the metal-binding site of FbpA has been investigated by several researchers, and has shown that, although *in vivo* the protein will preferentially bind a single ferric-ion with high affinity (10^{18} M^{-1}), *in vitro* the protein can be "re-loaded" with not only clusters of iron, but also with other metal ions and clusters, as well as iron-complexing ligands. Crystal structures of oxo-Fe_3, oxo-Hf_3 & Hf_5 clusters, oxo-Zr_3 (**Figure 2.14**), Ti, and a Fe-NTA (nitriloacetate) complex bound to FbpA have been published (22,28-30,63). There have also been structures determined for FbpA and its homologues in different conformations, such as the *apo*-open form, and the *holo*-open and closed forms (26,29). This is also the case for FbpA homologues from other bacteria, in which other synergistic anions have been crystallised in the binding site.

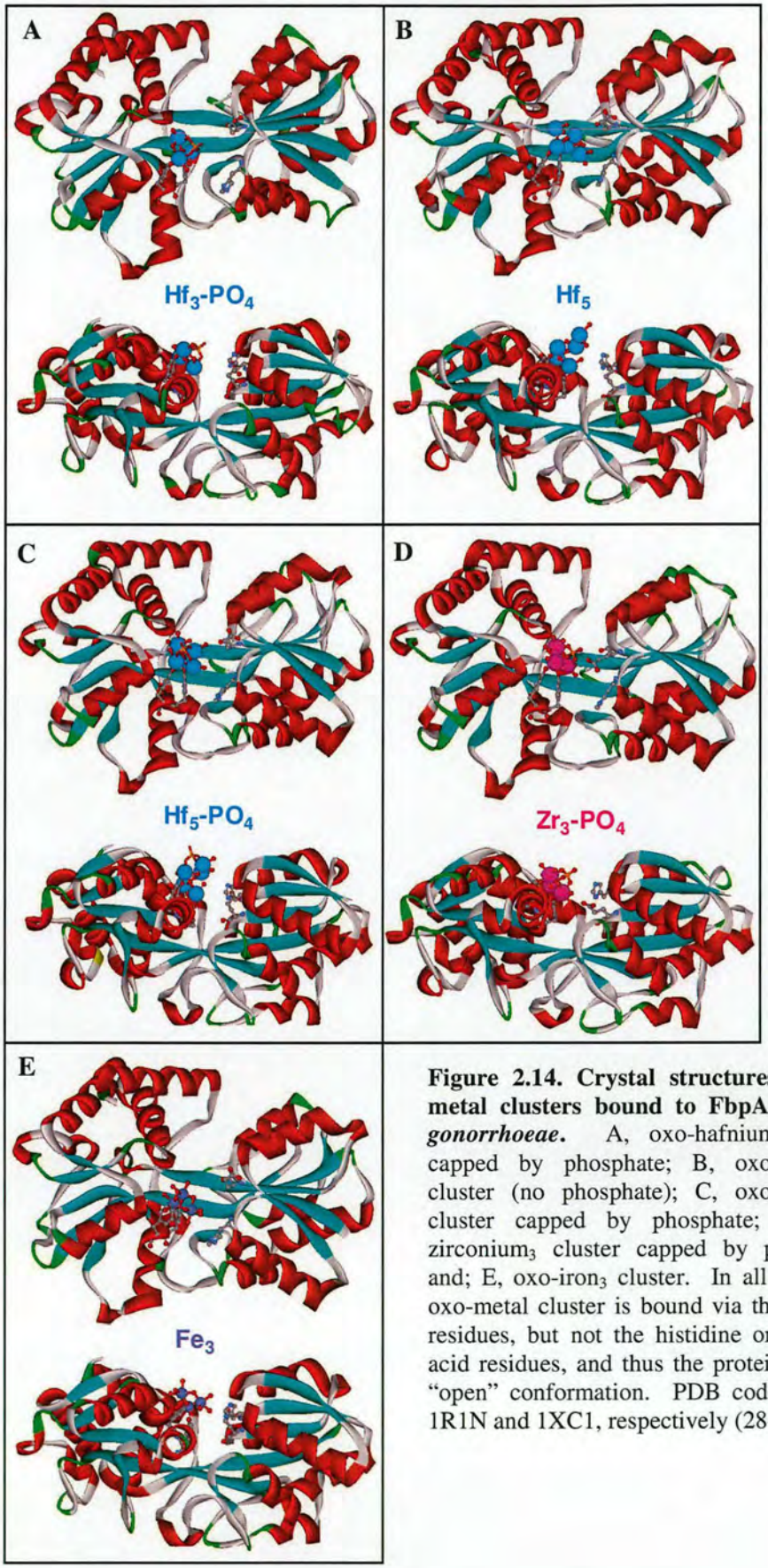

Figure 2.14. Crystal structures of oxo-metal clusters bound to FbpA from *N. gonorrhoeae*. A, oxo-hafnium$_3$ cluster capped by phosphate; B, oxo-hafnium$_5$ cluster (no phosphate); C, oxo-hafnium$_5$ cluster capped by phosphate; D, oxo-zirconium$_3$ cluster capped by phosphate, and; E, oxo-iron$_3$ cluster. In all cases the oxo-metal cluster is bound via the tyrosine residues, but not the histidine or glutamic acid residues, and thus the protein is in an "open" conformation. PDB codes: 1O7T, 1R1N and 1XC1, respectively (28-30).

The finding that FbpA can bind metal clusters suggests another mechanism for iron uptake: FbpA may be able to interact directly with the extracellular environment; a suggestion has been supported by work that has shown that anti-FbpA antibodies bind to the surface of whole cells expressing FbpA from *N. menigitidis* and the canine pathogen *Ehrlichia canis* (33,34). However, bioinformatic analysis of the amino acid sequence of FbpA yields a soluble protein that contains no predicted transmembrane-spanning domains. As such, this, and the lack of experimental evidence, means that this proposed mechanism of iron acquistion remains unproven.

Holo-FbpA is proposed to complex with the TMD component of the ABC transporter in the cytoplasmic membrane to facilitate translocation of the iron across this membrane. How these proteins associate and which residues are involved in docking is unknown, and little is known about how and in what form the iron is removed from FbpA.

2.2.3 Ferric Binding Protein B: FbpB

The *FbpB* gene (1527 bp) encodes the TMD that is proposed to form a dimer in the cytoplasmic membrane. The gene was first described and sequenced in 1996 as an extension of the original work performed on FbpA (46,47,64). The mature protein is predicted to be a 509-amino-acid long 56.3 kDa integral membrane protein that is proposed to form a homodimer in the functional ABC transporter complex (**Appendix 1**). The only previously published work on this protein was in one of the original FbpA papers. In that report the authors suggested that FbpB should contain

11 transmembrane spanning regions, meaning that the active permease would be composed of 22 transmembrane-spanning helices (46). This analysis was performed by sequence alignment with HitB and SfuB permease proteins from the homologous iron transporters from *Haemophilus influenzae* and *Serratia marcescens* (respectively), and revealed significant homology between the three proteins (64.4% and 34.9% identity, and 77.5% and 58.2% similarity, respectively). These researchers also identified the consensus permease motif EAA---G---------I-LP in these three proteins predicted to be located on cytoplasmic loops that interact with the NBD component of the transporters. Similar motifs have also been identified in other well-characterised TMD of ABC transporters that transport different ligands (46). These researchers also found that the protein was composed of 62% of hydrophobic residues, indicative of membrane proteins, and suggests that the protein would be insoluble in aqueous buffers (46).

2.2.4 Ferric Binding Protein C: FbpC

The *FbpC* gene (1056 bp) encodes the NBD. The gene was first described and sequenced in 1996 as an extension of the work performed on FbpA (46,47,64). The mature protein is predicted to be a 352-amino-acid 37.9 kDa membrane associated protein that would form a homodimer in the functional ABC transporter complex (**Appendix 1**). Previous investigations of this protein showed that FbpC can bind a non-hydrolysable radioactive ATP analogue and could hydrolyse ATP (65). Mutagenesis studies also revealed that the ATP-hydrolysing activity of the enzyme could be reduced 10-fold by mutation of the catalytic base in the Walker B motif (E164D), certainly suggesting that FbpC is a member of the ABC ATPase

family (65). However, the work did not specifically identify the protein by peptide mass fingerprinting, and no accurate mass was determined for the protein by mass spectrometry. Previous bioinformatic analysis published as part of the original FbpABC operon (from *N. gonorrhoeae* F62) work revealed that FbpC contained the characteristic Walker A and B motifs, but did not identify the other conserved motifs found in ABC ATPases (46). Sequence alignment with the HitC and SfuC NBD proteins from the homologous iron transporters from *Haemophilus influenzae* and *Serratia marcescens* (respectively) revealed significant homology between the three proteins (51% and 40% identity, and 68% and 58% similarity, respectively). These researchers also demonstrated that the protein was composed of 50.5% hydrophobic residues, suggesting that the protein may be relatively insoluble in aqueous buffers (46).

2.3 Aims

The aims of this thesis are as follows.

1. To further understanding of the complex transportation mechanisms of the FbpABC operon by cloning genomic DNA from a clinical isolate of *Neisseria gonorrhoeae*.

2. To overexpress the genes in *E. coli* and purify and characterise these proteins.

3. To mutate FbpA to allow attachment, via a linker molecule, to a sensor chip (and other solid phases) to facilitate investigation of the association of the protein complex.

4. To crystallise FbpC and the FbpBC complex in order to allow X-ray structure determination.

This study constitutes the first expression and purification of the transmembrane domain (FbpB) of this ABC transporter, and the first exploration of the crystal structure of FbpC. It is also the first investigation of the intact FbpABC complex *in vitro*.

2.4 Chapter 2 References

1. Locher, K. P., Rees, B., Koebnik, R., Mitschler, A., Moulinier, L., Rosenbusch, J. P., and Moras, D. (1998) *Cell* **95**, 771-778
2. Higgins, C. F., and Linton, K. J. (2004) *Nat. Struct. Mol. Biol.* **11**, 918-926
3. Higgins, C. F., and Linton, K. J. (2001) *Science* **293**, 1782-1784
4. Diederichs, K., Diez, J., Greller, G., Muller, C., Breed, J., Schnell, C., Vonrhein, C., Boos, W., and Welte, W. (2000) *Embo. J.* **19**, 5951-5961
5. Wolters, J. C., Abele, R., and Tampe, R. (2005) *J. Biol. Chem.* **280**, 23631-23636
6. Higgins, C. F., Callaghan, R., Linton, K. J., Rosenberg, M. F., and Ford, R. C. (1997) *Semin. Cancer Biol.* **8**, 135-142
7. Dawson, R. J., and Locher, K. P. (2006) *Nature* **443**, 180-185
8. Reyes, C. L., and Chang, G. (2005) *Science* **308**, 1028-1031
9. Andrews, S. C., Robinson, A. K., and Rodriguez-Quinones, F. (2003) *FEMS Microbiol. Rev.* **27**, 215-237
10. Patzlaff, J. S., van der Heide, T., and Poolman, B. (2003) *J. Biol. Chem.* **278**, 29546-29551
11. Horn, C., Jenewein, S., Sohn-Bosser, L., Bremer, E., and Schmitt, L. (2005) *J. Mol. Microbiol. Biotechnol.* **10**, 76-91
12. Schuurman-Wolters, G. K., and Poolman, B. (2005) *J. Biol. Chem.* **280**, 23785-23790
13. Lubelski, J., van Merkerk, R., Konings, W. N., and Driessen, A. J. (2006) *Biochemistry* **45**, 648-656

14. Pinkett, H. W., Lee, A. T., Lum, P., Locher, K. P., and Rees, D. C. (2007) *Science* **315**, 373-377

15. Ames, G. F. (1986) *Annu. Rev. Biochem.* **55**, 397-425

16. Dwyer, M. A., and Hellinga, H. W. (2004) *Curr. Opin. Struct. Biol.* **14**, 495-504

17. Quiocho, F. A., and Ledvina, P. S. (1996) *Mol. Microbiol.* **20**, 17-25

18. Clarke, T. E., Tari, L. W., and Vogel, H. J. (2001) *Curr. Top. Med. Chem.* **1**, 7-30

19. Tom-Yew, S. A., Cui, D. T., Bekker, E. G., and Murphy, M. E. (2005) *J. Biol. Chem.* **280**, 9283-9290

20. Shouldice, S. R., McRee, D. E., Dougan, D. R., Tari, L. W., and Schryvers, A. B. (2005) *J. Biol. Chem.* **280**, 5820-5827

21. Bruns, C. M., Nowalk, A. J., Arvai, A. S., McTigue, M. A., Vaughan, K. G., Mietzner, T. A., and McRee, D. E. (1997) *Nat. Struct. Biol.* **4**, 919-924

22. Shouldice, S. R., Skene, R. J., Dougan, D. R., McRee, D. E., Tari, L. W., and Schryvers, A. B. (2003) *Biochemistry* **42**, 11908-11914

23. Shouldice, S. R., Dougan, D. R., Skene, R. J., Tari, L. W., McRee, D. E., Yu, R. H., and Schryvers, A. B. (2003) *J. Biol. Chem.* **278**, 11513-11519

24. Bruns, C. M., Anderson, D. S., Vaughan, K. G., Williams, P. A., Nowalk, A. J., McRee, D. E., and Mietzner, T. A. (2001) *Biochemistry* **40**, 15631-15637

25. Shouldice, S. R., Dougan, D. R., Williams, P. A., Skene, R. J., Snell, G., Scheibe, D., Kirby, S., Hosfield, D. J., McRee, D. E., Schryvers, A. B., and Tari, L. W. (2003) *J. Biol. Chem.* **278**, 41093-41098

26. Shouldice, S. R., Skene, R. J., Dougan, D. R., Snell, G., McRee, D. E., Schryvers, A. B., and Tari, L. W. (2004) *J. Bacteriol.* **186**, 3903-3910

27. McRee, D. E., Bruns, C. M., Williams, P. A., Mietzner, T. A., and Nunn, R. (Unpublished)

28. Alexeev, D., Zhu, H., Guo, M., Zhong, W., Hunter, D. J., Yang, W., Campopiano, D. J., and Sadler, P. J. (2003) *Nat. Struct. Biol.* **10**, 297-302

29. Zhu, H., Alexeev, D., Hunter, D. J., Campopiano, D. J., and Sadler, P. J. (2003) *Biochem. J.* **376**, 35-41

30. Zhong, W., Alexeev, D., Harvey, I., Guo, M., Hunter, D. J., Zhu, H., Campopiano, D. J., and Sadler, P. J. (2004) *Angew. Chem. Int. Ed. Engl.* **43**, 5914-5918

31. Zhu, H. (2003) PhD thesis, University of Edinburgh Chemistry Dept, Edinburgh

32. Butler, A. (2003) *Nat. Struct. Biol.* **10**, 240-241

33. Doyle, C. K., Zhang, X., Popov, V. L., and McBride, J. W. (2005) *Infect. Immun.* **73**, 62-69

34. Ferreiros, C., Criado, M. T., and Gomez, J. A. (1999) *Comp. Biochem. Physiol. B. Biochem. Mol. Biol.* **123**, 1-7

35. Chang, C., Mooser, A., Pluckthun, A., and Wlodawer, A. (2001) *J. Biol. Chem.* **276**, 27535-27540

36. Koster, W. (2001) *Res. Microbiol.* **152**, 291-301

37. Borths, E. L., Locher, K. P., Lee, A. T., and Rees, D. C. (2002) *Proc. Natl. Acad. Sci. U S A* **99**, 16642-16647

38. Nikaido, K., Liu, P. Q., and Ames, G. F. (1997) *J. Biol. Chem.* **272**, 27745-27752

39. Kreimer, D. I., Chai, K. P., and Ferro-Luzzi Ames, G. (2000) *Biochemistry* **39**, 14183-14195

40. Linton, K. J., and Higgins, C. F. (2006) *Pflugers Arch.*

41. Hung, L. W., Wang, I. X., Nikaido, K., Liu, P. Q., Ames, G. F., and Kim, S. H. (1998) *Nature* **396**, 703-707

42. Chen, J., Lu, G., Lin, J., Davidson, A. L., and Quiocho, F. A. (2003) *Mol. Cell* **12**, 651-661

43. Borths, E. L., Poolman, B., Hvorup, R. N., Locher, K. P., and Rees, D. C. (2005) *Biochemistry* **44**, 16301-16309

44. Liu, C. E., and Ames, G. F. (1997) *J. Biol. Chem.* **272**, 859-866

45. Sharma, S., Davis, J. A., Ayvaz, T., Traxler, B., and Davidson, A. L. (2005) *J. Bacteriol.* **187**, 2908-2911

46. Adhikari, P., Berish, S. A., Nowalk, A. J., Veraldi, K. L., Morse, S. A., and Mietzner, T. A. (1996) *J. Bacteriol.* **178**, 2145-2149

47. Khun, H. H., Deved, V., Wong, H., and Lee, B. C. (2000) *Infect. Immun.* **68**, 7166-7171

48. Desai, P. J., Angerer, A., and Genco, C. A. (1996) *J. Bacteriol.* **178**, 5020-5023

49. Sebastian, S., Agarwal, S., Murphy, J. R., and Genco, C. A. (2002) *J. Bacteriol.* **184**, 3965-3974

50. Cornelissen, C. N., Kelley, M., Hobbs, M. M., Anderson, J. E., Cannon, J. G., Cohen, M. S., and Sparling, P. F. (1998) *Mol. Microbiol.* **27**, 611-616

51. Chen, C. Y., Berish, S. A., Morse, S. A., and Mietzner, T. A. (1993) *Mol. Microbiol.* **10**, 311-318

52. http://www.vetmed.iastate.edu/faculty_staff/users/phillips/Micro402/03-Gene%20expression/Rhoindependent.jpg.

53. Berish, S. A., Kapczunski, D., and Morse, S. A. (1990) *Nucleic Acids Res.* **18**, 4596

54. Berish, S. A., Chen, C.-Y., Mietzner, T. A., and Morse, S. A. (1991) *Mol. Microbiol.* **6**, 2607-2615

55. Boukhalfa, H., Anderson, D. S., Mietzner, T. A., and Crumbliss, A. L. (2003) *J. Biol. Inorg. Chem.* **8**, 881-892

56. Dhungana, S., Anderson, D. S., Mietzner, T. A., and Crumbliss, A. L. (2005) *Biochemistry* **44**, 9606-9618

57. Dhungana, S., Taboy, C. H., Anderson, D. S., Vaughan, K. G., Aisen, P., Mietzner, T. A., and Crumbliss, A. L. (2003) *Proc. Natl. Acad. Sci. U S A* **100**, 3659-3664

58. Gabricevic, M., Anderson, D. S., Mietzner, T. A., and Crumbliss, A. L. (2004) *Biochemistry* **43**, 5811-5819

59. Guo, M., Harvey, I., Yang, W., Coghill, L., Campopiano, D. J., Parkinson, J. A., MacGillivray, R. T., Harris, W. R., and Sadler, P. J. (2003) *J. Biol. Chem.* **278**, 2490-2502

60. Roulhac, P. L., Powell, K. D., Dhungana, S., Weaver, K. D., Mietzner, T. A., Crumbliss, A. L., and Fitzgerald, M. C. (2004) *Biochemistry* **43**, 15767-15774

61. Lam, S. L., Kirby, S., and Schryvers, A. B. (2003) *Microbiology* **149**, 3155-3164

62. Alexeev, D. (Unpublished)

63. Guo, M., Harvey, I., Campopiano, D. J., and Sadler, P. J. (2006) *Angew. Chem. Int. Ed. Engl.* **45**, 2758-2761

64. Khun, H. H., Kirby, S. D., and Lee, B. C. (1998) *Infect. Immun.* **66**, 2330-2336

65. Lau, G. H., MacGillivray, R. T., and Murphy, M. E. (2004) *J. Bacteriol.* **186**, 3266-3269

Chapter 3: Materials & Methods

3.1 General Materials

3.1.1 General Reagents

Chemicals and solvents were of the appropriate quality and were purchased from GE Healthcare, Promega, Sigma, Pierce, BioRad, Gibco BRL, Vivascience, New England Biolabs, Waters Micromass, Anatrace or Invitrogen unless otherwise stated.

Plasmid pTrc99A/FBP/NG (**Figure 3.1**) was a kind gift from Prof. Ross MacGillivray (University of British Columbia, Vancouver, Canada) and was renamed pTrc99A/FbpA/Ng to avoid confusion with other plasmids constructed for this study.

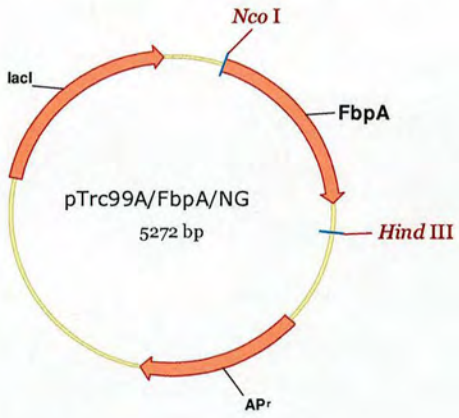

Figure 3.1. Plasmid pTrc99A/FbpA/Ng map.

Neisseria gonorrhoeae genomic DNA was a kind gift from Dr Helen Palmer (Scottish *Neisseria Gonorrhoeae* Research Laboratory, Edinburgh Royal Infirmary) and was purified from a clinical isolate of the bacteria by the author.

3.1.2 Solutions and Media

Buffers – All buffers were prepared fresh, as required, and were 0.2 μm filtered before use. Buffer recipes are described in the text where appropriate.

Sterilisation of media – All media was autoclaved at 121 °C for 15 min at 15 psi prior to use.

Agar plates – bacto-agar (15 g/L) was added to the specified media to prepare agar plates.

S-Gal/LB/amp plates – a pack of S-Gal/LB Agar Blend (Sigma) was dissolved in deionised water (1000 mL) and autoclaved. Ampicillin (100 μg/mL) was added to the solution to prepare plates.

Luria Bertani (LB) – tryptone (10 g/L), yeast extract (5 g/L), NaCl (10 g/L); pH adjusted to 7.5 with NaOH.

2xYT – tryptone (16 g/L), yeast extract (10 g/L), NaCl (5 g/L); pH adjusted to 7.5 with NaOH.

SOC – tryptone (20 g/L), yeast extract (5 g/L), NaCl (0.5 g/L), $MgSO_4$ (5 g/L), glucose (3.2 g/L); pH adjusted to 7.5 with NaOH.

Terrific Broth – tryptone (12 g/L), yeast extract (24 g/L), glycerol (4 mL/L), NaH_2PO_4 (2.31 g/L) and Na_2HPO_4 (12.54 g/L).

5x M9 Salts – Na_2HPO_4 (30 g/L), KH_2PO_4 (15 g/L), NaCl (2.5 g/L) and $(NH_4)Cl$ (5 g/L).

50x M – Na_2HPO_4 (177.5 g/L), KH_2PO_4 (170 g/L), NH_4Cl (134 g/L) and $NaSO_4$ (35.5 g/L)

250x Mg - 0.2 metals – 800 µL sterile water, 1000 µL sodium citrate (1 M), 2000 µL $MgSO_4$ (1 M), 200 µL 1000x trace metals (see below) (1).

1000x trace metals – 50 mM $FeCl_3$, 50 mM $CaCl_2$, 25 mM $MnCl_2$, 25 mM $ZnSO_4$, 2 mM $CoCl_2$, 5 mM $CuSO_4$, 2 mM $NiCl_2$, 2 mM Na_2MoO_4, 2 mM Na_2SeO_3, and 2 mM H_3BO_3, all in 50 mM HCl (*1*).

MDG media – 50x M, 40% glucose, 25% aspartic acid, 250x Mg-0.2 metals (1).

SeMet labelling media – 5x M9 salts (200 mL), 40% glucose (10 mL), 1 M $MgSO_4$ (1 mL), 1000x trace metals (200 µL), 0.1 M $FeCl_3$ in 0.1 M HCl (250 µL), biotin (10 mg/L), thiamine (10 mg/L), 100 µM vitamin B_{12} (1 mL), L-lysine (100 mg/L), L-phenylalanine (100 mg/L), L-threonine (100 mg/L), L-valine (50 mg/L), L-leucine (50 mg/L), L-isoleucine (50 mg/L) and L-selenomethionine (50 mg/L). Sterile water was added to the required volume.

3.2 Molecular Biology: DNA Manipulation

3.2.1 Bacterial Cell Lines

Table 3.1. Bacterial cell lines used in this study.

Strain	Genotype	Applications
Top 10™ (Invitrogen)	F'mcrA D(mrr-hsdRMS-mcrBC) Φ80lacZΔM15 ΔlacX74 deoR recA1 araD139 Δ(ara-leu)7697 gal/U gal/K rpsL endA1 nupG	Used For transforming DNA ligations. Expression host
BL21(DE3) (Novagen)	F^- omp $Thsds_b$ (r_B^- m_B^-) gal dcm (DE3)	General purpose expression host.

3.2.2 Oligonucleotide Primers

The following oligonucleotide primers were using in this study (**Table 3.2**). Restriction sites are highlighted.

Table 3.2. Oligonucleotide sequences used in this study. Mutant codons and restriction sites are shown in bold italics.

Name	Sequence (5'-3')
FbpA R48C For	AAA GAA GAA GGC AGC ***TGC*** AGC CCC GCC
FbpA R48C Rev	GGC GGG GCT ***GCA*** GCT GCC TTC TTC TTT
FbpA R83C For	ATC AAC GAA ACA ***TGC*** GGC AAA GGC GTG
FbpA R83C Rev	CAC GCC TTT GCC ***GCA*** TGT TTC GTT GAT
FbpA K111C For	GTT TAC GAC ACC CGC ***TGC*** CTG TCT GAA AAA
FbpA K111C Rev	TTT TTC AGA CAG ***GCA*** GCG GGT GTC GTA AAC
FbpA V272C For	AAT CCG CAC GTG ***TGC*** TCC ACC TTC AAT TTG
FbpA V272C Rev	CAA ATT GAA GGT GGA ***GCA*** CAC GTG CGG ATT
FbpB BamHI For	ACT GTC CGC CCG TT***G GAT CC***G ATG AAA AAC
FbpB HindIII Rev	GGC GGT CAT AGC G***AA GCT T***CC TCA AGC TGT
FbpC NdeI For	ACA GCT TGA GGA AGC ACC ***CAT ATG*** ACC GCC
FbpC Stop XhoI Rev	CTT GTG GAT GCT GC***C TCG AG***T CAG AGG GTA
FbpB NcoI For	CCC GTT TTG C***CC ATG GG***A AAC ACT ATG TCT
FbpB XhoI Rev	TTC CTC AAG ***CTC GAG*** TTT GAA GGC GTA TTT
FbpA NcoI For	GAG GAA ATC G***CC ATG GG***A ACA TCT ATC CGA
FbpC NcoI For	AGC ACC G***CC ATG GG***G GCC GCC CTG CAC ATC
FbpC XhoI Rev	***CTC GAG*** GGT ATT TCC GGG GAA GAA CAG GGC

3.2.3 Storage of Bacterial Stocks

Colonies of bacteria were stored on inverted agar plates at 4 °C for up to 28 days. Overnight cultures grown in non-inducing MDG media were stored at 4 °C for up to six weeks. LB or 2xYT medium containing the appropriate antibiotics was used for the short-term storage of *E. coli*.

3.2.4 Transformation of *E. coli* Competent Cells

Competent cells were transformed according to the manufacturers instructions. DNA (up to 40 ng) was added to an aliquot of competent cells and gently mixed. This was left on ice for 5 or 30 minutes before the cells were heat shocked (42 °C, 30 s). The cells were then grown in 80-250 µL SOC medium at 37 °C for 1 h. Finally, the cells were spread to dryness on selective agar plates and incubated at 37 °C overnight.

3.2.5 Preparation of Plasmid DNA

Plasmid DNA was prepared using QIAprep® Spin Miniprep Kit (Qiagen) following the manufacturers instructions.

3.2.6 Digestion of DNA with Restriction Endonucleases

The required amount of DNA (0.5-1 µg) was treated with the appropriate amount of endonuclease and buffer and incubated for at least 2 hours at 37 °C. Blue/orange loading dye (Promega) was added and the sample was subjected to electrophoresis on agarose. The gels were viewed and photographed under UV-light.

3.2.7 Electrophoresis of DNA

The required amount of agarose was added to 1x TAE buffer (typically 1.2 g/100 mL) and heated at 100 °C until it dissolved. The solution was allowed to cool to 55 °C and ethidium bromide was added to a final concentration of 0.5 μg/mL. The gel was then poured into the casting mould and allowed to set at room temperature. DNA was loaded and electrophoresed using a potential difference of 100 V for an adequate time to achieve separation of visible bands.

3.2.8 Purification of DNA

DNA was purified from agarose using QIAquick® Gel Extraction Kit (Qiagen) following the manufacturers instructions.

3.2.9 Amplification of DNA by PCR

Polymerase chain reactions (PCRs) and sequencing reactions were performed using a Perkin Elmer 480 thermal cycler. A typical reaction contained: 2 Ready-to-Go PCR™ beads (GE Healthcare), DNA template (1 μL), primer 1 (forward) (5 μL 10 μM), primer 2 (reverse) (5 μL, 10 μM), and distilled water (39 μL). Reactions were overlayed with oil and cycled 30 times at 95 °C for 1 min, 54 °C for 1 min and 72 °C for 2 min. Heating at 72 °C for 10 min terminated the reaction. The PCR product was then subjected to agarose gel electrophoresis and the required band excised and the DNA purified as described as above.

3.2.10 Site-Directed Mutagenesis PCR

The muatations were introduced by using the Quikchange Site-Directed Mutagenesis Kit (Stratagene). This is a cloneless system that uses the parent plasmid as a template and forward and reverse complementary primers designed to encode for the desired mutation.

Reactions were performed as follows: to a 0.5 ml PCR tube was added 5 μL (parent) plasmid DNA, 5 μL 10x reaction buffer, 1 μL forward mutagenic primer, 1 μL reverse mutagenic primer, 1 μL dNTPs, 36 μL water and 1 μL *PfuTurbo* DNA polymerase. This was mixed and overlaid with oil and cycled 17 times at 95 °C for 30 s, 55 °C for 30 s and 68 °C for 1 min/kbp. After the reaction was complete, 1 μL of *Dpn*I (restriction endonuclease) was added and the mixture and incubated for 1 h at 37 °C. *Dpn*I digested PCR product (10 μL) was then subjected to agarose gel electrophoresis to check the efficiency of the reaction, and 2 μL of the PCR product was then transformed into TOP10 *E. coli* as described above.

3.2.11 Cloning of PCR Products

PCR products were cloned into the pGEM T-Easy cloning vector (Promega) using the manufacturer's guidelines.

3.2.12 DNA Sequencing

Automated DNA sequencing was performed on an ABI prism 377 DNA sequencer using the Sanger dideoxy chain termination method. Each sequencing reaction typically contained: DNA template (~5 pmol, 2 μL), primer (10 μM, 1 μL), distilled

water (13 µL) and Big Dye 4.1 (4 µL; PE Biosystems, UK). The reaction performed on an Eppendorf Mastercycler Personal hot-lid PCR cycler and cycled 30 times at 96 °C for 30 sec, 45 °C for 15 sec and 60 °C for 4 min. Sequence data were analysed using Contig Express within the Vector NTI Advance™ v9 software package.

3.2.13 Cloning into Plasmid Vectors

The DNA fragment cut with suitable restriction enzymes (13 µL), the host vector cut with suitable restriction enzymes (4 µL), 10x T4 DNA ligase buffer (2 µL), and T4 DNA ligase (1 000 000 U, 2 µL) were gently mixed and incubated overnight at 16 °C. Reaction mixture (2 µL) was used to transform suitable competent cells.

3.3 Molecular Biology: Protein Expression & Purification

3.3.1 Polyacrylamide Gel Electrophoresis (PAGE)

SDS-PAGE was used to analyse proteins on the basis of their molecular mass. The technique used was the discontinuous buffer system of Laemmeli. Alternatively, proteins were analysed on precast 12% Bis-Tris Nu-PAGE gels (Invitrogen) according to manufacturers instructions.

Gels were visualised using Coomassie blue, GelCode Blue Stain reagent or Imperial stain (Pierce) in accordance with the manufacturers instructions.

3.3.2 Western Blot Analysis

Western Bolt analysis was performed to positively identify very small amounts of expressed tagged protein.

SDS-PAGE was performed and the gel fixed in transfer buffer (25 mM Tris buffer pH 8.3, 150 mM glycine and 10% methanol) for at least 15 min. The proteins were then transferred onto a nitrocellulose membrane (GE Healthcare) for 30 min at a potential difference of 15 V using a BioRad TransBlot according to the manufacturers instructions. The membrane was blocked for 1 hour at room temperature with PBS-0.05% Tween containing 5% non-fat dried milk (Marvel) followed by at least three washes (10 min each) with PBS-0.05% Tween. The membrane was hybridised for 1-16 hours with the relevant primary HRP-conjugated antibody dilution made up in PBS-0.05% Tween containing 5% non-fat dried milk, followed by at least three washes (10 min each) with PBS-0.05% Tween. The membrane was drained of excess PBS-tween and developed using ECL Plus Western Blotting Detection System (GE Healthcare) according to the manufacturers instructions. Radiographic films (BioMax XAR film, Kodak) were exposed in a dark room for 1 s-10 min and then developed using on a Compact X4 Automatic X-ray film processor (Xograph). The antibodies used for Western blot analysis were anti-C-terminal-His_6 (Invitrogen) or anti-his_6 (Sigma).

3.3.3 Large-Scale Expression of *N. gonorrhoeae* FbpA and Mutants in *E. coli*

TOP10 cells (Invitrogen) transformed with pTrc99A/FbpA/Ng were used to aseptically inoculate up to 500 ml of 2xYT medium containing ampicillin. This was then incubated for 16 h at 37 °C and 250 rpm. The cells were harvested by centrifugation at 4 000 x *g* for 10 min at 4 °C. The FbpA expressing pellet (red-

brown in colour) was collected and frozen at -20 °C before extraction and purification.

3.3.4 Purification of *N. gonorrhoeae* FbpA and Mutants

FbpA was purified by a slight modification of methods described previously (2). The pellet from the large-scale preparation was defrosted at room temperature and re-suspended (5 mL/g pellet) in 50 mM HEPES (pH 8.0) and 1% CTAB (cetyltrimethylammonium bromide, Fluka). This mixture was then stirred gently for 3-6 h at 37 °C. The white insoluble material was removed by centrifugation at 12 000 x *g* for 25 min at 4 °C. The supernatant (red) was 0.45 µm-filtered and dialysed overnight into 10 mM HEPES buffer (pH 8.0) to precipitate excess CTAB and re-filtered (0.45 µm). A 26/10 SP Sepharose Fast Flow (55 mL, GE Healthcare) column was washed according to the manufacturers instructions and equilibrated with 10 mM HEPES buffer (pH 8.0). The CTAB extract was loaded onto the column by FPLC (ÄKTA*Basic100*, GE Healthcare) and eluted with a high salt gradient (0-1 M) using a 10 mM HEPES, 1 M NaCl buffer (pH 8.0). Fractions (variable volumes) showing absorbance at 280 and 481 nm were collected and analysed by SDS-PAGE. FbpA containing fractions were concentrated by ultrafiltration (VivaSpin concentrator, 10 kDa molecular weight cut-off) and then desalted by either PD10 column or dialysis.

FbpA and mutants of the protein were also purified by a novel batch method using Fractogel EMD SO_3^--650(M) chromatography media (Merck). The bacterial pellet of overexpressed FbpA was treated in an identical fashion as described above,

but purification was performed by using 1-5 mL of washed and equilibrated (using the above buffers) with the Fractogel media. Protein was loaded onto the media by incubation at room temperature for 5 min, and the bound protein washed with 30 CV of wash buffer in a batch fashion using a centrifuge (1 min, 500 x *g*) to pellet the media between washes. The media was then washed with 20 CV of wash buffer containing 100 mM NaCl, and then bound protein eluted in an appropriate volume of wash buffer containing 250 mM NaCl.

3.3.4.1 Preparation of *apo*-FbpA

Apo-FbpA was prepared by dialysing the *holo* form of the protein against 50 mM *tri*-sodium citrate (pH 6.0) for 2 hours. The *apo*-FbpA was then dialysed (8 000 M_r cut-off) against 3 x 1 L of 10 mM HEPES buffer (pH 8.0) and then treated with Chelex 100™ resin to remove any trace metals. The protein was stored at -20 °C until required.

3.3.5 Expression of *N. gonorrhoeae* FbpC in *E. coli*

The FbpC construct pET-28a/FbpC/Ng, was used to transform *E. coli* expression strain BL21(DE3) and grown on LB/kanamycin (30 µg/mL) agar plates. Small-scale induction screens (20 mL) were performed at 25 °C using 0.2 mM IPTG overnight to verify the FbpC protein expression (by SDS-PAGE) of the clones.

For large-scale expression, one colony was picked and used to inoculate 200 mL of 2xYT or MDG media containing kanamycin (30 µg/mL) and grown overnight at 37 °C with agitation (250 rpm). The 200 mL overnight culture was used to inoculate 5 L of Terrific broth (TB) and grown to an OD_{600} of 0.8 at 25 °C and

then induced with 0.2 mM IPTG for three hours at 25 °C. Cells were harvested by refrigerated centrifugation at 4 000 x *g* for 10 min immediately after induction. Cell pellets were frozen in liquid nitrogen and stored at -20°C until required.

3.3.6 Expression of SeMet Labelled *N. gonorrhoeae* FbpC in *E. coli*

The FbpC construct pET-28a/FbpC/Ng was transformed into *E. coli* expression strain BL21(DE3) and grown on LB/kanamycin (30 μg/mL) agar plates.

For large-scale expression, one colony was picked and used to inoculate 200 mL of MDG media containing kanamycin (30 μg/mL) and grown overnight at 37 °C with agitation (250 rpm). The 200 mL overnight culture was used to inoculate 5 L of M9 media supplemented with $MgSO_4$, glucose, thiamine, biotin and trace metals and grown to an OD_{600} of 0.7-0.8 at 25 °C. Amino acids were added (K, F, T, I, L, V and selenomethionine) and vitamin B_{12}, and the cells grown for a further 15 min before being induced with 0.2 mM IPTG for three hours at 25 °C. Cells were harvested by refrigerated centrifugation at 4 000 x *g* for 10 mins immediately after induction. Cell pellets were frozen in liquid nitrogen and stored at -20°C until required.

3.3.7 Purification of Wild-Type and SeMet Labelled *N. gonorrhoeae* FbpC

The FbpC expressing pellet was resuspended (5 mL/g wet cell pellet) in 25 mM Tris buffer (pH 8.0) containing ATP (5 mM), EDTA (0.1 mM), 20% glycerol (resuspension buffer (RB)) with 1 protease inhibitor cocktail tablet (EDTA-free), and

10 mg of DNase added, and then homogenised. The resuspended pellet was sonicated for 15 min (30 s on/30 s off) on ice and was then centrifuged at 25 000 x *g* for 30 mins at 4 °C to remove insoluble debris.

Ni-NTA silica (1-5 mL; Promega) was used to purify the extracted FbpC. The resin was first washed with water and then equilibrated with 10 column volumes (CV) of RB containing 20 mM imidazole at 4 °C. The filtered (0.45 μm) sonication supernatant was added to the resin and stirred gently at 4°C for 1-2 hours.

The resin was packed by centrifugation (1 min at 500 x *g*). The flow through fraction was collected and the packed beads washed with 30 CV of 25 mM tris buffer (pH 8.0) containing NaCl (500 mM), imidazole (50 mM), ATP (5 mM), EDTA (0.1 mM) and 20% glycerol (wash buffer (WB)), and the wash fractions collected. Bound protein was eluted with imidazole (250 mM, 5mL fractions) in wash buffer. SDS-PAGE was used to determine fractions containing FbpC, and these fractions were pooled and frozen at -20 °C.

A second round of purification using TALON resin (cobalt-affinity chromatography) was performed if necessary. Fractions containing FbpC were diluted in RB containing no EDTA to a final imidazole concentration of 20 mM (~10-fold dilution), and incubated at 4 °C with washed and equilibrated TALON resin for 1-2 hours with gentle stirring. Bound protein was washed and eluted as described above and the purity of the eluted protein checked by SDS-PAGE.

Purification of SeMet labelled FbpC was identical except that all buffers also contained 0.5-1 mM tris(carboxyethyl)phosphine (TCEP) as a reducing agent to avoid oxidation of incorporated selenomethionine residues.

3.3.8 Co-Expression of *N. gonorrhoeae* FbpBC in *E. coli*

The FbpBC constructs, pETDuet-1/FbpB/FbpC/Ng or pET-28a/FbpBC/Ng, were used to transform *E. coli* expression strain BL21(DE3) and grown on LB/kanamycin (30 μg/mL) agar plates, for the pET-28a construct and LB/ampicillin (100 μg/mL), for the pETDuet-1 construct. Small-scale inductions (20 mL) were performed at 25 °C using 0.2 mM IPTG for 3 hours to verify expression (by SDS-PAGE) of FbpB and FbpC.

For large-scale expression, one colony was picked and used to inoculate 200 mL of 2xYT or MDG media containing kanamycin (30μg/mL) or ampicillin (100 μg/mL), as appropriate, and grown overnight at 37°C with agitation (250 rpm). The 200 mL overnight culture was used to inoculate 6 L of Terrific broth (TB) and grown to an OD_{600} of 0.8 at 25°C and then induced with 0.2 mM IPTG for three hours at 25°C. Pre- and post-induction aliquots were taken to check protein expression level by SDS-PAGE. Cells were harvested by refrigerated centrifugation at 4 000 x *g* for 10 min immediately after induction. Cell pellets were frozen in liquid nitrogen and stored at -20°C until required.

3.3.9 Purification of the *N. gonorrhoeae* FbpBC Complex

The FbpBC expressing pellet was resuspended (5 mL/g wet cell pellet) in 25 mM tris buffer (pH 8.0) containing ATP (5 mM), EDTA (0.1 mM) (resuspension buffer(RB1)) with 5 mM benzamidine, and then homogenised. DNase (10 mg) and lysozyme (5 mg/mL) were added to this and the mixture stirred briskly at 4 °C for 30 mins. This was then sonicated for 15 min (30 s on/30 s off) on ice and then

centrifuged at 25 000 x *g* for 30 min at 4 °C to remove insoluble debris. The opaque supernatant was decanted and ultracentrifuged at 120 000 x *g* for 2 hours at 4 °C. The resulting dense golden pellets were resupended in a minimal amount of 25 mM tris (pH 8.0) and frozen in 1 mL aliquots at -20 °C until required. A BCA assay was performed to determine the total protein concentration in these enriched inner membranes.

Aliquots of enriched inner membranes were solubilised (6 mg/mL total protein, final concentration) in 25 mM tris buffer (pH 8.0) containing 500 mM NaCl, ATP (5 mM), 20% glycerol and 1% n-dodecyl-β-D-maltopyranoside (DDM) at 4 °C for 3 hours with gentle agitation (resolubilisation buffer (RB2)). The extraction mixture was centrifuged for 30 min at 25 000 x *g* and 4 °C to remove any remaining unsolubilised material. TALON metal affinity resin (1-5 mL; Clontech) was washed three times in water and then three times in RB2. The extract supernatant was incubated with the equilibrated TALON resin for 1-2 hour at 4 °C with gentle agitation. The resin was then pelleted by centrifugation (1 min, 500 x *g*). The flow through fraction was collected and the packed beads washed with 30 column volumes of 25 mM tris buffer (pH 8.0) containing NaCl (500 mM), ATP (5 mM), 20 % glycerol, 0.1 % DDM and 20 mM imidazole (wash buffer). Bound protein was eluted with a 250 mM imidazole in wash buffer. Fractions were collected and SDS-PAGE and Western blot analysis performed to check the purity of the eluted proteins.

3.4 Protein Chemistry

3.4.1 Modification of FbpA Cysteine-Containing Mutants

3.4.1.1 Modification with Iodoacetamide

Iodoacetamide (**Figure 3.2**) and iodoacetic acid are widely used to alkylate sulfhydryl groups irreversibly, thus covalently modifying reactive cysteine residues (3). This procedure is used to assess the ability for modification of the free thiol in the protein with a useful prosthetic group.

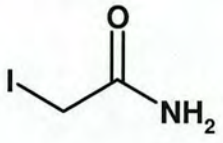

Figure 3.2. Structure of iodoacetamide.

The procedure was performed as follows: the protein was first reduced by addition of TCEP (1 mM final concentration) to 2.5 mL of protein (1 mg/mL) and incubated for 5-10 min at room temperature. Iodoacetamide (20 µL, 1 M made up in 1 M NaOH) was added and the mixture incubated for 30 min in the dark, at room temperature. Unreacted iodoacetamide and excess TCEP was removed by PD10 column chromatography (GE Healthcare) which was used to exchange the modified protein into ammonium acetate buffer (10 mM, pH 8.0) for mass spectrometry (4). LC-MS was performed as described in Section 3.5.2.

Protein modified with iodoacetamide should yield a mass increase of 57 Da.

3.4.1.2 Modification with AMS

4-Acetamido-4'-maleimidylstilbene-2,2'-disulfonic acid (AMS, **Figure 3.3**) is a thiol-reactive reagent that is water-soluble, with high polarity and membrane impermeability (5). This polysulfonated dye is useful for determining whether thiol-containing proteins and polypeptide chains are exposed at the extracellular or cytoplasmic membrane surface. This molecule was used in this study to assess the reactivity of the surface thiol group on the mutant protein.

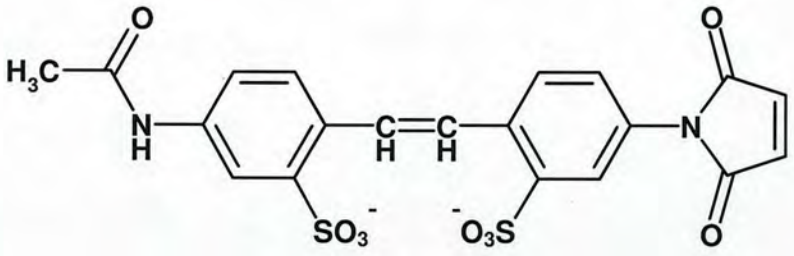

Figure 3.3. Structure of 4-acetamido-4'-maleimidylstilbene-2,2'-disulfonic acid.

The procedure for modifying a protein containing a reactive thiol was as follows: 1 mg/mL of mutant FbpA in 25 mM HEPES (pH 7.5) was reduced with 1 mM TCEP for 5-10 min at room temperature. AMS (20-fold molar excess) dissolved in 25 mM HEPES (pH 7.5) was added dropwise with stirring, and the reaction allowed to procede for 2 hours at room temperature. Unreacted AMS was quenched with TCEP. The mixture was centrifuged and the supernatant applied to a PD10 column (GE Healthcare) to remove excess AMS and TCEP and to exchange the modified protein into ammonium acetate buffer (10 mM, pH 8.0) for mass spectrometry (6).

Protein modified with AMS should yield a 425 Da mass increase by LC-MS.

3.4.1.3 Modification with EZ-Link™ Maleimide-PEO_2-Biotin

Maleimide-PEO_2-biotin (Pierce, **Figure 3.4**) is a water-soluble sulfhydryl-reactive biotinylation reagent that covalently modifies reactive cysteine residues. The reagent is used to modify a reactive thiol group on the surface of a protein, via the maleimide moiety, by Michael addition. The molecule contains a maleimide moiety and a biotin moiety that are linked by a polyethyleneoxide (PEO_2) chain, rendering the biotin group ~29 Å away from the reactive thiol group on protein surface. Biotin is a small naturally occurring vitamin that binds with high affinity to avidin and streptavidin proteins: the bond formation between biotin and avidin is rapid and, once formed, is unaffected by most extremes of pH, organic solvents and other denaturing agents. As such maleimide-PEO_2-biotin is an excellent molecule for the biotinylation of reactive thiol containing proteins for attachment to a avidin/streptavidin coated surface (sensor chip), as the protein of interest is held away from the surface due to the length of the PEO_2 linker (7).

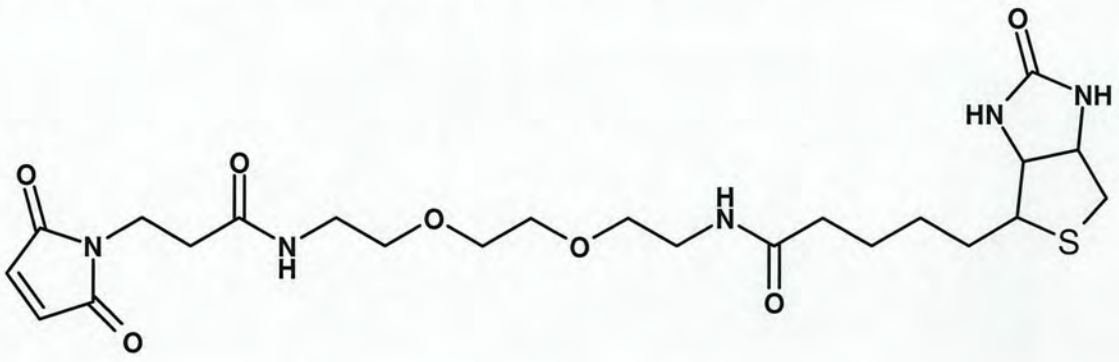

Figure 3.4. Structure of maleimide-polyethyleneoxide$_2$-biotin. The maleimide moiety on the left is linked to the biotin moiety on the right by a polyethyleneoxide$_2$ chain.

The procedure for modifying a protein containing a reactive thiol was as follows: 1 mg/mL of mutant FbpA in PBS (pH 7.2) was reduced with 1 mM TCEP for 10 min at room temperature. To this was added maleimide-PEO_2-biotin (20 mM; final concentration 0.8 mM) dissolved in PBS (pH 7.2), and the reaction allowed to procede overnight at room temperature (7). Unreacted maleimide-PEO_2-biotin and excess TCEP were removed by PD10 column chromatography (GE Healthcare). This was also used to exchange the modified protein into ammonium acetate buffer (10 mM, pH 8.0) for mass spectrometry. The biotinylated FbpA (named FbpA-V272C-(M-PEO_2-B)) was stored at 4 °C for up to 2 weeks.

LC-MS was performed as described in Section 3.5.2. A protein modified with maleimide-PEO_2-biotin should yield a 525 Da mass increase by LC-MS.

3.4.1.4 Modification with Iodoacetamidofluorescein (IAF)

This molecule relies on the same chemistry as iodoacetamide to modifiy a reactive thiol containing protein with the fluorescent molecule fluoroscein (**Figure 3.5**). Fluorescein has an absorption maximum at 490 nm and an emission maximum at 514 nm, making the molecule fluoresce green when excited with the correct wavelength of light. Modification of a protein with IAF is useful for studying the formation of protein complexes *in vitro*, and for tracking proteins within a cell. The procedure for modification with IAF is identical to that described above for iodoacetamide.

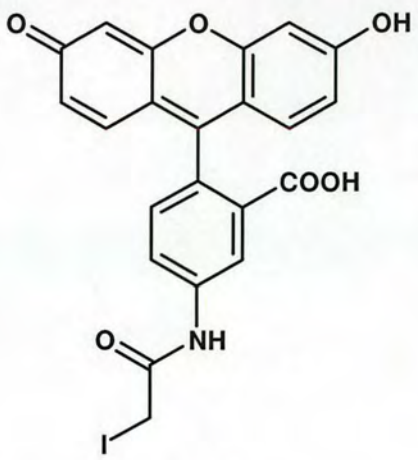

Figure 3.5. Structure of iodoacetamidofluorescein.

3.4.2 Reloading of *apo*-FbpA with Ruthenium and Osmium

3.4.2.1 Preparation of Ruthenium Reloaded FbpA

Reloaded Ru-FbpA was prepared by adding a 5-fold molar excess of Ru(III), in the form of $RuCl_3.xH_2O$ (1 mM stock solution, made up in water; pH 4.5), to *apo*-FbpA in 50 mM HEPES, pH 8.0. The mixture was incubated at room temperature for 3 h and was then dialysed into 3 x 1 L of 10 mM HEPES, pH 8.0. Chromatography was then performed using a Tricorn™ MonoS cation exchange column (GE Healthcare) on a ÄKTA*Basic100* (GE Healthcare). The load and wash buffer was 10 mM HEPES, pH 8.0 and bound protein was eluted with a 0-1 M salt gradient in wash buffer.

3.4.2.2 Preparation of Osmium Reloaded FbpA

Reloaded Os-FbpA was prepared by adding a 5-fold molar excess of Os(III), in the form of $OsCl_3.3H_2O$ (1 mM, made up in water, pH 4.5), to *apo*-FbpA in 10 mM HEPES, pH 8.0. The mixture was incubated at room temperature for 3 hours and

was then dialysed into 3 x 1 L of 10 mM HEPES, pH 8.0. Chromatography was then performed using a Tricorn™ MonoS cation exchange column (GE Healthcare) on a ÄKTA*Basic100* (GE Healthcare). The load and wash buffer was 10 mM HEPES, pH 8.0 and bound protein was eluted with a 0-1 M salt gradient in wash buffer.

3.4.2.3 Preparation of Ru-FbpA samples for EXAFS

The proteins contained in two major peaks from cation exchange chromatography were collected and concentrated to ~1 mM by ultrafiltration (Viva Life Sciences, 10 000 M_r cut-off). These were stored at 2-8 °C until transported to the Central Laboratory for the Research Councils (CLRC) Synchrotron Radiation Source (SRS) at Daresbury Laboratory (UK) for EXAFS. Samples were frozen in liquid nitrogen prior to being mounted and loaded into the cryostat for analysis. Analysis was performed at 100 K with X-ray scan traversing 22.1214 keV (0.56047 Å, ruthenium edge position) by Dr Ian Harvey (Station Scientist; Daresbury Lab).

3.4.3 ATPase Assay of FbpC

An ATPase assay was performed to determine that the purified FbpC protein was correctly folded and could hydrolyse ATP. The method uses the properties of molybdenum (as molybdate) to complex inorganic phosphate (P_i) in a specific manner at acidic pH values. This method was used because the assay, unlike other phosphate determination assays, is not affected by high concentrations of ATP and glycerol (8).

An ATPase assay was performed as previously reported (8), and the amount of inorganic phosphate (P_i) liberated determined by colourimetric assay (8-10). Briefly, FbpC or FbpBC in 25 mM tris buffer (pH 8.0) containing NaCl (40 mM),

ATP (5 mM), DTT (1 mM), EDTA (0.1 mM) and 20% glycerol was incubated at 37°C for 3 min and the reaction initiated by the addition of 100 mM $MgCl_2$ to a final concentration of 2 mM. Aliquots were removed from the reaction at specific time points and added directly to an equal volume of 12% SDS and mixed. An equivalent volume of 6% SDS, 0.5% ammonium molybdate and 3% ascorbic acid in 0.5 N HCl was then added. The mixture was incubated at room temperature for 5 min before the addition of an equivalent volume of 2% sodium citrate, 2% sodium (meta)arsenite and 2% acetic acid. This was incubated at 37 °C for 10 min to allow any colour to develop, and the absorbance of each reaction read at 850 nm on a Varian Cary 300 fitted with a temperature control system. A negative control was also assayed and a standard curve of KH_2PO_4 was used to determine the amount of P_i liberated.

3.4.4 FbpBC Pull-Down with Biotinylated FbpA

Magnetic streptavidin beads (100 µL, New England Biolabs) were washed three times (1 mL each) in water and then equilibrated with three washes (1 mL each) of PBS using a magnetic separation rack (New England Biolabs). 0.05 mg of FbpA-V272C-(M-PEO_2-B) (biotinylated FbpA) was incubated with the beads for 10 min at room temperature and then the beads washed three times (1 mL each) in PBS. The FbpA-V272C-(M-PEO_2-B) flow through and wash fractions were retained for analysis by SDS-PAGE and Western blot. To the washed beads coated with FbpA-V272C-(M-PEO_2-B) was added ~0.5 mg of the FbpBC complex. This was incubated for 10 min at room temperature, and then the beads washed three times (1 mL each) in 25 mM tris (pH 8.0) containing 2 mM ATP, 20 % glycerol, 150 mM NaCl and

0.1 % DDM. The FbpBC flow through and wash fractions were retained for analysis by SDS-PAGE and Western blot. Bound protein was eluted from the streptavidin beads by boiling for 5 min. The elution supernatant was analysed by SDS-PAGE and Western blot.

3.4.5 Surface Plasmon Resonance of the FbpABC Complex

Surface plasmon resonance (SPR) is a phenomenon that occurs when light is reflected off thin metal films (11). A fraction of the light energy incident at a sharply defined angle can interact with the delocalised electrons in the metal film (plasmon) thus reducing the reflected light intensity. The precise angle of incidence at which this occurs is determined by a number of factors, but the principal determinant is the refractive index close to the backside of the metal film, to which target molecules are immobilised and addressed by ligands in a mobile phase running along a flow cell. If binding occurs to the immobilised target the local refractive index changes, leading to a change in SPR angle, which can be monitored in real-time by detecting changes in the intensity of the reflected light, producing a sensorgram. The rates of change of the SPR signal can be analysed to yield apparent rate constants for the association and dissociation phases of the reaction. The ratio of these values gives the apparent equilibrium constant (affinity). The size of the change in SPR signal is directly proportional to the mass being immobilised and can thus be interpreted crudely in terms of the stoichiometry of the interaction. Signals are easily obtained from sub-microgram quantities of material. Since the SPR signal depends only on binding to the immobilised template, it is also possible to study binding events from molecules in extracts, and thus it is not necessary to have highly purified components (12).

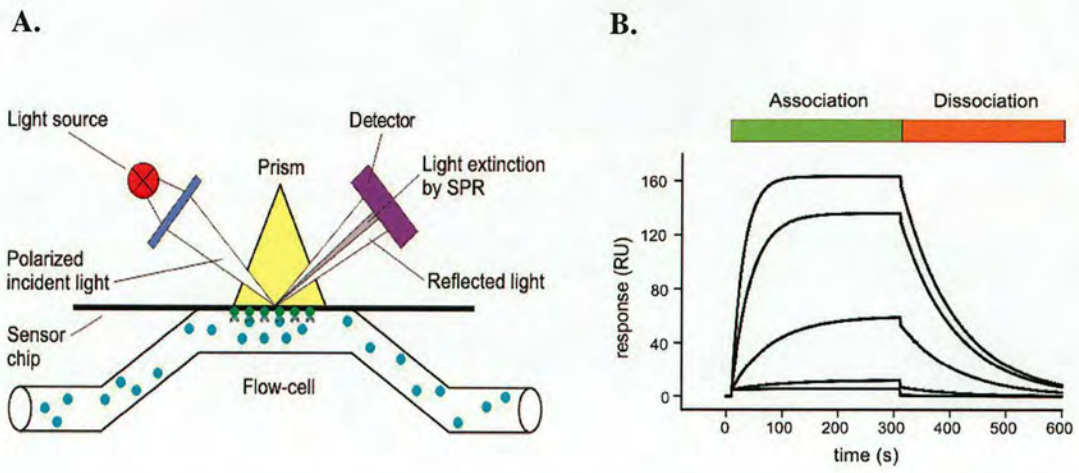

Figure 3.6. Diagrammatic representation of surface plasmon resonance. **A**, a light source is shone through a prism at the back of a sensor surface onto which a capture molecule (green) is immobilised. Changes of mass upon binding of partner (cyan) causes the incident angle (SPR angle) of refracted light to change. This change in SPR angle is deconvoluted and displayed in real time as a sensogram (**B**) from which affinity and kinetic data can be extrapolated (13).

SPR was performed on the FbpABC complex using a BiaCore T100 instrument in a similar manner to the pull-down experiment described above. A streptavidin derivatised SPR sensor chip was used to bind FbpA-V272C-(M-PEO_2-B) (40 nM) to maximum of ~100 Response Units (RU), manually at 10 µL/min, using the control software (14). Six serial dilutions of the FbpBC complex were prepared from 0-2400 nM, and a method written in the Biacore T100 control software to inject set volumes (88 µL) of each dilution, waiting 3000 s between injections, and the method was run overnight. Analysis of the results was performed using the Biacore T100 control software.

3.4.6 FbpABC Iron-59 Uptake Assay

Iron-59 (^{59}Fe) was bought from GE Healthacre in the form of $^{59}FeCl_3$ in 0.5 M HCl. ^{59}Fe is a β radiation emitter with some associated low energy γ emissions, and has a half-life of 44.5 days (15), making it useful for performing *in vivo* iron-uptake assays.

The ability of cells expressing *FbpABC* to take up radioactive ^{59}Fe (GE Healthcare) into the cytoplasm was compared to a non-FbpABC expressing negative control. BL21(DE3) cells were transformed with pET-28a/FbpABC/Ng and grown overnight in TB media containing kanamycin. Cells were diluted to OD_{600} of ~0.2 in fresh TB medium and grown at 25 °C to an OD_{600} of 0.7. The cells were then induced with 0.2 mM IPTG for 2 hours at 25 °C. This procedure was repeated with pET-28a/FbpC/Ng expressing cells as a negative control. An uninduced sample of FbpABC transformed cells was also retained as a negative control. After induction the cells were washed in MDG medium containing no iron and resuspended in the same medium to an OD_{600} of 1.0. Cultures were pre-incubated at 37 °C before the addition of $^{59}FeCl_3$ in 0.1 mM HCl to a final concentration of 2 μM. Aliquots (1 mL) were removed from the cultures at specific time points and immediately centrifuged for 2 mins at 11 000 x *g*, after which the supernatant was thoroughly removed and added to 2 mL of scintillation fluid. The pellets were immediately incubated with 50 mM HEPES (pH 8.0) and 1% CTAB for 2 hours at 37 °C to extract the periplasmic fraction. The periplasmic extraction was centrifuged for 5 min at 11 000 x *g* after which the supernatant was thoroughly removed and added to 2 mL of scintillation fluid. Scintillation fluid (2 mL) was also added to the remaining

cytoplasmic pellet. Radioactivity of all fractions was counted on a Packard liquid scintillation counter. Results were then plotted as a percentage (average of triplicates) of radioactivity taken up into the periplasm and cytoplasm.

3.5 Protein Charcterisation

3.5.1 UV-Visible Spectroscopy

The UV-Vis spectra were obtained on a Varian Cary 300 fitted with a temperature control system or a Hewlett Packard 8452A diode array spectrophotometer in 1 cm quartz cuvettes. Solvent was used as reference unless otherwise stated.

UV-Vis spectroscopy was used to determine the concentration of some proteins. Proteins have characteristic absorbance at 280 nm, and their concentrations can be determined if the molar extinction coefficient (ε) is known at these wavelengths. This is achieved by using the Beer-Lambert Law ($c = A/\varepsilon l$, c is concentration, A is absorbance, ε is the extinction coefficient at a specific wavelength [$M^{-1}cm^{-1}$], and l is the path length (4)).

The molar extinction coefficient at 280 nm can be calculated for proteins with known amino acid constituents by using the equation $\varepsilon = 5\,500N_{Trp} + 1\,490N_{Tyr} + 125N_{s\text{-}s}$ (16).

3.5.2 Liquid Chromatography-Mass Spectrometry (LC-MS)

LC-MS was performed on a MicroMass Platform II quadrupole mass spectrometer equipped with an electrospray ion source. The spectrometer cone voltage was ramped from 40 to 70 V and the source temperature set to 90 °C. Protein samples

were separated with a Waters HPLC 2690 with a Jupiter C5 reverse phase column (5 μm, 250 x 4.6 mm, Phenomenex) directly connected to the spectrometer. Proteins were eluted from the column with a 5-95% acetonitrile (containing 0.01% TFA) gradient at a flow rate of 0.2 mL/min. The total ion count in the range 500-2000 m/z was scanned at 0.1 s intervals. The scans were accumulated, spectra combined and the molecular mass determined by the MaxEnt and Transform algorithms of the Mass Lynx software (Micromass, U.K.).

3.5.3 Inductively Coupled Plasma Optical Emission Spectrometry (ICP-OES)

Inductively coupled plasma optical emission spectrometry (ICP-OES) is a technique used for the detection and quantification of elements in a sample. Up to 40 elements can be analysed simultaneously, and detection limited for most elements is typically at the μg/L (ppm) level for aqueous solutions.

ICP-OES was performed on a Thermo Jarrell Ash IRIS instrument and standards for the analytes under investigation were prepared to give a standard curve for each of those analytes. Concentrations of analytes in the samples were extrapolated from the relevant standard curves.

3.5.4 Extended X-ray Absorbance Fine Structure (EXAFS)

EXAFS is a technique for determining the atomic number, distance and coordination number of the atoms surrounding a metal. A monochromatic X-ray beam (from a synchrotron radiation source) is directed at the sample. The photon energy of the X-

rays is gradually increased, by a monochromator, such that it passes through the absorption edge of the element of interest contained in the sample. Below the absorption edge, the photons cannot excite the electrons of the relevant atomic level and thus absorption is low. However, when the photon energy is sufficient to excite the electrons, a large increase in absorption is observed; this is known as the absorption edge. The resulting photoelectrons with low kinetic energy can be backscattered by the atoms surrounding the emitting atom. This backscattering is dependent on the energy of the photoelectrons. Hence, the observed X-ray absorption will depend on the photon energy (as the photoelectron energy will depend on the photon energy). The net result is a series of oscillations on the high photon energy side of the absorption edge, and it is these oscillations that can be used to determine the atomic number, distance and coordination number of the atoms surrounding the element whose absorption edge is being examined (17).

EXAFS was performed on the ruthenium reloaded form of FbpA at the CCLRC synchrotron radiation source at Daresbury laboratory, UK, in collaboration with Dr Ian Harvey.

3.5.5 Peptide Mass Fingerprinting of SDS-PAGE Bands

A NuPAGE gel was run on the samples to be identified and then stained using a (colloidal) Coomassie stain compatible with mass spectrometric analysis, as described above. The bands of interest were cut out and placed in clean Eppendorf tubes. To one gel slice was added 200 µL of 50% acetonitrile followed by a 5 min incubation at RT. The liquid was removed and discarded and the procedure repeated.

The tubes were then placed in a Gyrovap for 15 min or until the slice was dry and moved freely in tube. An aliquot of 10 mM DTT, 0.2% EDTA in 100 mM ammonium bicarbonate was added to just cover the dried gel slice and then incubated at 56 °C for 30 min, after-which the mixture was cooled to RT. The DTT solution was removed and 50 mM iodoacetamide (made up in 100 mM ammonium bicarbonate) was added to just cover the gel slice, and this incubated in the dark for 30 min at RT. This liquid was then removed and the slices washed with 200 µL of 100 mM ammonium bicarbonate for 10 min. The slices were then dehydrated with the addition of 200 µL of neat acetonitrile for 10 mins and then the liquid discarded. This was repeated once and then the slices dried in a Gyrovap for 15 min. Trypsin solution was added directly to the slice and incubated at 2-8 °C for 30 min and then 37 °C for 15 min or until all the liquid was absorbed. A volume of ammonium bicarbonate (50 mM) was added to just cover the slice and then the tube sealed and placed on a shaker set at 250 rpm for 12-16 hours at 37 °C.

The digest liquid was removed from the tube and placed in a fresh Eppendorf tube. Just enough 5% trifluoroacetic acid made up in 50% acetonitrile was added to cover the gel slice and this then incubated with shaking at RT for 30-60 min. This was centrifuged for 2 min at 11 000 x *g* and the supernatant combined with the supernatant from above. The sample was then placed in a Gyrovap until dry and then resuspended in 20 µL of 0.1% formic acid made up in water (ZipTip wash buffer) and a washed and equilibrated C_{18} ZipTip (Millipore Corp,) used according to the manufacturers instructions to load the peptides onto the ZipTip resin. Peptides were eluted from the ZipTip with 10 µL of 50% acetonitrile made up in 0.1% formic acid in water (ZipTip elution buffer). This elution procedure was repeated twice.

Samples were spotted onto a MALDI plate and analysed on a MALDI-TOF spectrometer (Tof-Spec 2E, Micromass, U.K). Spectrum analysis was performed using Voyager software and peptide fragment analysis performed using either the MS-Fit or ProFind databases.

3.5.6 Bioinformatics

3.5.6.1 Basic Local Alignment Search Tool (BLAST)

Similar protein sequences were identified using BLASTp [BLAST 1.5.4-Paracel] accessed via ExPASy/SIB (http://ca.expasy.org/tools/blast/), against the ExPASy/UniprotKB database (18,19). Amino acid sequences of FbpB and FbpC from *N. gonorrhoeae* were used as query sequences.

3.5.6.2 Vector NTI 9

Vector NTI version 9 suite (Invitrogen) was used for drawing plasmid maps, manipulating nucleic acid and amino acid sequences, designing primers and for performing amino acid sequence alignments (using the Align X function).

3.5.6.3 Structure Analysis

Structure analysis of the FbpB and FbpC sequences was performed using topology programmes TMHMM version 2 (http://www.cbs.dtu.dk/services/TMHMM-2.0) and TopPred (http://bioweb.pasteur.fr/seqanal/interfaces/toppred/html) (20-23).

3.5.6.4 Structure Modelling

A model of the FbpC predicted structure was generated by submitting the amino acid sequence of the protein to the Swiss-Model database on the ExPASy Proteomics server using T.l.MalK as a template.

3.5.7 Crystallisation Trials of FbpC

Crystallisation trials of FbpC were performed in collaboration with Dr Simon Newstead/Prof. So Iwata at Imperial College, London, in the Membrane Protein Crystallography Group. FbpC was prepared in Edinburgh as described above and transported to London on dry ice. Clean-up purification was performed if required as described above and the protein exchanged into crystallisation buffer: 10 mM HEPES buffer (pH 7.5), 5 mM ATP, 2 mM EDTA and 20% glycerol (> 99.5 pure). FbpC was then concentrated to 5 mg/mL using a spin concentrator (10 000 MWCO, VivaSpin).

A Cartesian crystallisation robot was used to set up nanolitre-scale sitting-drop crystal trials in either a 1:1 or 2:1, precipitant:protein volume ratio (~800 conditions screened in total). The commercial screens used are listed in **Table 3.3**. Conditions that yielded small crystals were repeated on a microlitre scale, and crystals that grew were taken to the ESRF synchrotron radiation source in Grenoble, France. Diffraction images were collected on beamline ID23eh2 microfocus.

SeMet labelled protein was prepared in the same way and trials were set up using crystallisation conditions that had been optimised for the unlabelled protein.

Table 3.3. Table of commercial crystallisation screens used for structural investigation of FbpC.

Commercial Screens	Number of conditions
Hampton Research Crystal Screen 1	50
Hampton Research Crystal Screen 2	48
Wizard I random sparse matrix crystallization screen	48
Wizard II random sparse matrix crystallization screen	48
PEG/Ion screen	48
JCSG+ refill-hit solutions	96
PACT Suite refill-hit solutions	96
Molecular Dimensions MemSys	48
Molecular Dimensions MemStart	48
Natrix	48

3.6 Chapter 3 References

1. Studier, F. W. (2005) *Protein Expr. Purif.* **41**, 207-234
2. Zhu, H., Alexeev, D., Hunter, D. J., Campopiano, D. J., and Sadler, P. J. (2003) *Biochem. J.* **376**, 35-41
3. Adamczyk, M., Gebler, J. C., and Wu, J. (1999) *Rapid Commun. Mass Spectrom.* **13**, 1813-1817
4. http://www.ionsource.com/Card/cmc/method.htm.
5. Hagting, A., Kunji, E. R., Leenhouts, K. J., Poolman, B., and Konings, W. N. (1994) *J. Biol. Chem.* **269**, 11391-11399
6. http://probes.invitrogen.com/media/pis/mp00003.pdf.
7. http://www.piercenet.com/files/0748dh5.pdf.
8. Gonzalez-Romo, P., Sanchez-Nieto, S., and Gavilanes-Ruiz, M. (1992) *Anal. Biochem.* **200**, 235-238
9. Nikaido, K., Liu, P. Q., and Ames, G. F. (1997) *J. Biol. Chem.* **272**, 27745-27752
10. Chifflet, S., Torriglia, A., Chiesa, R., and Tolosa, S. (1988) *Anal. Biochem.* **168**, 1-4
11. Attridge, J. W., Daniels, P. B., Deacon, J. K., Robinson, G. A., and Davidson, G. P. (1991) *Biosens. Bioelectron.* **6**, 201-214
12. Torreri, P., Ceccarini, M., Macioce, P., and Petrucci, T. C. (2005) *Ann. Ist Super. Sanita.* **41**, 437-441
13. http://images.google.co.uk/imgres?imgurl=http://www.fz-juelich.de/ibi/ibi-1/datapool/page/130/Principle%2520of%2520surface.jpg&imgrefurl=http://w

ww.fz-juelich.de/ibi/ibi-1/protein-protein_interaction&h=257&w=500&sz=40&hl=en&start=2&tbnid=b5k6Nghl_eSjLM:&tbnh=67&tbnw=130&prev=/images%3Fq%3Dsurface%2Bplasmon%2Bresonance%26svnum%3D10%26hl%3Den%26lr%3D%26client%3Dfirefox-a%26rls%3Dorg.mozilla:en-GB:official%26sa%3DN.

14. Morgan, H., and Taylor, D. M. (1992) *Biosens. Bioelectron* **7**, 405-410

15. httpwww6.gelifesciences.com/applic/upp00738.nsf/vLookupDoc/250151221-B653/$file/IFS1.pdf.

16. Pace, C. N., Vajdos, F., Fee, L., Grimsley, G., and Gray, T. (1995) *Protein Sci.* **4**, 2411-2423

17. http://www.uksaf.org/tech/exafs.html.

18. Altschul, S. F., Gish, W., Miller, W., Myers, E. W., and Lipman, D. J. (1990) *J. Mol. Biol.* **215**, 403-410

19. Altschul, S. F., Madden, T. L., Schaffer, A. A., Zhang, J., Zhang, Z., Miller, W., and Lipman, D. J. (1997) *Nucleic Acids Res.* **25**, 3389-3402

20. Krogh, A., Larsson, B., von Heijne, G., and Sonnhammer, E. L. (2001) *J. Mol. Biol.* **305**, 567-580

21. Sonnhammer, E. L., von Heijne, G., and Krogh, A. (1998) *Proc. Int. Conf. Intell. Syst. Mol. Biol.* **6**, 175-182

22. Vonheijne, G. (1992) *J. Mol. Biol.* **10**, 685

23. Claros, M. G., and von Heijne, G. (1994) *Comput. Appl. Biosci.* **10**, 685-686

Chapter 4: Results and Discussion: FbpA

4.1 Results: FbpA

4.1.1 Purification of *N. gonorrhoeae* FbpA Wild-Type and Mutants

Purification of FbpA was optimised as part of this study. A novel procedure for the purification of FbpA and mutants of the protein was devised to speed up the purification process. The protein extraction process was retained except that the method of purification that had previously been used included high concentrations (1 M) of Tris buffer in the extraction buffer. The buffer was changed to HEPES (100 mM), due to the possible metal chelating properties of Tris buffer, and the concentration of HEPES was kept low throughout the purification. The previous method also involved an overnight dialysis step at 4 °C of the crude extract to precipitate excess cetylmethylammonium bromide (CTAB) which is the cationic detergent used in the extraction of the protein from *E. coli*, and to dilute the concentrated tris buffer (1,2). This step was replaced with a 30 min incubation on ice of the crude cell-free extract, followed by centrifugation and purification. Previous purification was performed on various cation exchange columns (GE Healthcare) using an ÄKTA*Basic* FPLC system, followed by clean-up purification on a gel filtration column if required. The new purification method was performed using a batch method, in a centrifuge tube, with Fractogel EMD SO_3^--650(M) chromatography resin (Merck) and produced protein that was > 98% pure, judged by SDS-PAGE, in a single purification step. The new method also cut the purification time to one day, from two-three days.

This improved method was used for purification of all mutant FbpA proteins described in the following sections.

4.1.2 Production of *N. gonorrhoeae* FbpA Mutants

4.1.2.1 Identification of Potential Residues for Mutational Studies

The fact that FbpA from *N. gonorrhoeae* does not contain any cysteine residues was exploited to investigate the interactions with the proposed protein partners from the FbpABC operon. By introducing a cysteine residue on the surface of the protein, thus introducing a reactive thiol group, the protein can be derivatised using commercially available compounds that selectively irreversibly modify such groups. The use of members of the PBP family as tools and biosensors has been investigated in detail by Hellinga and co-workers (3-5). In this research the authors classify mutations dependent upon where the mutation is located on the PBP surface. Mutations in, or very close to, the substrate-binding site are termed *endosteric* sites; mutations located on the binding rim, close by the substrate-binding site are referred to as *peristeric* sites; and mutations located some distance away from the substrate-binding site are classed as *allosteric* sites (3).

Mutants of FbpA were produced by site-directed mutagenesis in order to perform protein-protein interaction studies with the other components of the FbpABC ABC transporter complex. Potential residues for mutation were identified by modelling the wild-type *N. gonorrhoeae* protein (PDB code 1D9Y) in WebLab and Swiss-pdb viewer programmes. As the protein was to be modified with a linker molecule for attachment to a sensor surface, only residues on the surface of the protein were chosen as potential candidates for mutation. To limit the potential structural effects of introducing mutants on the surface of the protein, only residues that were not thought to be involved in maintaining tertiary structure or in iron

coordination were chosen as suitable candidates, and residues that were not highly conserved throughout the ferric-ion binding protein PBP family were selected.

Residues that were suitable candidates were arginine residues in positions 48 and 83, a lysine residue in position 111 and a valine residue in position 272. These residues were classified as either peristeric or allosteric in position (**Table 4.1** and **Figure 4.1**).

Table 4.1. Mutation sites on FbpA and a description of their location and classification. Mutation residues are colour coded to those shown in **Figure 4.1** below.

Mutation	Description	Classification
R48C	N-terminal domain, outside rim of binding site	Peristeric
R83C	Lower face, hinge region	Allosteric
K111C	C-terminal domain, outside rim of binding site	Peristeric
V272C	Lower face, hinge region	Allosteric

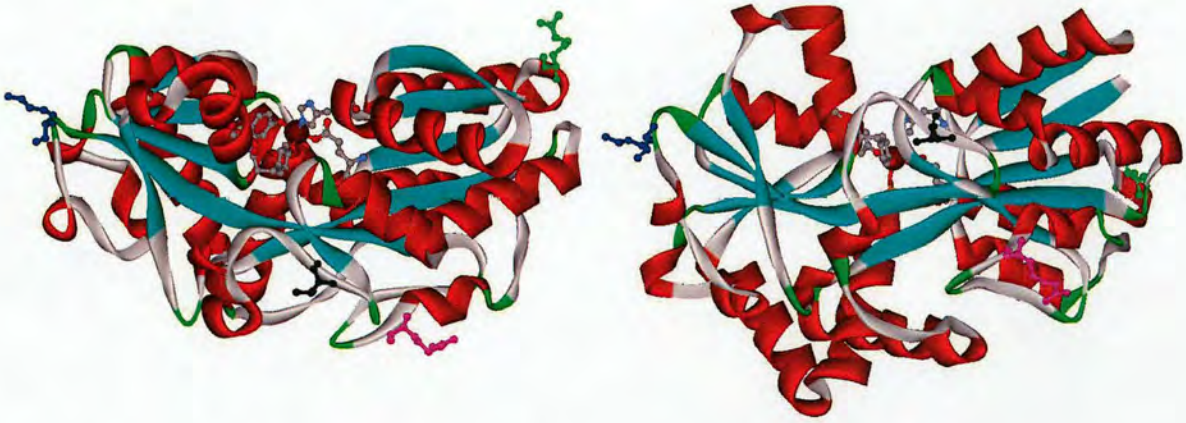

Figure 4.1. Model of FbpA from *N. gonorrhoeae* showing residues selected for mutation to cysteine. Left, side view; and right, bottom view. The residues are colour coded to those presented in **Table 4.1** above.

4.1.2.2 Site-Directed Mutagenesis of *N. gonorrhoeae* FbpA

PCR reactions were performed using the wild-type pTrc99A/FbpA/Ng plasmid as a template. The QuikChange Stratagene site-directed mutagenesis kit utilises a mutated version of the *Pyrococcus furians* DNA polymerase, renamed *PfuTurbo*, in a single PCR reaction to insert, remove or mutate single amino acid DNA base pair codons. The basic procedure utilizes a supercoiled double-stranded DNA (dsDNA) vector with an insert of interest (eg pTrc99A/FbpA/Ng) and two synthetic oligonucleotide primers containing the desired mutation (6). Oligonucleotide primers containing the required mutant codon were designed, each complementary to the opposite strand of the vector, and were extended during temperature cycling by *PfuTurbo* DNA polymerase. Incorporation of the oligonucleotide primers generated a mutated plasmid containing staggered nicks. Following the PCR reaction, the product was treated with the restriction endonuclease *Dpn*I. *Dpn*I endonuclease (target sequence: 5´-Gm6ATC-3´) is specific for methylated and hemimethylated DNA and is used to digest the original parental DNA template (pTrc99A/FbpA/Ng) and to select for synthesised DNA containing the desired mutation (7).

FbpA mutants were generated using the Stratagene QuikChange site-directed mutagenesis kit in accordance with the manufacturer's instructions. Reactions were performed with the relevant mutagenic primers as described above. DNA agarose gels of the reaction products are shown in **Figure 4.2**.

Figure 4.2. Agarose DNA gels showing products from site-directed mutagenesis PCR reactions after *Dpn*I digest. 1, R48C; 2, R83C; 3, K111C; and 4, V272C. M, hyperladder I marker (Bioline).

DNA from reactions was used to transform TOP10 *E. coli* cells, and the DNA purified from the cells using a Qiagen mini-prep kit. The mutant DNA was verified by DNA sequencing and was used for expression trials of the mutant proteins.

PCR reactions for the R48C, R83C and V272C mutants yielded DNA that contained the correct specific mutations, however, the DNA sequenced from the K111C reaction yielded only wild-type DNA. The reaction was repeated five times with no success: suggesting there was a problem with the DNA primers.

4.1.2.3 Small-Scale Expression of Mutant of FbpA in *E. coli*

Expression trials of the mutant FbpA proteins were performed using small-scale (10 mL) cultures. The mutant protein was expressed in an identical fashion to the wild-type protein. Briefly, single colonies from a freshly transformed LB/amp agar plate were picked and used to inoculate 10 mL of LB or 2xYT media containing ampicillin (100 µg/mL) and grown for 16 hours at 37 °C with agitation (250 rpm). Cultures were centrifuged for 10 min at 4000 x *g* and expression of the mutant

protein first checked visually by looking for the deep brown-red colour that is characteristic of the wild-type *holo*-protein, and then by SDS-PAGE.

FbpA-R48C expressing pellets were brown-red in colour and two large bands were observed at the expected molecular mass of FbpA (~35 kDa; on SDS-PAGE), and at a mass twice that of FbpA (~67 kDa). This mutant was deemed suitable for further studies.

FbpA-R83C expressing pellets were creamy-white in colour and no band was observed at the expected molecular mass of FbpA by SDS-PAGE (data not shown). It was assumed that the mutant DNA did not express. Several expression attempts were performed with no success, and thus, this mutant was deemed unsuitable for further study.

FbpA-V272C expressing pellets were brown-red in colour and a large band was observed at the expected molecular of FbpA by SDS-PAGE. This mutant was deemed suitable for further studies.

4.1.2.4 Large-Scale Expression of FbpA-R48C and FbpA-V272C in *E. coli*

Large-scale expression was carried out in an identical fashion to the wild-type protein. Two-litre cultures were prepared on both mutants and the resulting large cell pellets (~7 g) were dark brown-red in colour, suggesting good expression of the mutant *holo* forms of the proteins. The pellets were stored at –20 °C until further purification.

4.1.2.5 Purification of FbpA-R48C and FbpA-V272C

Purification of the mutant proteins was carried out in an identical fashion to the wild-type protein, as described above. SDS-PAGE of the purification of FbpA-R48C and FbpA-V272C are shown in **Figure 4.3**.

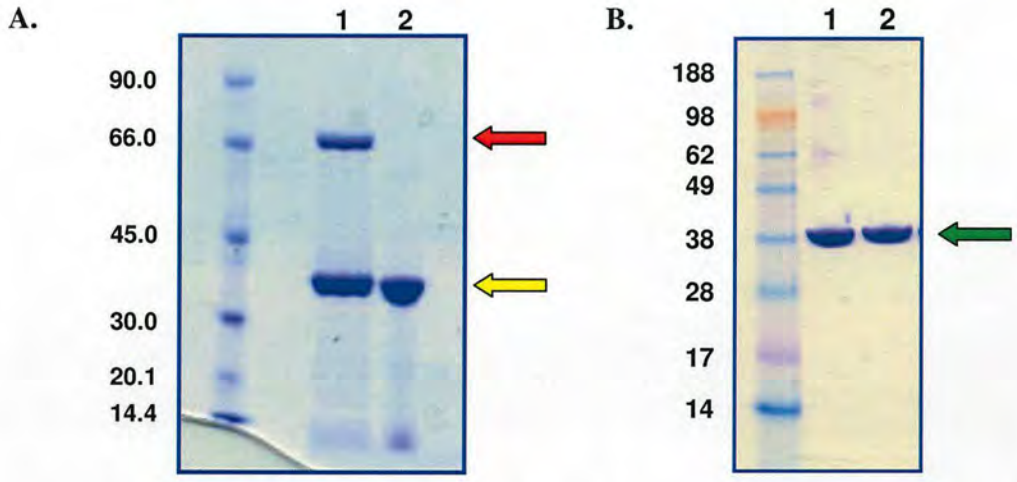

Figure 4.3. A, SDS-PAGE of purified FbpA-R48C. 1, non-reducing conditions; 2, reduced (β-mercaptoethanol) sample. The non-reduced sample revealed a band that was not present in the reduced sample. The band at 67 kDa (red arrow) was therefore assigned as a FbpA-R48C dimer and the other band assigned as monomer (yellow arrow). **B, SDS-PAGE of purified FbpA-V272C.** 1, non-reducing conditions; 2, reduced (β-mercaptoethanol) sample. Only the monomer (green arrow) was observed in the unreduced sample of FbpA-V272C.

Interestingly, the purification of the R48C mutant yielded two highly pure bands when run under partially denaturing conditions (no reducing agent in the loading buffer). The lower band was observed at a molecular mass of ~34 kDa, which was the expected mass of FbpA-R48C, and the upper band was observed at ~67 kDa. The upper band was assigned as FbpA-R48C dimer, as reducing SDS-PAGE conditions yielded a single band at ~34 kDa. The finding that ~20% of the "as purified" protein was in a dimeric form strongly suggested that the introduced

thiol group on the surface of the protein was both solvent exposed and reactive. The yield of the FbpA-R48C protein was estimated to be 30-40 mg/L culture.

No such corresponding dimer was observed in the purified FbpA-V272C protein, as the SDS-PAGE yielded only one highly pure band at ~34 kDa when non-reducing and reducing conditions were tested. The finding that no dimer was present in the purified protein suggested that the introduced cysteine residue may not be solvent exposed and/or not reactive. The yield of the FbpA-V272C protein was estimated to be 40-50 mg/L culture.

4.1.3 UV-Visible Spectroscopy of *N. gonorrhoeae* FbpA Mutants

To investigate whether the mutant FbpA proteins showed the same UV-vis spectrum as the wild-type FbpA, both mutants were scanned over a range of 250-700 nm. The traces are presented in **Figure 4.4**.

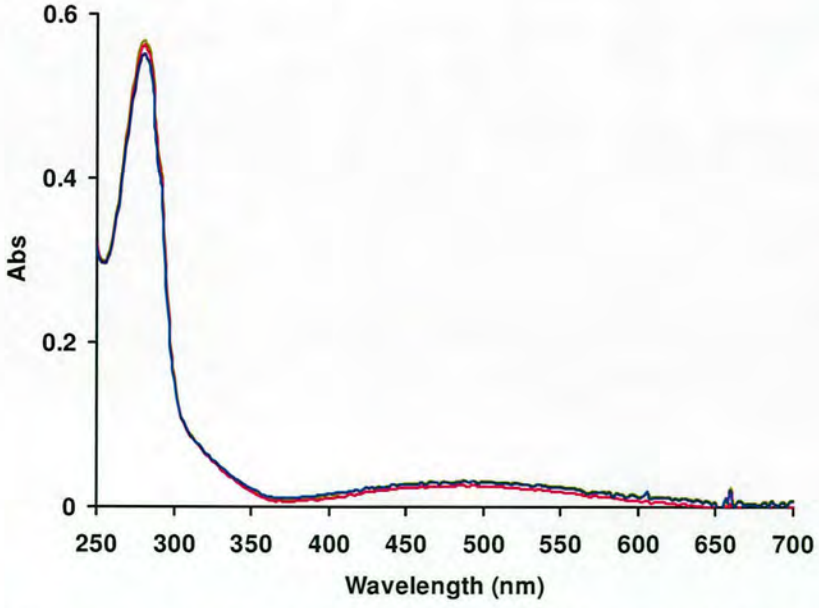

Figure 4.4. Comparison of the UV-Visible spectra of wild-type FbpA (blue) compared to FbpA-R48C (pink) and FbpA-V272C (green); all ~0.4 mg/mL. Note the identical shape of all three curves, suggesting that iron binding is not altered in the mutant proteins.

The UV-vis spectra show that the *holo* forms of FbpA-R48C and FbpA-V272C have almost identical UV-visible spectra when compared to wild-type *holo*-FbpA, suggesting that the iron-binding site in the mutant proteins do not differ greatly from the wild-type protein. UV-visible spectra were also obtained of FbpA-V272C modified with both maleimide-polyethylene-biotin (M-PEO_2-B) and iodoacetamidofluoroscein (IAF) to investigate if the modification interfered with iron binding. The spectra are shown in **Figure 4.5**.

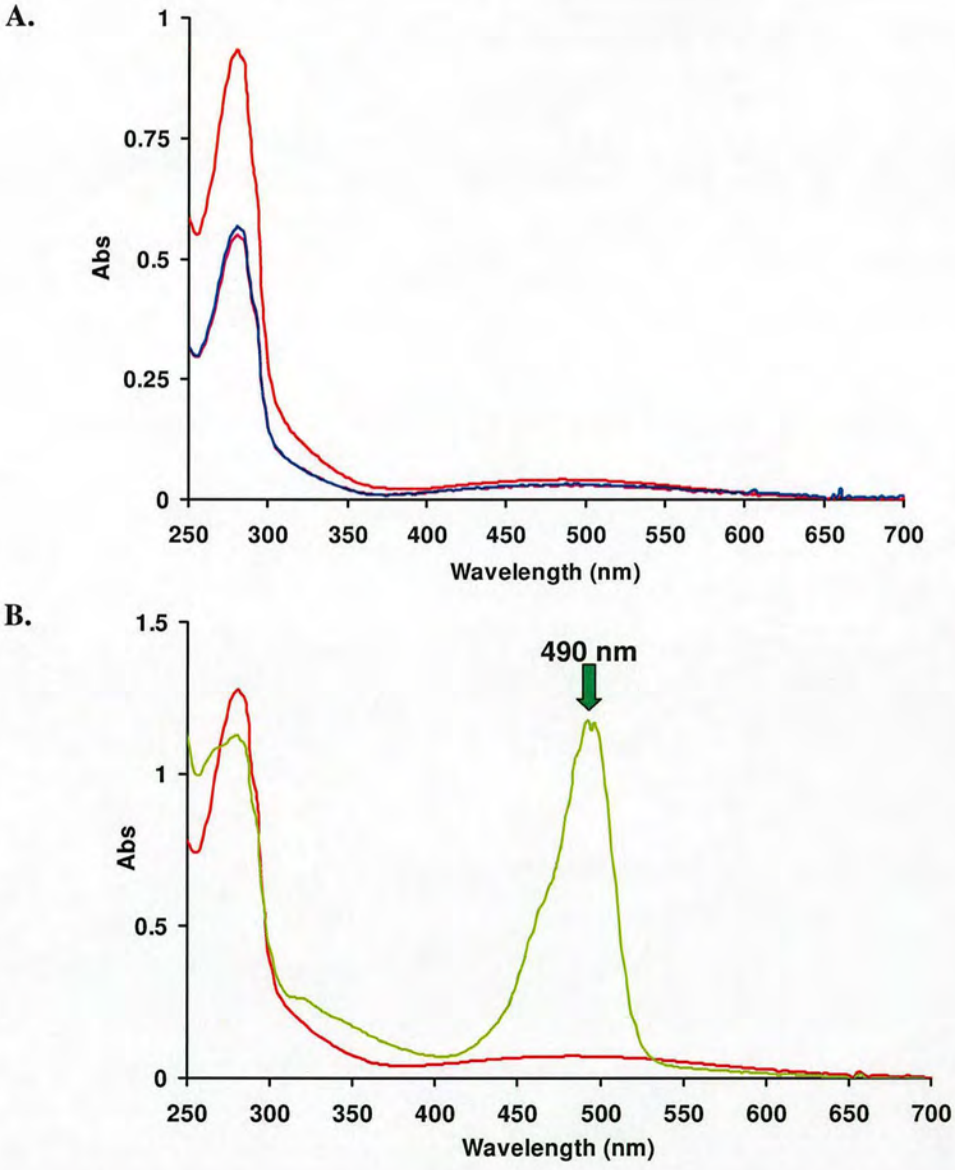

Figure 4.5. A. UV-Visible spectra of wild-type FbpA (blue) compared to FbpA-V272C (pink) (both 0.4 mg'mL) and FbpA-V272C-(M-PEO_2-B) (red, 0.7 mg/mL). Note the virtually identical shape of all three curves, suggesting that iron binding is not altered in the modified mutant proteins. **B. UV-Visible spectra of FbpA-V272C (red) compared to FbpA-V272C-IAF (green).** The modified protein shows a large absorbance peak at ~490 nm due to the presence of the iodoacetamidofluorescein moiety.

4.1.4 Mass Spectrometry of *N. gonorrhoeae* FbpA Mutants

4.1.4.1 Mass Spectrometry of Purified Mutants

The accurate mass of the two mutant proteins was determined by electro-spray ionisation mass spectrometry (ESI-MS). All masses obtained are presented in **Table 4.2** and all spectra are provided in **Appendix 2**.

FbpA-R48C: Due to the presence of the dimer observed by SDS-PAGE, an unreduced and reduced (using 1 mM TCEP) sample of the protein was subjected to ESI-MS. When the unreduced sample was analysed by ESI-MS a mass corresponding to the dimer (67 198 ± 11.4 Da) was observed, as well as masses for the monomer and several other peaks that suggested FbpA-R48C had also been modified by other molecules *in vivo*. The theoretical mass for FbpA-R48C is 33 588 Da and a peak was observed at 33 583 ± 4.9 Da along with peaks at 33 706.50 ± 4.9 Da (+118 Da) and 33 886.50 ± 4.9 (+300 Da) which were assigned as cysteinylation and glutathionylation (γ-Glu-Cys-Gly) of the protein, respectively. On reduction with TCEP the ESI-MS spectra obtained yields only a single mass (33 585 ± 5.0 Da) that is in agreement with the theoretical mass of the R48C mutant. From this it was clear that the introduced cysteine mutation was reactive and had been modified *in vivo* by cysteine and glutathione.

FbpA-V272C: On reduction with TCEP the mass obtained for FbpA-V272C was 33 640.86 ± 2.3 Da which is concordant with the theoretical mass expected for this mutant (33 643 Da). Since the theoretical mass for the mutant protein was four Daltons different from wild-type FbpA, it was not possible to prove from the mass spectrometry data alone that the V272C mutation had been correctly inserted.

4.1.4.2 Mass Spectrometry of Modified Mutants

To verify that the mutant proteins could be derivatised using thiol reactive molecules, both mutant proteins were modified with a number of different prosthetic groups.

FbpA-R48C: This mutant was modified with iodoacetamide and AMS (4-acetamido-4'-maleimidylstilbene-2,2'-disulfonic acid). Modification with iodoacetamide is an example of a S-amidomethylation reaction, whereas modification with AMS is via a maleimide moiety, by Michael addition to the reduced thiol group. Both derivatisations were successfully performed, but there were solubility issues with both modified proteins. Approximately 30% of the iodoacetamide modified protein, and more than 90% of the AMS modified protein precipitated during the reaction. Nevertheless, sufficient quantities of modified protein could be isolated for binding studies. Accurate masses were determined for both conjugated mutants. Masses obtained for the modified proteins are shown in **Table 4.2**. The iodoacetamide modified protein remained stable at 2-8 °C for several weeks, but the AMS modified protein continued to precipitate for several days after storage.

Due to the solubility issues for the modified protein, and the position of the mutation on the rim of the metal-binding site, it was decided not to pursue binding studies with other component proteins of the ABC transporter with this particular protein.

FbpA-V272C: This protein was successfully modified with iodoacetamide, iodoacetamidofluorescein and maleimide-polyethyleneoxide$_2$-biotin (M-PEO$_2$-B). M-PEO$_2$-B was the molecule to be used for attachment of the mutant protein to a

streptavidin-coated surface (chip) to perform protein-binding studies. The mass spectrum for the reaction product showed there was a mixture of modified and unmodified protein, with a ratio of about 65%:35% modified:unmodified protein. There was no precipitation of the protein during the reaction, and the modified protein was stable at 2-8 °C for several weeks. Accurate masses were obtained for the iodoacetamide and M-PEO_2-B derivatised proteins, but no mass was obtained for the protein modified with iodoacetamidofluorescein. Masses obtained for the modified proteins are shown in **Table 4.2**.

Due to the stability of the modified proteins, and the position of the mutation (away from the metal binding site) on the "underside" of the molecule, this protein was used to perform binding studies with the BC component proteins of the FbpABC ABC transporter.

Table 4.2. Masses obtained for mutant proteins and derivatives. AMS: 4-acetamido-4'-maleimidylstilbene-2,2'-disulfonic acid; M-PEO_2-B: maleimide-polyethyleneoxide-biotin; IAA: iodoacetamidofluorescein – : no mass obtained.

Modification	FbpA-R48C	FbpA-V272C
Theoretical mass	**33 588**	**33 643**
As Purified	**67 198** ± 11.4 (dimer) **33 585** ± 5.0 (monomer) **33 706** ± 4.9 (cysteinylation) **33 886** ± 4.9 (glutathionylation)	**33 640** ± 2.3
Iodoacetamide	**33 644** ± 5.0	**33 707** ± 6.7
AMS	**33 094** ± 5.9	–
M-PEO_2-B	–	**34 180** ± 4.9
IAF	–	–

4.1.5 Loading FbpA with Ruthenium

4.1.5.1 Characterisation of Reloaded Ru-FbpA by UV-Vis

UV-Visible spectra were recorded of a sample of *apo*-FbpA at various times after addition of $RuCl_3$. A peak was observed that appeared at 410 nm and which shifted to 425 nm over a period of 3 h (**Figure 4.6**).

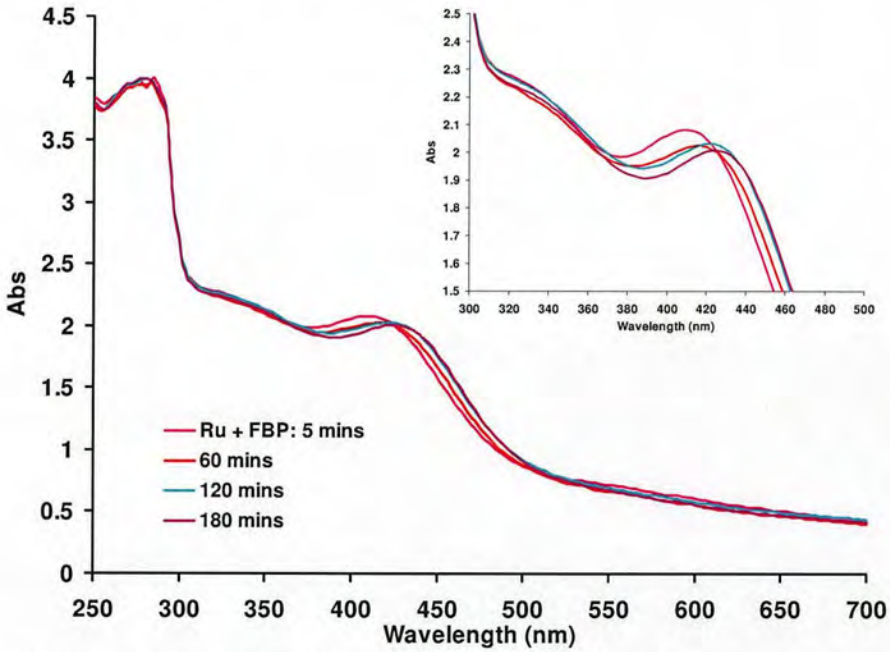

Figure 4.6. UV-visible spectra of FbpA incubated with $RuCl_3$. Over time there is a band shift from 410-425 nm. Bands in this region are probably due to Ru *d-d* or charge-transfer transitions.

4.1.5.2 Characterisation of Ru-FbpA by Chromatography

Chromatography was performed by FPLC on a ÄKTA *Basic100* (Amersham Biosciences) using a Tricorn™ MonoS (GE Healthcare) cation exchange column. Two major peaks were observed at 280 nm (protein absorbance) and 430 nm (ruthenium absorbance) and several other minor peaks were also present: all peaks eluted between 190-220 mM NaCl (**Figure 4.7**). This revealed that ruthenium had

bound to FbpA and had resulted in at least three different species. Peak 1 and 2 were collected and concentrated by ultrafiltration (Viva Life Sciences, 10 000 M_r cut-off).

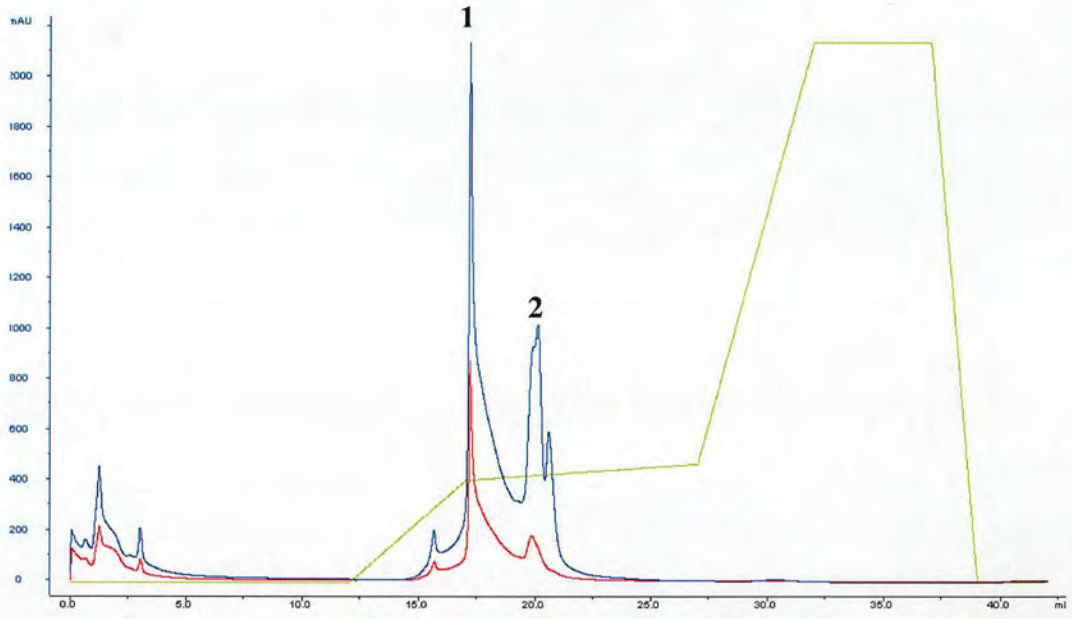

Figure 4.7. Chromatogram of Ru-FbpA purified by cation ion-exchange. Two main species were observed. Peaks 1 and 2 were resolved, collected and analysed by ICP-OES. Both protein species were associated with four ruthenium metal ions. Blue line: A_{280} (protein absorbance); red line: A_{430} (ruthenium absorbance); green line: concentration percentage of buffer B.

4.1.5.3 Characterisation of Ru-FbpA by ICP-OES

The Ru:P:S ratio for the Ru-FbpA species in peaks 1 and 2 from the above chromatogram was determined by ICP-OES; the molar concentration of sulphur was used to assess the concentration of protein, as the each protein molecule contains one sulphur (methionine residue). The Analytical data are shown in **Table 4.3**. Multiple ruthenium binding was observed for both species. For both adducts the Ru:FbpA ratio was 4:1.

Table 4.3. ICP-OES analysis of peaks 1 and 2 from Figure 4.7.

Sample	Mol element per mol protein	
	Ru	P
Peak 1	4.2	1.8
Peak 2	4.1	1.2

The data in **Table 4.3** suggest the presence of two forms of a bound Ru_4 cluster; one form capped by two phosphate (peak 1) ions and one capped by one phosphate (peak 2). This is strongly reminiscent of the Fe_3, Hf_3 and Hf_5 and Zr_3 oxo clusters previously reported by our group, and an Fe_4 cluster in FbpA reported by other researchers (1,8-10). However, an oxo-metal cluster capped by two phosphate molecules would be a novel species. When both species were analysed by ESI-MS, the ion-envelope obtained for the protein was that of *apo*-FbpA, thus signifying that ruthenium was lost from the protein during the ionisation process. This is common for metalloproteins as the metal ligand bonds are coordination bonds, which are weaker than covalent bonds.

4.1.5.4 Characterisation of Reloaded Ru-FbpA by EXAFS

Extended X-ray absorbance fine structure (EXAFS) analysis was performed on peaks 1 and 2 on Station 16.5 at the CCLRC SRS at Daresbury Laboratory, by beamline scientist Dr Ian Harvey. The X-ray absorbance near edge structure (XANES), EXAFS and Fourier transform spectra are shown in **Figure 4.8**.

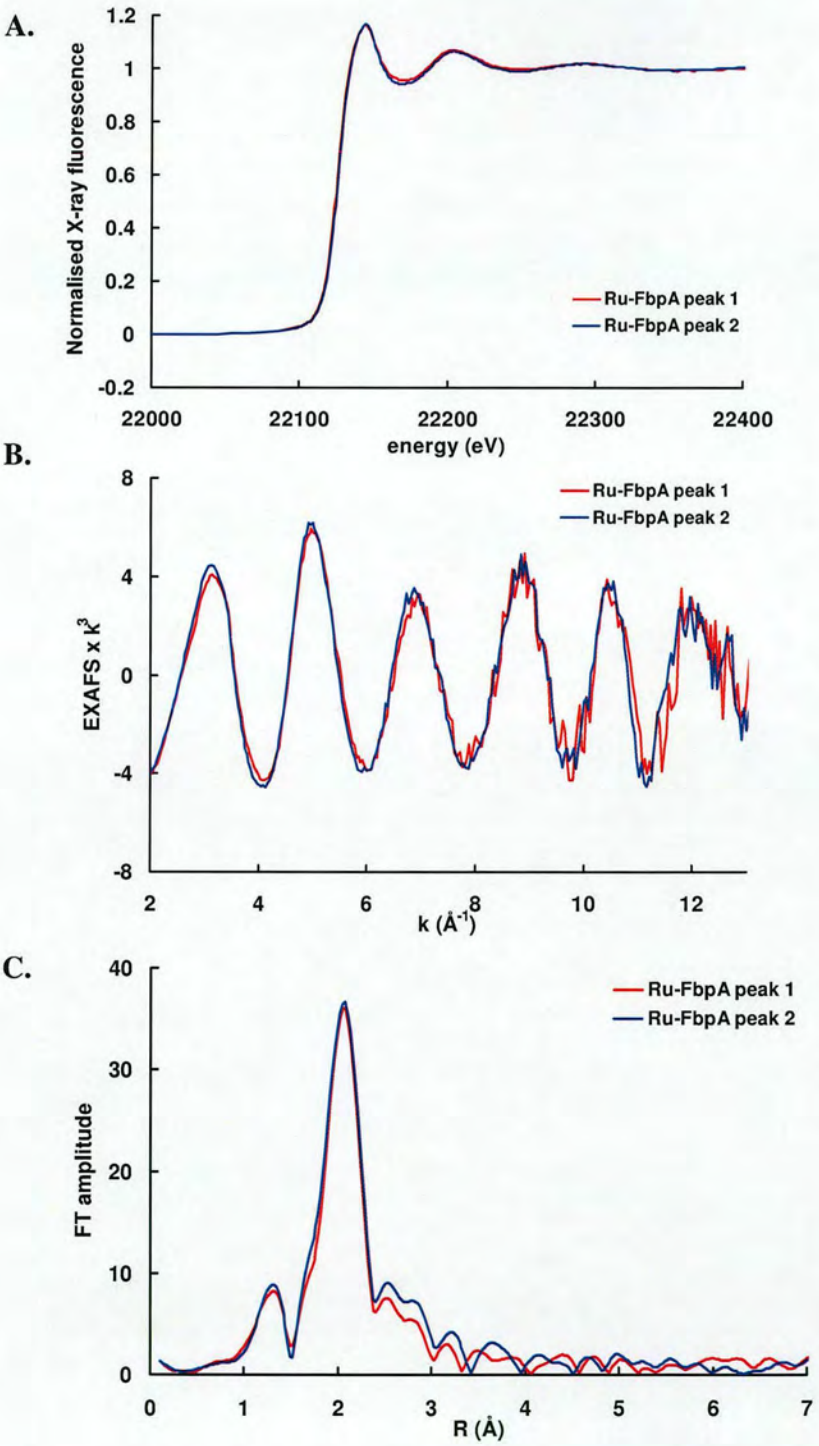

Figure 4.8. A, XANES spectra of Ru-FbpA species present in peaks 1 and 2. Ru-FbpA spectra are almost identical apart from a small difference at ~22 160 eV. **B, EXAFS spectra.** Both species yield very similar EXAFS spectra. **C, Fourier transform of EXAFS data.** The data suggests that the species are very similar, but do differ slightly in the bond lengths at ~2.2-4 Å.

The XANES spectra show the K edge absorbance spectra from which the oxidation state of the metal being probed can be determined. Initial findings suggest that the energy observed in the spectra are comparable with oxidation states of Ru(V) or Ru(VI), when compared to ruthenium oxidation-state standards. This is an unexpected finding and further investigation of this conclusion is required.

Fourier transform of the EXAFS spectra revealed a main peak that fits 3-4 oxygens at ~2.05 Å. There is also a small contribution at a shorter bond distance (1.2 Å), however, this requires further investigation. The peaks at ~2.7 Å and 2.9 Å do not fit either tyrosine- or histidine-type bonds, but may be a very small contribution from another ruthenium atom, possibly through a bridging oxygen, or may also be due to the possible presence of a phosphate synergistic anion. Analysis of the data is still in progress.

4.1.6 Loading of FbpA with Osmium

4.1.6.1 Characterisation of Os-FbpA by UV-Vis

UV-Visible spectra were recorded of a sample of *apo*-FbpA at various times after addition of $OsCl_3$. A peak was observed at 360 nm that shifted to 370 nm over a period of 2 h (**Figure 4.9**).

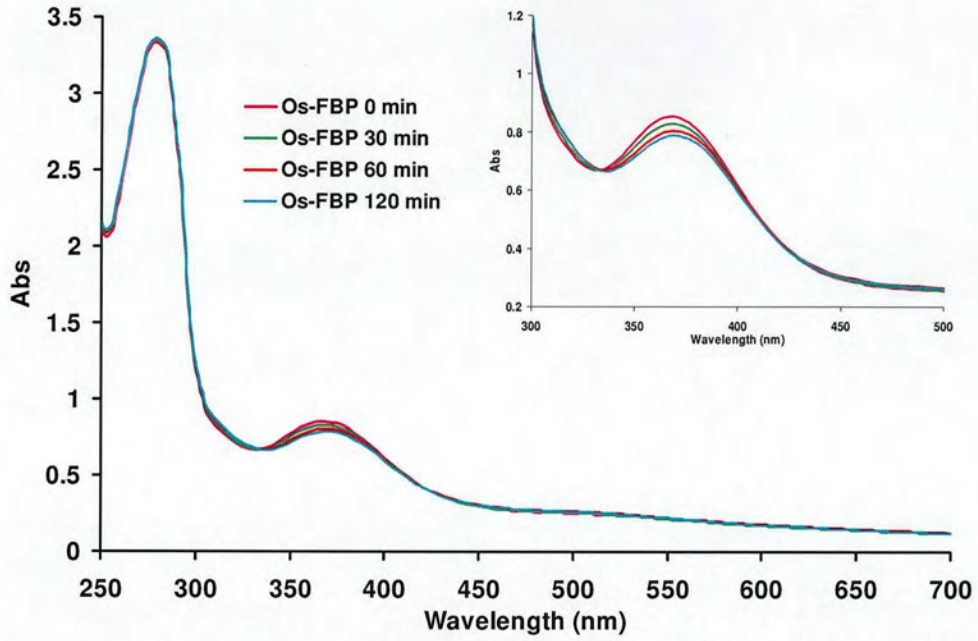

Figure 4.9. UV-visible spectroscopy of FbpA incubated with $OsCl_3$. Over time there is a band shift from 360 to 370 nm in the osmium absorbance region.

4.1.6.2 Characterisation of Os-FbpA by Chromatography

Two major peaks were observed at 280 nm (protein absorbance) and 330 nm (osmium absorbance): both peaks eluted from the cation exchange column between 190-220 mM NaCl (**Figure 4.10**). This revealed that at least two different species formed after the addition of $OsCl_3$ to *apo*-FbpA. Peaks 1 and 2 were collected and concentrated by ultrafiltration (Viva Life Sciences, 10 000 M_r cut-off).

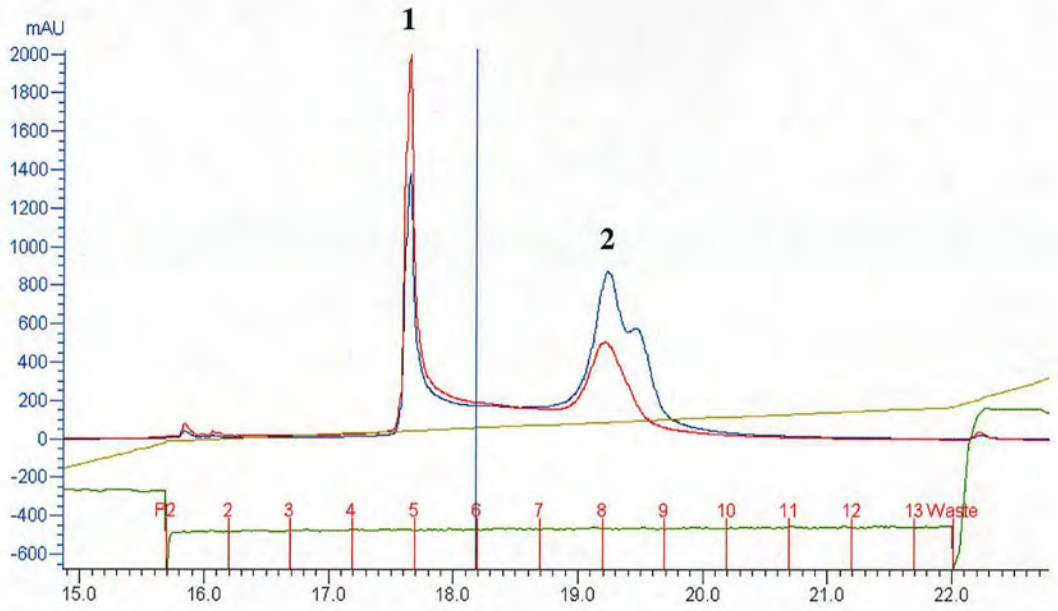

Figure 4.10. Chromatogram of Os-FbpA purified by cation ion-exchange. Two main species were observed (Peaks 1 nd 2). Blue line: A_{280} (protein absorbance); red line: A_{360} (osmium absorbance); green line: concentration percentage of buffer B.

4.1.6.3 Characterisation of Os-FbpA by ICP-OES

The Os:P:S ratio of the species formed that are represented by peaks 1 and 2 from the above chromatogram were determined by ICP-OES; the molar concentration of sulphur was used to assess the concentration of protein, as the each protein molecule contains one sulphur (methionine residue). The results are shown in **Table 4.4**.

Table 4.4. ICP-OES analysis of peaks 1 and 2 from Figure 4.10.

Sample	Mol element per mol protein	
	Os	P
Peak 1	4.0	1.9
Peak 2	3.9	1.3

The data in **Table 4.4** suggests the presence of two forms of Os_4 cluster with ratios of Os:P:S of *ca.* 4:2:1 ratio for peak 1, and 4:1:1 for peak 2. This suggests that two forms of Os_4 cluster can bind to FbpA; one form capped by two phosphates (peak 1) and one capped by one phosphate (peak 2). The behaviour of osmium(III), like ruthenium(III) above, is strongly reminiscent of that for iron(III), hafnium(IV) and zirconium(IV) oxo clusters previously reported for FbpA (1,8,9). However, an oxo-osmium cluster capped by two phosphate molecules would be a novel FbpA species. There was insufficient sample to allow characterisation by mass spectrometry, however, it may be assumed that the bound metal ions would dissociate during the ionisation process as observed for the ruthenium adduct.

4.2 Discussion: FbpA

4.2.1 FbpA Purification and Modification of Mutant Proteins

The purification of FbpA was optimised by changing buffer systems and by the use of a batch purification method. The new procedure reduced purification time from three days, to a one-day process. Large quantities of very pure protein were produced in a single purification step in a short time. This new method limits the time that the protein is in contact with proteases that may be present in the cell-free extract, and thus reduces the potential risk of degradation during purification.

FbpA was successfully mutated to incorporate a single thiol residue and allowed covalent modification with several functional prosthetic groups. Mutations were classified by the position of the mutation of the surface of the protein using a system outlined by Hellinga and co-workers (3). FbpA-V272C was modified to

yield a biotinylated FbpA (FbpA-V272C-(maleimide-polyethyleneoxide$_2$-biotin)) that allowed attachment of the mutant protein to a streptavidin-coated surface for protein-protein interaction studies with FbpB and C (**Chapter 5**). FbpA-V272C was also modified with a fluorescent tag (iodoacetamidofluoroscein; IAF) to allow complex formation studies in future work. Accurate masses were determined for the unmodified protein and for FbpA-V272C-(maleimide-polyethyleneoxide$_2$-biotin), but not for FbpA-V272C-IAF. All masses obtained were within experimental error.

Interestingly, the mutant FbpA-R48C formed a dimer *in vivo* – the first time such a bacterial two-lobe "pseudo-transferrin" molecule has been described. The monomeric form of FbpA-R48C was modified with iodoacetamide and 4-acetamido-4'-maleimidylstilbene-2,2'-disulfonic acid. These probes were used to determine the reactivity of the introduced thiol group, but showed that, although the protein could be modified *in vitro*, the resulting derivatised proteins were unstable. Accurate masses were determined for the unmodified protein, including the observed dimer, and for FbpA-R48C-iodoacetamide and FbpA-R48C-AMS. The instability of the modified proteins may have been because residue 48 may play an important role in maintaining tertiary structure of the protein, and modification at this position causes denaturation of FbpA.

This study has shown that FbpA from *N. gonorrhoeae* is a suitable protein for mutational studies, and can be modified and employed as a tool for performing binding studies with the other gene products of the *FbpABC* operon: FbpB and FbpC.

4.2.2 Loading of FbpA with Ruthenium and Osmium

FbpA was loaded with the transition metal ions ruthenium(III) and osmium(III) in order to further investigate the specificity of the metal-binding site. Both metals were found to bind to FbpA, and appeared to form very similar species that could be separated chromatographically.

The finding by ICP-OES and EXAFS (for the ruthenium species) that FbpA bound four atoms of either ruthenium or osmium is similar to results previously published for iron(III), hafnium(IV) and zirconium(IV) clusters in FbpA (1,8,9). Assuming that the metals have bound as a cluster, and not at four distinct binding sites elsewhere on the protein, the possible presence of a oxo-metal cluster potentially capped by two phosphate ions is novel for metal clusters bound to FbpA. EXAFS revealed that the ruthenium cluster present in the Ru-FbpA, may contain ruthenium in the (V) or (VI) oxidation state, which would be very unusual, as, although ruthenium can rarely form these oxidation states as well as the (VII) and (VIII) oxidation states, this metal is usually found in the form of Ru(II), Ru(III) or Ru(IV) in aqueous systems (Ru(IV) being readily reduced to Ru(III) in such systems) (11). From previous work on FbpA, it is known that the protein can stabilise higher oxidation states of bound metal clusters, as revealed in the oxo-$(Fe^{III})_3$, oxo-$(Hf^{IV})_{3\ \&\ 5}$, Ti(IV) and oxo-$(Zr^{IV})_3$ FbpA crystal structures (1,8,9,12). However, if the ruthenium clusters in FbpA do contain ruthenium in the (V) and/or (VI) oxidation states, this would be unexpected, and would be the first report of such clusters bound to a protein.

Ruthenium and osmium oxo-bridged clusters have been described in the literature, although oxo-Ru_4 and oxo-Os_4 clusters are relatively rare. A search of the Cambridge Crystallographic Data Centre (CCDC) revealed that only two structures containing Ru_4, and one $Os(IV)_4$, hydroxo-bridged clusters have been determined (13-15), and all the clusters had been produced synthetically. Tri-Ru and -Os clusters and higher number (5, 6, 8 and 9) clusters of both metals are more commonly described in the literature, and the clusters often contain other metals (such as molybdenum). There were also several examples of M-phenoxide (M = Ru or Os) bonds in the CCDC, but most were present with a second, chelating bond from another position on the adjacent aromatic ring. Three examples could be found of a single M-phenoxide bond for each metal (16-19), suggesting that these bounds can be formed.

If the Ru- and Os-FbpA species isolated in this study contain oxo-metal clusters, maintained in unusually high oxidation states, and bound via one or two tyrosine residues, this would be of great interest with regards to how this protein binds these precious metals, and how FbpA stabilises these metal clusters in high oxidation states.

Preliminary crystal screens performed on both the ruthenium and osmium reloaded proteins did not yield any crystals, although different conditions may allow the structures of both proteins to be determined in the future.

4.3 Chapter 4 References

1. Zhu, H., Alexeev, D., Hunter, D. J., Campopiano, D. J., and Sadler, P. J. (2003) *Biochem. J.* **376**, 35-41
2. Guo, M., Harvey, I., Yang, W., Coghill, L., Campopiano, D. J., Parkinson, J. A., MacGillivray, R. T., Harris, W. R., and Sadler, P. J. (2003) *J. Biol. Chem.* **278**, 2490-2502
3. Dwyer, M. A., and Hellinga, H. W. (2004) *Curr. Opin. Struct. Biol.* **14**, 495-504
4. de Lorimier, R. M., Smith, J. J., Dwyer, M. A., Looger, L. L., Sali, K. M., Paavola, C. D., Rizk, S. S., Sadigov, S., Conrad, D. W., Loew, L., and Hellinga, H. W. (2002) *Protein Sci.* **11**, 2655-2675
5. de Lorimier, R. M., Tian, Y., and Hellinga, H. W. (Epub 2006) *Protein Sci.* **15**, 1936
6. Papworth, C., Bauer, J. C., Braman, J., and Wright, D. A. (1996) *Strategies* **9**, 3
7. Nelson, M., and McClelland, M. (1992) *Methods Enzymol.* **216**, 279-303
8. Alexeev, D., Zhu, H., Guo, M., Zhong, W., Hunter, D. J., Yang, W., Campopiano, D. J., and Sadler, P. J. (2003) *Nat. Struct. Biol.* **10**, 297-302
9. Zhong, W., Alexeev, D., Harvey, I., Guo, M., Hunter, D. J., Zhu, H., Campopiano, D. J., and Sadler, P. J. (2004) *Angew. Chem. Int. Ed. Engl.* **43**, 5914-5918
10. Shouldice, S. R., Skene, R. J., Dougan, D. R., McRee, D. E., Tari, L. W., and Schryvers, A. B. (2003) *Biochemistry* **42**, 11908-11914

11. Greenwood, N. N., and Earnshaw, A. (1997) *Chemistry of the Elements* (2nd, Ed.), Elsevier

12. Guo, M., Harvey, I., Campopiano, D. J., and Sadler, P. J. (2006) *Angew. Chem. Int. Ed. Engl.* **45**, 2758-2761

13. Gould, R. O., Jones, C. L., Robertson, D. R., Tocher, D. A., and Stephenson, T. A. (1982) *J. Organomet. Chem.* **226**, 199-207

14. Gould, R. O., Jones, C. L., Stephenson, T. A., and Tocher, D. A. (1984) *J. Organomet. Chem.* **264**, 365-378

15. Gould, R. O., Jones, C. L., Robertson, D. R., and Stephenson, T. A. (1977) *Chem. Commun.*

16. Collman, J. P., Barnes, C. E., Brothers, P. J., Collins, T. J., Ozawa, T., Gallucci, J. C., and Ibers, J. A. (1984) *J. Am. Chem. Soc.* **106**, 5151-5163

17. Pizzotti, M., and Crotti, C. (1984) *J. Chem. Soc. Dalton Trans.*, 735-738

18. Stokes Jr, S. M., Ding, F., Smith, P. L., Keane, J. M., Kopach, M. E., Jervis, R., Sabat, M., and Harman, W. D. (2003) *Organometallics* **22**, 4170-4171

19. Che, C.-M., Huang, J.-S., Li, Z.-Y., Poon, C.-K., Tong, W.-T., Lai, T.-F., Cheng, M.-C., Wang, C.-C., and Wang, Y. (1992) *Inorg. Chem.* **31**, 5220-5225

Chapter 5: Results and Discussion: FbpABC

5.1 Results: FbpC

5.1.1 Bioinformatic Analysis of *N. gonorrhoeae* FbpC

Due to the lack of published literature on this protein, some preliminary bioinformatic studies were performed on the amino acid sequence of FbpC.

FbpC is encoded for by the third gene in the *FbpABC* operon: *FbpC*, 1059 bp. Bioinformatic analysis of the amino acid sequence using Vector NTI v9 (Invitrogen) revealed that the mature protein is predicted to contain 352 amino acids and have a molecular mass of 37 900 Da (**Appendix 1**). The protein has a predicted pI of 6.91, making the protein have no overall net charge at physiological pH. Other biochemical characteristics of the protein are summarised in **Table 5.1**.

Table 5.1. Amino acid composition of FbpC. The protein is composed of ~40% hydrophobic residues, suggesting that the protein may have solubility problems in aqueous buffers.

Amino acids	Number	% by weight	% by frequency
Hydrophobic	136	37.08	38.64
Charged	89	31.13	25.28
Polar	79	22.74	22.44
Basic	34	12.82	9.66
Acidic	35	11.17	9.94

Bioinformatic analysis of the amino acid composition of FbpC revealed that a large proportion of the amino acid sequence is comprised of hydrophobic residues, suggesting that the protein may not be soluble in aqueous buffers. However, hydrophobicity profiling using a topology prediction programme (TMHMM) available on the ExPASy (**Ex**pert **P**rotein **A**nalysis **Sy**stem) Proteomics server

revealed that FbpC is expected to be a soluble protein with no transmembrane helices (**Figure 5.1**). The probability of the protein containing any transmembrane domains was virtually zero for the entire amino acid sequence. The degree of hydrophobicity of the protein is perhaps not surprising considering that FbpC is expected to be closely associated with the cytoplasmic side of the cytoplasmic membrane.

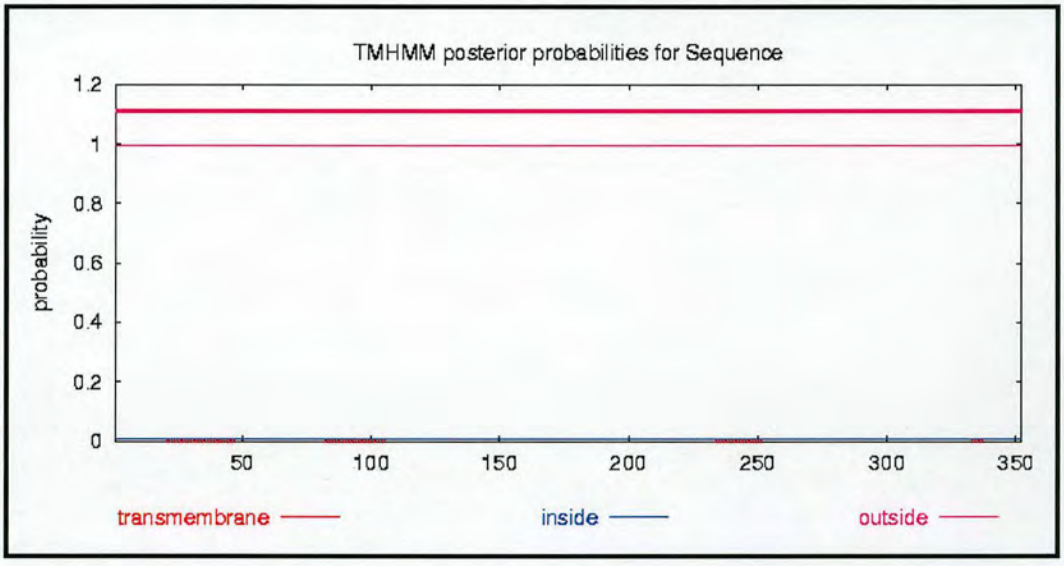

Figure 5.1. Topology modelling of FbpC. Using the topology modelling program TMHMM v2, FbpC is predicted to be a soluble protein with no predicted transmembrane helices (red line). This figure should be compared with **Figure 5.12 "Topology modelling of FbpB"** which shows predicted transmembrane helices for that protein.

The Basic Local Alignment Search Tool (BLAST) was used to identify known proteins with similar alignment sequences. The results are summarised in **Table 5.2**.

Table 5.2. Top 20 results of the BLAST search performed using the amino acid sequence of FbpC as the query sequence.

Gene description	Species	Accession Number	BLAST Score	E value	Sequence Length	
					Identities	%
ABC transporter, ATP-binding protein, iron related	*Neisseria gonorrhoeae* FA 1090	YP_207380	672	0	352/352	100
Iron(III) ABC transporter, ATP-binding protein	*Neisseria meningitides* MC58	NP_273675	660	0	343/352	97
Ferric cations import ATP-binding protein FbpC	*Neisseria gonorrhoeae* (no strain given)	Q50966	639	0	336/352	95
HitC	*Haemophilus influenzae* (no strain given)	AAB32112	378	2×10^{-103}	189/344	54
ABC-type spermidine/putrescine transport systems, ATPase components	*Haemophilus influenzae* R2866	ZP_00203259	378	3×10^{-103}	189/344	54
Ferric cations import ATP-binding protein fbpC 2	*Haemophilus influenzae* (no strain given)	P44513	377	6×10^{-103}	188/344	54
Iron-utilization ATP-binding protein hFbpC	*Haemophilus influenzae* 86-028NP	YP_247822	376	8×10^{-103}	188/344	54
Iron(III) ABC transporter ATP-binding protein	*Haemophilus influenzae* Rd KW20	NP_438273	376	8×10^{-103}	188/344	54
ABC-type spermidine/putrescine transport systems, ATPase components	*Haemophilus influenzae* R2846	ZP_00154826	374	5×10^{-102}	188/344	54
ABC transporter related	*Roseiflexus castenholzii* DSM 13941	ZP_01530879	249	1×10^{-64}	141/300	47
ABC transporter related	*Mycobacterium sp* JLS	ZP_01279931	249	1×10^{-64}	138/282	48
ABC transporter related	*Mycobacterium sp* MCS	ZP_01286100	248	3×10^{-64}	138/282	48
Iron(III) ABC transporter, ATP-binding protein	*Marine actinobacterium* PHSC20C1	ZP_01130545	247	7×10^{-64}	158/353	44
Iron(III) ABC transporter, ATP-binding protein	*Pseudomonas fluorescens* Pf-5	YP_260146	243	8×10^{-63}	136/281	48
ABC transporter ATP-binding protein	*Thermosynechococcus elongates* BP-1	NP_682282	243	1×10^{-62}	135/295	45
ABC transporter component	*Rhodospirillum rubrum* ATCC 11170	YP_425858	242	2×10^{-62}	140/285	49
ABC-type spermidine/putrescine transport systems, ATPase components	*Yersinia frederiksenii* ATCC 33641	ZP_00831119	241	3×10^{-62}	131/289	45
ABC transporter-like	*Pseudomonas fluorescens* PfO-1	YP_348570	241	3×10^{-62}	139/298	46
ABC transporter related	*Herpetosiphon aurantiacus* ATCC 23779	ZP_01427854	241	4×10^{-62}	150/348	43
ABC transporter ATP-binding protein	*Vibrio fischeri* ES114	YP_205532	240	6×10^{-62}	121/287	42

The BLAST results reveal that the ABC transporter family ATPases show very high sequence homology between individual family members, not only between the iron ABC transporters, but amongst members of the family that transport diverse ligands. Proteins with E values of less than 10^{-5} are considered to have "good" identity to the query sequence. Of the BLAST search performed for this study the top 100 hits all had E values of 10^{-49} or less, suggesting that this very large diverse family share significant sequence homology between transporters that transport diverse ligands. Included in the first 100 hits were many iron ABC transporter ATPases and putative ATPases from ABC transporters, but also spermidine/putrescine, sulfate and polyamine ABC transporter ATPases.

When the amino acid sequence of FbpC was aligned with the four proteins for which the crystal structures have been determined discussed in Section 2.1.4 (2 x MalK, HisP and BtuD), it is clear that FbpC contains all the characteristic elements of a NBD from the ABC transporter family. FbpC contains Walker A and B motifs, as well as the Q-loop, H-Loop, D-loop and ABC signature sequences. It also revealed that the amino acid identity is highest for the MalK sequences and lowest for BtuD protein: 31.6% identity (46.4% consensus) with T.l.MalK, 27.6% identity with E.c.MalK, 22.6% identity (34.6% consensus) with His P, and only 16.7% (28.4% consensus) with BtuD. Not surprisingly, this high homology with MalK is due in part to the presence of a ~80 amino acid C-terminal extension observed in FbpC, suggesting that the protein may contain a similar domain to that found in these two proteins. Amino acid sequence alignments are shown in **Figure 5.2** and **5.3**.

FbpC was modelled using the T.l.MalK structure as a template using Swiss-Model database on the ExPASy Proteomics server. The modelled theoretical structure of FbpC is shown in **Figure 5.4**, and reveals that FbpC should adopt a similar overall fold as is found in these proteins.

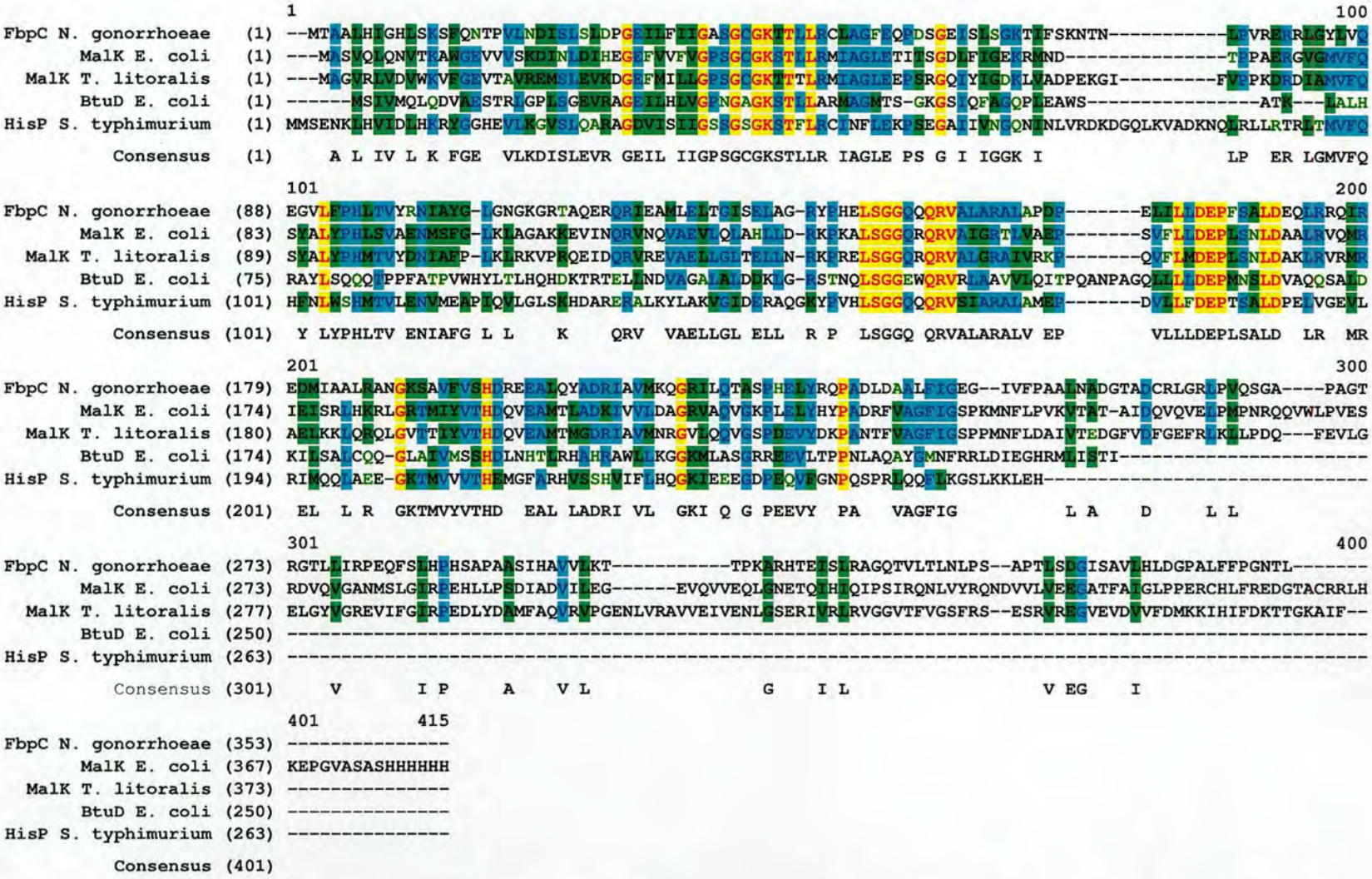

Figure 5.2. Sequence alignment and consensus of FbpC from *N. gonorrhoeae*, MalK from *E. coli* and *T. litoralis*, BtuD from *E.coli* and HisP from *S. typhimurium*. X - Identical residues, X - conserved residues, X - block of similar, X - weakly similar, and X - non-similar. Note the C-terminal extension on FbpC and MalK sequences.

Figure 5.3. Sequence alignment of FbpC from *N. gonorrhoeae* against MalK from E. coli and *T. litoralis*, BtuD from *E.coli* and HisP from *S. typhimurium* showing conserved motifs. FbpC contains the essential ABC motifs that define the family of ATPase proteins of ABC transporters. Note the C-terminal domain present in FbpC.

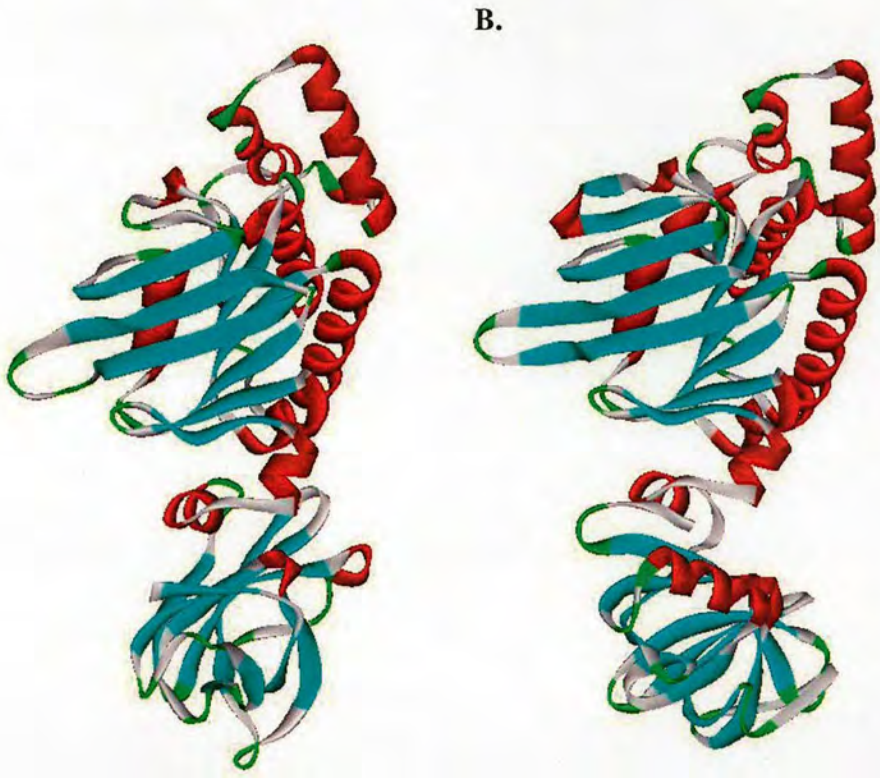

Figure 5.4. A, Model of the predicted structure of N.g.FbpC using T.l.MalK (B) as a template. Note the similarity of both structures, including the C-terminal extension present in FbpC that is proposed to be involved in signal transduction (1).

5.1.2 Cloning of FbpC from *N. gonorrhoeae* Genomic DNA

Ferric-ion binding protein C (*FbpC*) gene was amplified from *Neisseria gonorrhoeae* genomic DNA by PCR using the primers FbpC *Nco*I For and FbpC *Xho*I Rev. Primers were designed to incorporate *Nco*I and *Xho*I restriction enzyme sites at the 5' and 3' end of the gene, respectively. The resulting PCR product was cloned into cloning vector pGEM T-Easy (Promega) and the constructs verified by DNA sequencing. Plasmid containing the *FbpC* gene insert was digested with *Nco*I and *Xho*I and the fragment corresponding to the correct insert size (~1050 bp) was ligated into pET-28a expression plasmid (Novagen) cut with *Nco*I and *Xho*I. This vector

was chosen in order to incorporate a hexahistidine tag on the C-terminal of the protein. The ligation mixture was transformed into DH5α *E. coli* cells (Invitrogen) and the plasmid DNA purified (Qiagen mini-prep). Restriction digests confirmed the presence of the correct sized insert, and the construct containing *FbpC* was named pET-28a/FbpC/Ng. The hexahistidine tagged protein was expected to have a molecular mass of 38 808 Da (359 amino acids) by Vector NTI bioinformatic analysis. DNA gels and constructed plasmid maps are provided in **Figure 5.5**.

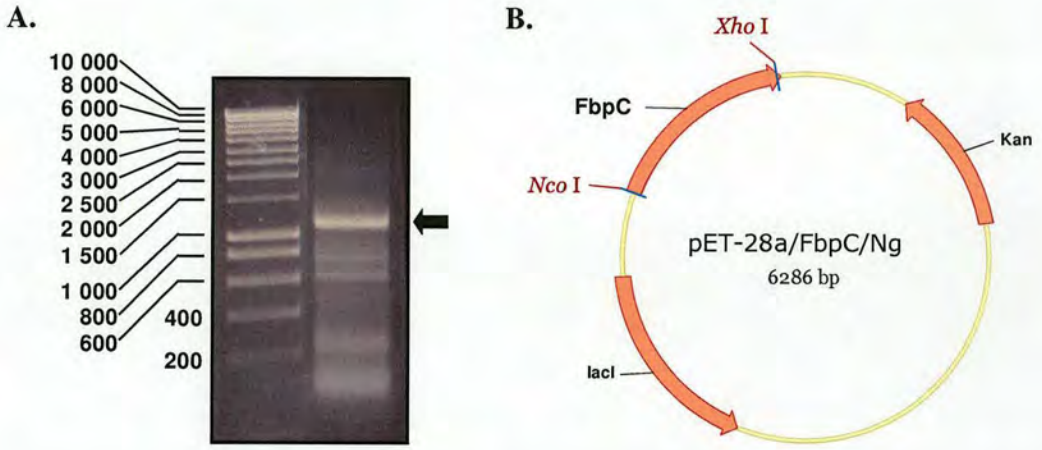

Figure 5.5. A. Agarose DNA gel showing the PCR product from reaction from *N. gonorrhoeae* genomic DNA. The DNA fragment corresponding to the FbpC gene is highlighted (arrow). **B. Vector map of pET-28a/FbpC/Ng.**

5.1.3 Expression of *N. gonorrhoeae* FbpC-His$_6$ in *E. coli*

pET-28a/FbpC/Ng plasmid was transformed into *E. coli* expression strain BL21(DE3) and grown on LB/kanamycin (30 μg/mL) agar plates. Small-scale inductions in this broth at 37 °C with 1 mM IPTG for 3 hours produced large quantities of FbpC. However, when large-scale inductions repeated these conditions it was discovered that ~90% of the expressed protein was insoluble (possibly by forming inclusion bodies), so alternative induction conditions were tested.

Conditions that yielded the highest expression of soluble protein were chosen for large-scale expression. Induction at OD_{600} 0.8 with 0.2 mM IPTG for 4-5 hours at 25 °C gave the best expression of soluble protein. Terrific broth was chosen as the preferred medium as this broth allowed high-density cell growth that produced large quantities of soluble FbpC. Other media tested were 2xYT and an auto-induction media, but this, and the use of different *E. coli* expression cell lines (HMS174(DE3) and B834(DE3)) produced less overall soluble protein.

5.1.4 Purification of *N. gonorrhoeae* FbpC-His_6

Several methods of purification were investigated to obtain pure FbpC-His_6. Ni^{2+}-affinity chromatography was used as a first step purification in all trials, and several different affinity resins from various commercial sources were tested. Ni^{2+}-NTA Sepharose High Performance resin (GE Healthcare), Ni^{2+}-NTA agarose (Invitrogen) and His-Link silica resin (Promega) all bound FbpC-His_6 to high capacity (> 2 mg/mL FbpC-His_6/mL resin), but differed in the amount of unspecific binding of non-His-tagged proteins in the cell-free extract. Ni^{2+}-NTA Sepharose High Performance resin bound FbpC-His_6 to the highest capacity, but also bound large amounts of untagged protein (> 30%), possibly via anionic interactions with the resin. Increasing the concentration of NaCl did not decrease the amount of non-specific binding, nor did increasing the concentration of imidazole in the wash buffer (this caused leaching of the bound FbpC-His_6 into the wash fractions). Ni^{2+}-NTA agarose had less unspecific protein binding to the resin (< 10%), but had the lowest binding capacity of all three resins, whereas the His-Link resin had an acceptable

level of unspecific binding (< 10%) to the resin but also had a high binding capacity. His-Link resin was therefore chosen for the first round of purification of FbpC-His_6.

The optimum concentration of imidazole in the load and wash buffers was determined to be 20 mM and 50 mM, respectively, and 250 mM in the elution buffer. Attempts to dialyse the protein into wash buffer containing no imidazole resulted in the precipitation of FbpC-His_6, even at 4 °C. Desalting by PD10 column resulted in loss of >80% of the protein, and thus protein was frozen (-20 °C) at this stage if it was to be stored for any more than a few hours, until further purification (**Figure 5.6**).

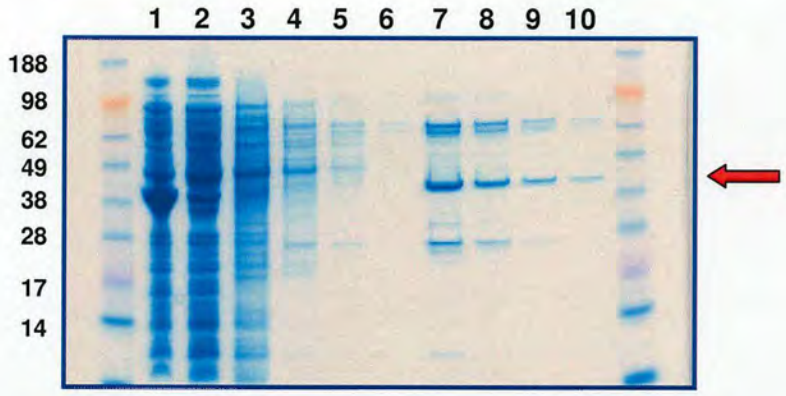

Figure 5.6. SDS-PAGE of Ni^{2+}-NTA purification of FbpC-His_6. Lanes 1-6, cell-free extract, flow-through and wash fractions; lanes 7-10, elution fractions containing FbpC-His_6 (~40 kDa; red arrow).

As a second round of purification, anion exchange chromatography (Capto Q; GE Healthcare) was originally chosen. This did provide relatively pure protein (~98% by SDS-PAGE), but purity varied from batch to batch and ~10% of FbpC was lost during the process. Therefore other methods were investigated. Gel filtration with a 26/60 Sephadex 75 High Performance Prep Grade (GE Healthcare) did not adequately purify the FbpC-His_6, probably due to the high concentration of glycerol

in the buffers. It was also noted that ~15% of the total FbpC-His_6 was lost during this type of purification. Cobalt-affinity chromatography (TALON resin; Clontech) was performed to investigate if the final purity and recovery of FbpC-His_6 could be improved. This form of affinity chromatography binds hexahistidine tags with higher specificity, thus improving purity, but with lower affinity. The trade-off for this higher specificity is that the resin has a much lower binding capacity (~1-5 mg/mL resin) compared with Ni^{2+}-NTA resin (typically 10-20 mg/mL resin). This purification step required dilution of the protein from the first round of purification with wash buffer (containing no imidazole) to reduce the concentration of imidazole to ~20 mM and then incubation with equilibrated TALON (Co^{2+}-affinity) resin (Clontech) for 1-2 hours. The resin was then washed in a similar fashion to the first round of purification except that the concentration of imidazole was kept at 20 mM, and the bound protein eluted with 200 mM imidazole. This method yielded the purest protein (>99% by SDS-PAGE) with the best recovery (>95%), and thus this two-stage affinity purification was chosen as the preferred method for the purification of FbpC-His_6 (**Figure 5.7**).

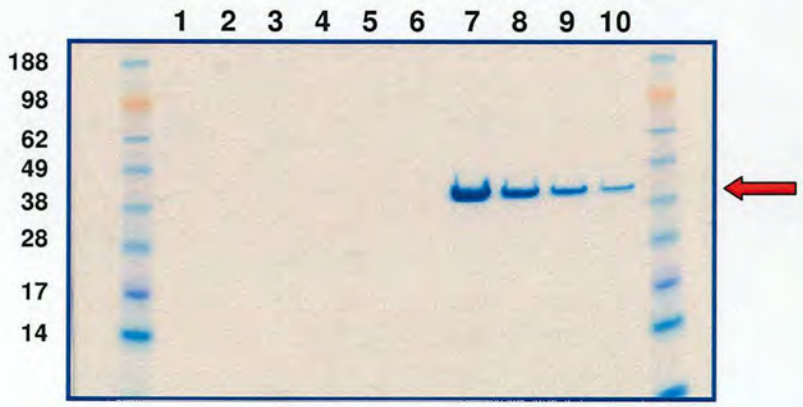

Figure 5.7. SDS-PAGE of TALON resin purification of FbpC-His_6. Lanes 1-6, flow-through and wash fractions; lanes 7-10, elution fractions containing pure FbpC-His_6 (~40 kDa; red arrow).

Purified FbpC-His_6 was routinely stored at –20 °C in aliquots with no loss of activity after repeated freeze-thaw cycles.

The yield of soluble FbpC was typically determined to be ~5 mg/L cell culture.

5.1.5 Expression of SeMet labelled *N. gonorrhoeae* FbpC-His_6 in *E. coli*

Selenomethionine labelling of FbpC was conducted to aid crystal structure determination, and involved replacing native methionine residues in the protein with the selenium containing analogue. This introduces a heavy atom(s) into the protein that allows for phasing of the crystal structure. Two different methods of selenomethionine labelling were attempted. The first of these was by a method published by Studier and co-workers, that utilises an auto-inducing SeMet labelling protocol (2). This procedure did not produce high amounts of soluble SeMet labelled FbpC, and thus another method for SeMet labelling was sought.

A novel method was optimised for the production of large quantites of SeMet labelled protein based on an existing minimal media protocol (3). Briefly, to a 1x M9 salts media was added $MgSO_4$, glucose, thiamine and biotin (as essential co-factors), and a trace metal solution containing a high concentration (10 μM) iron (to allow the production cytochromes for aerobic growth). BL21(DE3) cells transformed with pET-28a/FbpC/Ng were grown in this media (typically 6 L culture) to an OD_{600} of 0.7-0.8, and then amino acids (K, F, T, I, L and V) and selenomethionine were added. Vitamin B_{12} was also added to stimulate the regeneration of selenomethionine from selenohomocysteine via the homocysteine

methyltransferase pathway (*MetH*) (2). Growth was continued for 15 min to allow the inhibition of methionine synthesis to start, and then the cells were induced with 0.2 mM IPTG for 3 hours at 25 °C. Induction at 37 °C with 1 mM IPTG produced large amounts of insoluble protein in a similar fashion to that observed for the wild-type protein. The cells would routinely grow to an OD_{600} of 4-5 at 25 °C.

5.1.6 Purification of SeMet labelled *N. gonorrhoeae* FbpC-His_6

SeMet labelled FbpC-His_6 was purified using an identical method that was optimised for the wild-type protein. A reducing agent (1 mM TCEP) was added to all buffers throughout the purification to inhibit the oxidation of selenomethionine residues that had been incorporated into the protein. The yield of SeMet labelled FbpC-His_6 was determined to be 2-5 mg/L culture (**Figure 5.8**).

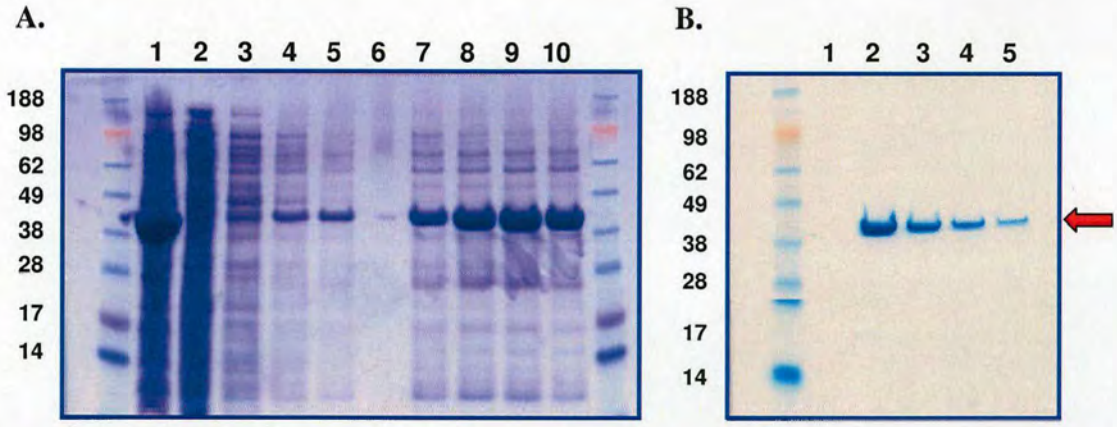

Figure 5.8. A. SDS-PAGE of Ni^{2+}-NTA purification of SeMet-FbpC-His_6. Lanes 1-6, cell-free extract, flow-through and wash fractions; lanes 7-10, elution fractions containing SeMet-FbpC-His_6 (~40 kDa). **B. SDS-PAGE of TALON resin purification of SeMet-FbpC-His_6.** Lanes 2-5, elution fractions containing pure SeMet-FbpC-His_6 (~40 kDa; red arrow).

SeMet labelled protein was no less stable that wild-type FbpC-His_6 and was stored at -20 °C with no loss of activity. Incorporation of selenomethioine residues and the number of SeMet per molecule of FbpC could not be confirmed by mass spectrometry (data not shown).

5.1.7 ATPase Activity of Wild-Type and SeMet labelled *N. gonorrhoeae* FbpC-His_6

5.1.7.1 ATPase Activity of Wild-Type *N. gonorrhoeae* FbpC-His_6

Several different methods of determining the amount of ATP hydrolysis were investigated, including a pyruvate kinase/lactose dehydrogenase (PK/LDH) assay, a malachite green assay and a commercially available kit (EnzCheck) manufactured by Invitrogen (4,5). However, the presence of high concentrations of glycerol and ATP in the reaction buffer caused interference with all of these colorimetric assays, and yielded erroneous results. The assay eventually chosen for the determination of the ATPase activity of FbpC-His_6 did not suffer from these interferences, and measured the amount of inorganic phosphate (P_i) liberated by the hydrolysis of ATP. The assay is dependent upon the formation of a complex between phosphate and molybdate in acid solution to form a yellow-coloured phosphomolybdate complex $\{12\ MoO_3 + H_2PO_4^- \longrightarrow (H_2PMo_{12}O_{40})^-\}$. The phosphomolybdate complex is then reduced by ascorbic acid, causing a characteristic molybdenum blue species that has an absorbance maximum at 850 nm (6,7). Results of the ATPase assay for wild-type assay are presented in **Figure 5.9**.

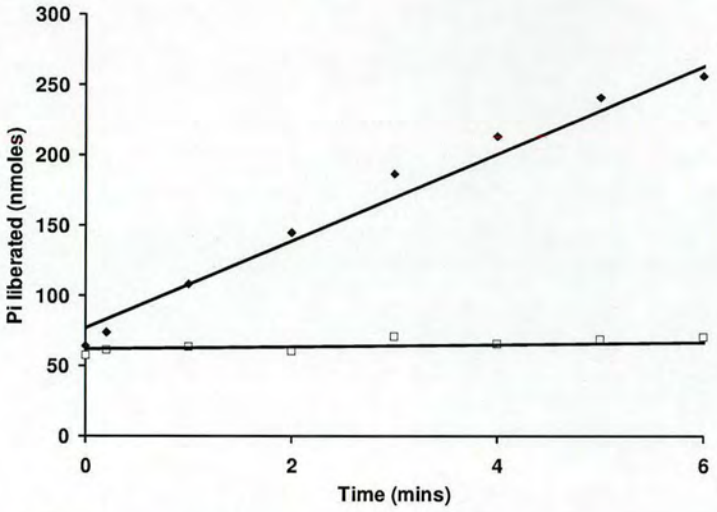

Figure 5.9. ATPase assay of FbpC. The activity of the protein was determined to be 0.4-0.6 μmols P_i liberated/min/mg of FbpC-His_6. ◆ Assay plus $MgCl_2$, □ assay minus $MgCl_2$. Results are an average of three repeats.

Analysis of the rate of ATP hydrolysis yielded that the activity of wild-type protein was in the range of 0.4-0.6 mols P_i liberated/min/mg of FbpC-His_6. Analysis of the kinetics of ATP hydrolysis could not be fitted to Michaelis-Menton analysis, as at low ATP concentrations FbpC was insoluble.

5.1.7.2 ATPase Activity of SeMet Labelled *N. gonorrhoeae* FbpC-His_6

The effect of incorporation of selenomethionine residues upon ATPase activity was determined by the same method as that performed for the wild-type protein. Results of the ATPase assay performed on SeMet labelled FbpC-His_6 are presented in **Figure 5.10**.

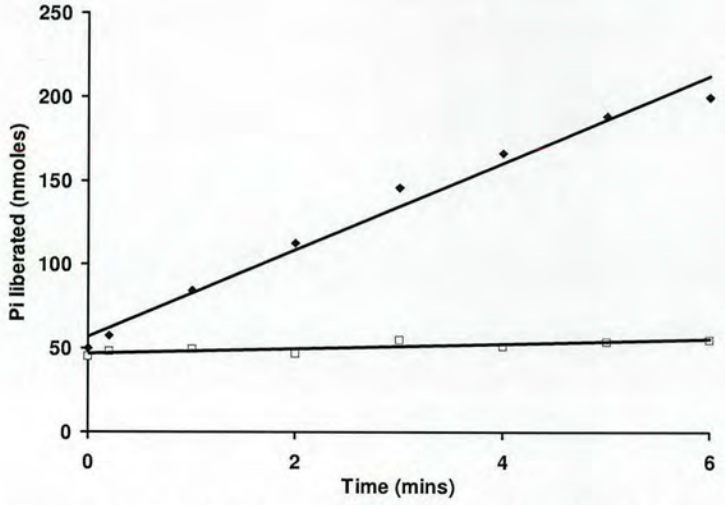

Figure 5.10. ATPase assay of SeMet-FbpC-His$_6$. The activity of the protein was determined to be 0.4-0.6 µmols P_i liberated/min/mg of SeMet-FbpC-His$_6$. ◆ Assay plus $MgCl_2$, □ assay minus $MgCl_2$. Results are an average of three repeats.

Analysis of the rate of ATP hydrolysis yielded that the activity of wild-type protein was in the range of 0.4-0.6 mols P_i liberated/min/mg of SeMet-FbpC-His$_6$. Again, Analysis of the kinetics of ATP hydrolysis could not be fitted to Michaelis-Menton analysis, as at low ATP concentrations FbpC was insoluble.

5.1.8 Peptide Mass Fingerprinting of *N. gonorrhoeae* FbpC-His$_6$

SDS-PAGE was performed on a sample of FbpC-His$_6$. The band proposed to be FbpC-His$_6$ was cut-out of the gel and was subjected to in-gel tryptic digest. Analysis of the peptide fragments obtained from the tryptic digest identified FbpC from *N. gonorrhoeae* as a best match with a MOWSE score of 2.2×10^6. The next closest match had a MOWSE score of 90.4.

The MALDI-TOF spectrum obtained for the in-gel trypsin digest of the gel band observed at ~40 kDa is provided in **Appendix 3**.

5.1.9 Crystallisation Trials of *N. gonorrhoeae* FbpC-His_6

Crystallisation trials were carried out in collaboration with Dr Simon Newstead working in Prof So Iwata's Membrane Protein Crystallography Group at Imperial College, London.

Conditions that yielded crystals are summarised in **Table 5.3**.

Table 5.3. Crystallisation conditions that yielded crystals of FbpC.

Crystallisation condition
0.2 M magnesium acetate tetrahydrate, 0.1 M sodium cacodylate pH 6.5, 20% PEG 8000
0.2 M calcium acetate hydrate, 0.1 M sodium cacodylate pH 6.5, 18% PEG 8000
0.2 M calcium acetate hydrate, 0.1 M MES pH 6.0, 20% PEG 8000
0.2 M magnesium acetate tetrahydrate, 20% PEG 3350, pH 7.7
0.1 M succinic acid pH 7.0, 15% PEG 3350
0.15 M DL-malic acid pH 7.0, 20% PEG 3350
0.2 M sodium malonate, 20% PEG 3350
0.2 M sodium bromide, 0.1 M Bis-tris propane pH 6.5, 20% PEG 3350
0.2 M calcium chloride, 0.1 M MES pH 6.50, 20% PEG 6000
0.1 M sodium chloride, 0.1 M sodium HEPES pH 7.5, 12% PEG 4000
0.1 M tris HCl pH 8.5, 10% PEG 8000
0.1 M potassium chloride, 0.01 M magnesium chloride, 0.05 M MES pH 6.0, 10% PEG 400
0.1 M potassium chloride, 0.01 M magnesium chloride, 0.05 M sodium cacodylate pH 6.5, 30% PEG 4000
0.08 M magnesium acetate, 0.05 M sodium cacodylate pH 6.5, 30% PEG 4000
0.1 M potassium chloride, 0.1 M magnesium acetate, 0.05 M sodium cacodylate pH 6.5, 10% PEG 8000

Crystals of wild-type and Se-Met-FbpC were obtained in several of the screening conditions, however, crystals that produced the highest resolution diffraction data of 2.7 Å crystallised out of 0.2 M calcium chloride, 0.1 M MES

buffer pH 6,50 and 20% PEG 6000 (**Figure 5.11**). Preliminary modelling of the data suggested two molecules per asymmetric unit.

A.

B.

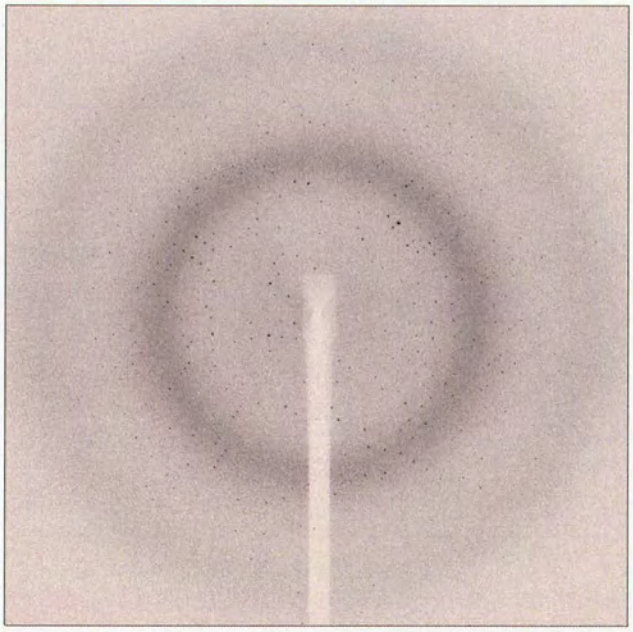

Figure 5.11. A. Crystals of wild-type FbpC that diffracted to 2.7 Å. Crystallisation conditions were 0.2 M $CaCl_2$, 0.1 M MES buffer pH 6,50 and 20% PEG 6000. **B. X-ray diffraction pattern from crystals shown in A.** Crystals were analysed at the ESRF synchrotron radiation source (SRS) in Grenoble, France, and the CCLRC Daresbury SRS, UK.

The structure of FbpC shows strong homology with other members of the NBDs from ABC transporters: The functional complex is composed of a dimer of two FbpC subunits (**Figure 5.12**). The structure obtained in this study appears to have Ca^{2+}-ATP bound at the interface of the two subunits. The ATP bound form was probably isolated due to the high concentrations of Calcium (0.2 M) in the crystallisation buffer keeping the ATP in a non-hydrolysable conformation. The C-terminal regulatory domain appears to have novel fold not previously described for an ABC transporter NBDs. Full analysis of the data is pending.

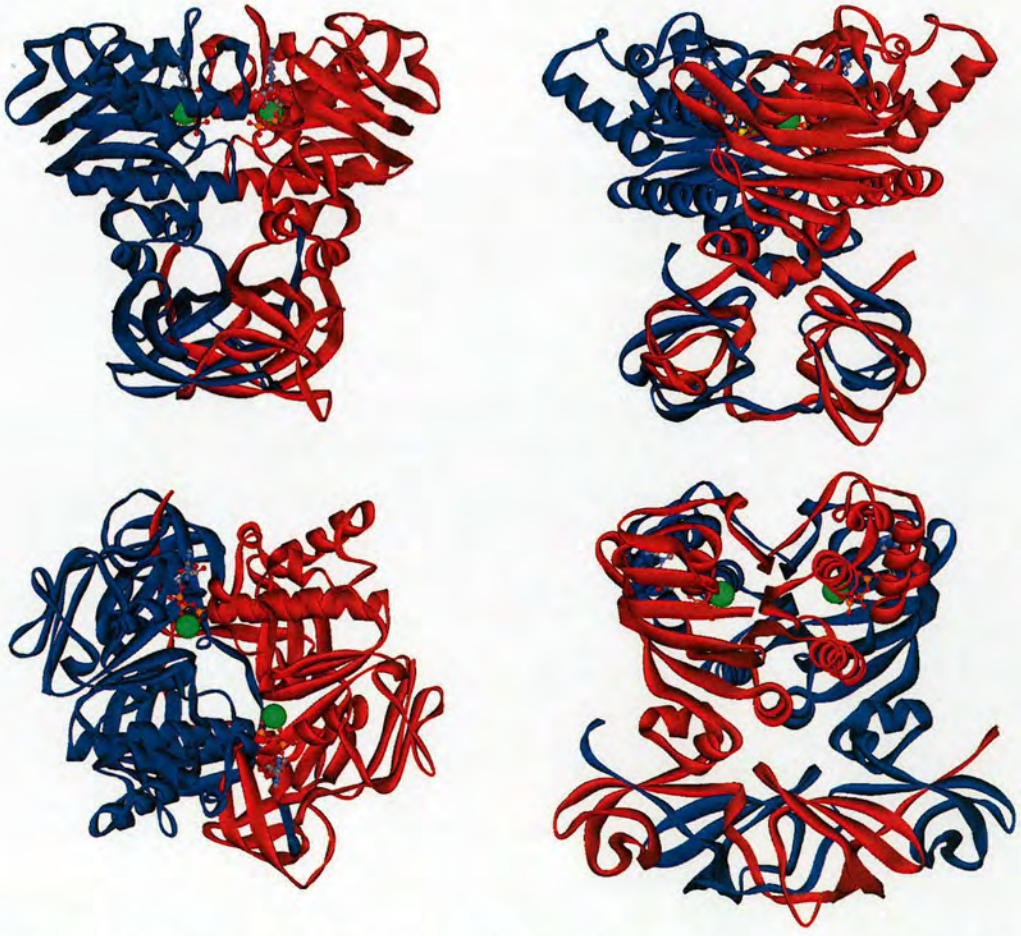

Figure 5.12. 2.7 Å crystal structure of FbpC from *N. gonorrhoeae*. Various views of the FbpC dimer. The FbpC monomers have been coloured red and blue, ATP in ball and stick representation and calcium ions is shown in CPK green. Note the highly structured C-terminal regulatory domain.

5.1.10 Discussion: FbpC

5.1.10.1 Bioinformatic Analysis of FbpC

FbpC is proposed to be the nucleotide-binding domain (NBD) of the FbpABC iron-uptake ABC transporter. FbpC is expected to form a dimer located on the cytoplasmic face of the cytoplasmic membrane in the active form of the complex, and is thought to provide the power-stroke for ligand translocation across the cytoplasmic membrane, via FbpB. Bioinformatic analysis of the amino acid sequence of FbpC revealed that the protein contains all of the ATPase motifs that define this very large family of enzymes. Sequence alignment between FbpC and other members of the NBD from bacterial ABC importers that transport unrelated substrates revealed that FbpC contains a C-terminal domain that is likely to play a role in signal transduction within the cytoplasm. This study is the first to highlight the possible dual role of FbpC *in vivo*: ATPase domain for substrate translocation and a signal transduction domain. These sequence alignments, along with the BLAST results, also emphasise the highly conserved homology among this family of proteins. Interestingly, the BLAST search using the amino acid sequence of FbpC yielded top 20 results that revealed matches for NBD that transport diverse ligands, and very few involved in iron transport. This shows that although a consensus homology is conserved within this protein family, the amino acid sequence varies between the iron-uptake NBD.

5.1.10.2 Expression and Purification of FbpC-His_6

Optimisation of the expression and purification of FbpC-His_6 was performed based on a partially described method (8). FbpC-His_6 was purified to a high level using

Ni^{2+} and Co^{2+}-affinity chromatography, and yields of typically 10-20 mg of protein were produced (2-4 mg/L). FbpC-His_6 was assayed to determine the activity of the enzyme by the use of a previously described ATPase and colorimetric assay (6,7,9). The results of the assays were concordant with values previously published for FbpC-His_6 (8). This previous work (8) determined the rate of ATP hydrolysis by FbpC-His_6 to be 0.5 ± 0.1 μmole P_i liberated/min/mg enzyme: results that are supported by this study. This study also positively identified FbpC-His_6 by peptide mass fingerprinting, however, no accurate mass of full-length FbpC-His_6 could be determined by ESI-MS due to ionisation problems.

Pure FbpC-His_6 was sent to Imperial College for crystallographic screening in order to elucidate the structure of the protein.

5.1.10.3 Expression and Purification of SeMet-FbpC-His_6

Selenomethionine labelled FbpC-His_6 was produced to facilitate crystal structure determination. The protein was labelled by a modification previously described that allowed yields of up to 10 mg to be produced and purified (2). Purification was performed using a two-stage metal-affinity chromatography method: Ni^{2+}-NTA purification followed by TALON resin (Co^{2+}-NTA) chromatography. This purification produced very pure protein (as determined by SDS-PAGE). SeMet-FbpC-His_6 was determined to have the same enzymatic activity as the wild-type protein. The SeMet-labelled protein was sent to Dr Simon Newstead at Imperial College for crystallographic studies.

5.1.10.4 Crystallisation Studies of FbpC-His_6

The X-ray crystallography yielded the 2.7 Å structure of FbpC, and that the NBD contains two molecules per unit cell. This is similar to previously published structures of the nucleotide binding domains of the histidine, vitamin B_{12} and maltose ABC transporters from other Gram-negative bacteria: the resolution of these structures range from 1.5-3.2 Å, and all have two molecules per unit cell (1,10,11). The structure of FbpC obtained had Ca^{2+}-ATP bound and contains a regulatory domain with a novel fold, analogous to that found in MalK, that is proposed to play a role in signal transduction within the cell (1).

5.2 Results: FbpBC

5.2.1 Bioinformatic Analysis of FbpB

FbpB is encoded for by the second gene in the *FbpABC* operon: *FbpB*, 1527 bp. Due to the lack of published literature on FbpB, preliminary bioinformatic analysis was performed on the amino acid sequence (**Appendix 1**). Bioinformatic analysis of the amino acid sequence using Vector NTI v9 (Invitrogen) revealed that the mature protein is expected to contain 509 amino acids and have a molecular mass of 56 310 Da. The protein has a predicted pI of 9.67, making the protein cationic at physiological pH. Other biochemical characteristics of the protein are summarised in **Table 5.4**.

Table 5.4. Amino acid composition of FbpB. The protein is composed of 50% hydrophobic residues, a common finding in membrane proteins.

Amino acids	Number	% by weight	% by frequency
Hydrophobic	256	50.32	50.29
Polar	120	23.53	23.58
Charged	85	20.55	16.70
Basic	36	8.81	7.07
Acidic	19	4.14	3.73

Bioinformatic analysis of the amino acid composition of FbpB revealed that 50% of the amino acid residues are hydrophobic. This, combined with the low percentages of charged, acidic and basic residues, suggests that the protein will be insoluble in aqueous buffers. This is common for integral membrane proteins and hydrophobicity profiling of FbpB using topology prediction programmes (TMHMM and TopPred) available on the ExPASy (**Ex**pert **P**rotein **A**nalysis **Sy**stem) Proteomics server revealed that FbpB is expected to contain 12 transmembrane helices. This indicates that the assembled homodimeric transporter will be composed of 24 transmembrane helices in all (**Figure 5.13**). This modelling also revealed that the N- and C-terminals of FbpB are expected to be cytoplasmic.

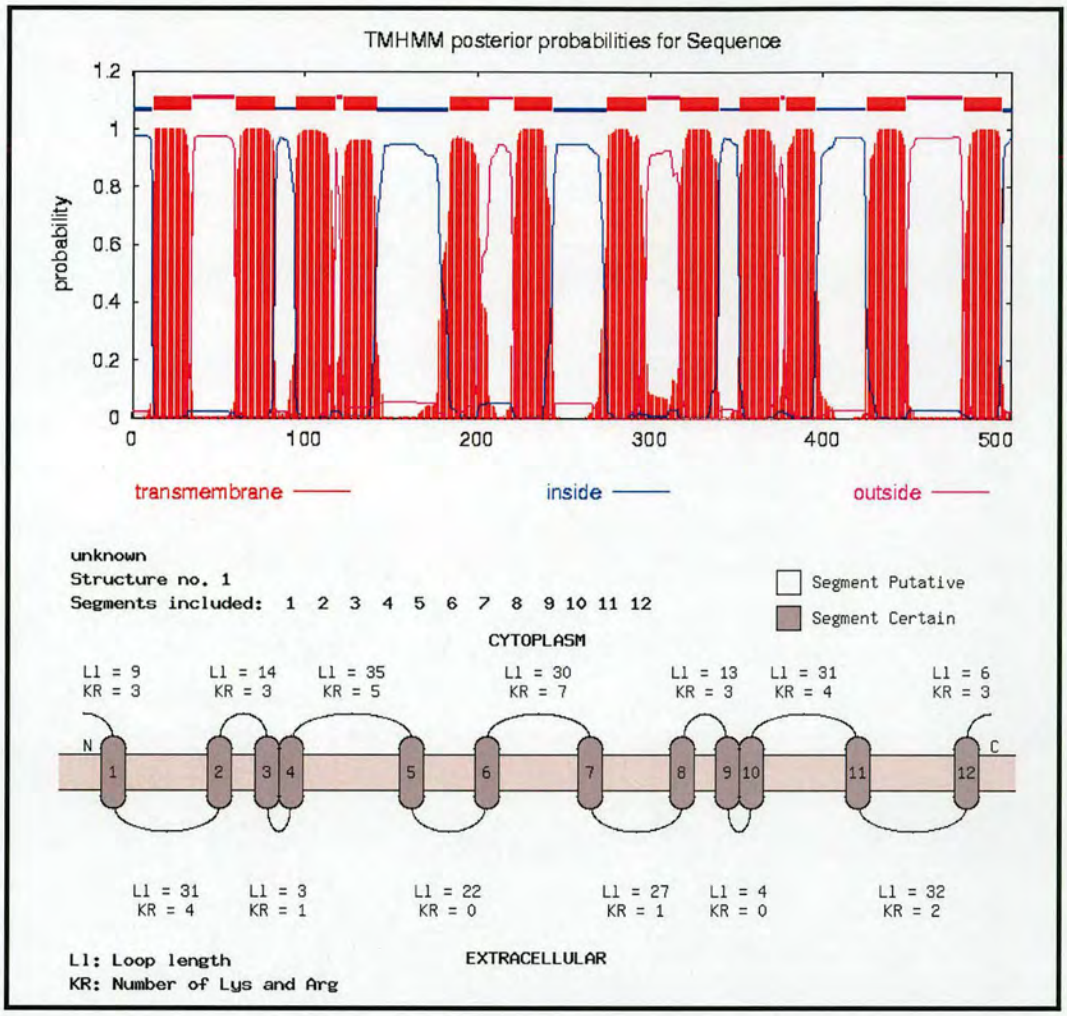

Figure 5.13. Topology mapping of the amino acid sequence of FbpB. FbpB is predicted to contain 12 transmembrane helices when the amino acid sequence is analysed using the topology mapping programmes TMHMM (top) and TopPred (bottom).

The **B**asic **L**ocal **A**lignment **S**earch **T**ool (BLAST) was used to identify known proteins with similar alignment sequences and the results are summarised in **Table 5.5**.

Table 5.5. Top 20 results of the BLAST search performed using the amino acid sequence of FbpB as the query sequence.

Gene description	Species	Accession Number	BLAST Score	E value	Sequence Length	
					Identities	%
ABC transporter, permease protein, iron related	*Neisseria gonorrhoeae* FA 1090	YP_207381	864	0	509/509	100
Iron-uptake permease inner membrane protein	*Neisseria meningitidis Z2491*	NP_283635	849	0	503/509	98
Iron(III) ABC transporter, permease protein	*Neisseria meningitidis* MC58	NP_273676	842	0	502/505	99
FbpB	*Neisseria gonorrhoeae* (no strain given)	AAB63560	770	0	464/511	90
HitB	*Haemophilus influenzae* (no strain given)	AAB32111	608	3×10^{-172}	362/505	71
ABC-type Fe3+ transport system, permease component	*Haemophilus influenzae* R2846	ZP_00154825	607	3×10^{-172}	362/505	71
Iron(III)-transport system permease protein (hFbpB)	*Haemophilus influenzae* 86-028NP	YP_247821	605	2×10^{-171}	360/505	71
Iron(III)-transport system permease protein fbpB 2	*Haemophilus influenzae* (no strain given)	P71338	600	7×10^{-170}	360/505	71
Iron(III) ABC transporter permease protein	*Haemophilus influenzae* Rd KW20	NP_438272	586	1×10^{-165}	343/478	71
Iron(III) ABC transporter, permease protein (hitB)	*Haemophilus influenzae* Rd KW20	AAC21774	580	8×10^{-164}	340/473	71
ABC-type Fe3+ transport system, permease component	*Haemophilus influenzae* R2866	ZP_00203258	567	4×10^{-160}	332/459	72
Iron ABC transporter, permease protein	*Pseudomonas putida* KT2440	NP_746986	348	3×10^{-94}	229/499	45
Iron ABC transporter, permease protein	*Pseudomonas entomophila* L48	YP_610363	337	7×10^{-91}	223/496	44
Binding-protein-dependent ABC transporter inner membrane component	*Pseudomonas fluorescens* PfO-1	YP_346263	330	8×10^{-89}	222/496	44
Hypothetical protein PaerP_01005765	*Pseudomonas aeruginosa* PA7	ZP_01292354	325	3×10^{-87}	232/504	46
Putative iron ABC transporter, permease protein	*Pseudomonas aeruginosa* UCBPP-PA14	YP_793150	324	6×10^{-87}	230/504	45
Iron (III)-transport system permease (HitB)	*Pseudomonas aeruginosa* PAO1	NP_253377	324	6×10^{-87}	230/504	45
Hypothetical protein PaerPA_01000654	*Pseudomonas aeruginosa* PACS2	ZP_01363556	324	8×10^{-87}	229/504	45
ABC-type Fe3+ transport system, permease component	*Pseudomonas aeruginosa* 2192	ZP_00971472	323	1×10^{-86}	229/504	45
ABC-type Fe3+ transport system, permease component	*Pseudomonas aeruginosa* C3719	ZP_00965766	323	1×10^{-86}	229/504	45

The results of the BLAST sequence analysis reveal that the sequence of *N. gonorrhoeae* FbpB shares the highest homology (90-99%), perhaps not surprisingly, to several strains of the *Neisseria spp* FbpB. It also showed significant homology (~71%) to the permease component (HitB) of various strains of the *H. influenzae* iron-uptake ABC-transporter, *HitABC*. Interestingly, FbpB also shares considerable homology (~45%) with the permease component of iron-uptake ABC transport systems and other putative ABC-type permeases from the *Pseudomonas spp*. Unlike FbpC, the FbpB homology shows that the proteins that share closest homology are all involved in iron transport, strongly suggesting that permeases involved in the transport of similar ligands share the strongest sequence homology.

5.2.2 Cloning of FbpBC from *N. gonorrhoeae* Genomic DNA

Two different FbpBC constructs were prepared for this study: pETDuet-1/FbpB/FbpC/Ng and pET-28a/FbpBC/Ng. The pETDuet construct incorporates an N-terminal hexahistidine tag on FbpB (His_6-FbpB), whereas the pET-28a construct incorporates a C-terminal hexahistidine tag on FbpC (FbpC-His_6).

pETDuet-1/FbpB/FbpC/Ng: Ferric-ion binding protein B and C (*FbpBC*) genes were amplified independently from *Neisseria gonorrhoeae* genomic DNA by PCR using FbpB *Bam*HI For and FbpB *Hind*III Rev (for FbpB), and FbpC *Nde*I For and FbpC Stop *Xho*I Rev (for FbpC). Primers were designed to incorporate *Bam*HI and *Hind*III restriction enzyme sites at the 5' and 3' ends of *FbpB*, respectively, and *Nde*I and *Xho*I at the 5' and 3' ends of *FbpC*, respectively. The resulting PCR products were cloned independently into the cloning vector pGEM T-Easy

(Promega) and the constructs verified by DNA sequencing. Plasmids containing the *FbpB* and *FbpC* gene inserts were digested with the relevant restriction enzymes and the fragments corresponding to the correct insert size (~1500 bp for *FbpB* and ~1050 bp for *FbpC*) were ligated into pETDuet-1 co-expression plasmid. Firstly, *FbpC* was ligated into pETDuet-1 cut with *Nde*I and *Xho*I and the ligation mixture transformed into DH5α cells. Transformants containing the pETDuet-1/FbpC construct had their DNA purified by standard procedures using a Qiagen mini-prep kit. The purified pETDuet-1/FbpC plasmid was then cut with the restriction enzymes *Bam*HI and *Hind*III. *FbpB*, cut similarly, was then ligated into the cut vector. The ligation mixture was transformed into DH5α and successful transformants were analysed by restriction digest to confirm the presence of the correct sized inserts. The pETDuet-1 vector not only allows the co-expression of two genes independently but also incorporates an N-terminal hexahistidine tag on the first gene insert (*FbpB*). The construct containing *FbpB* and *FbpC* genes was named pETDuet-1/FbpB/FbpC/Ng (**Figure 5.14**).

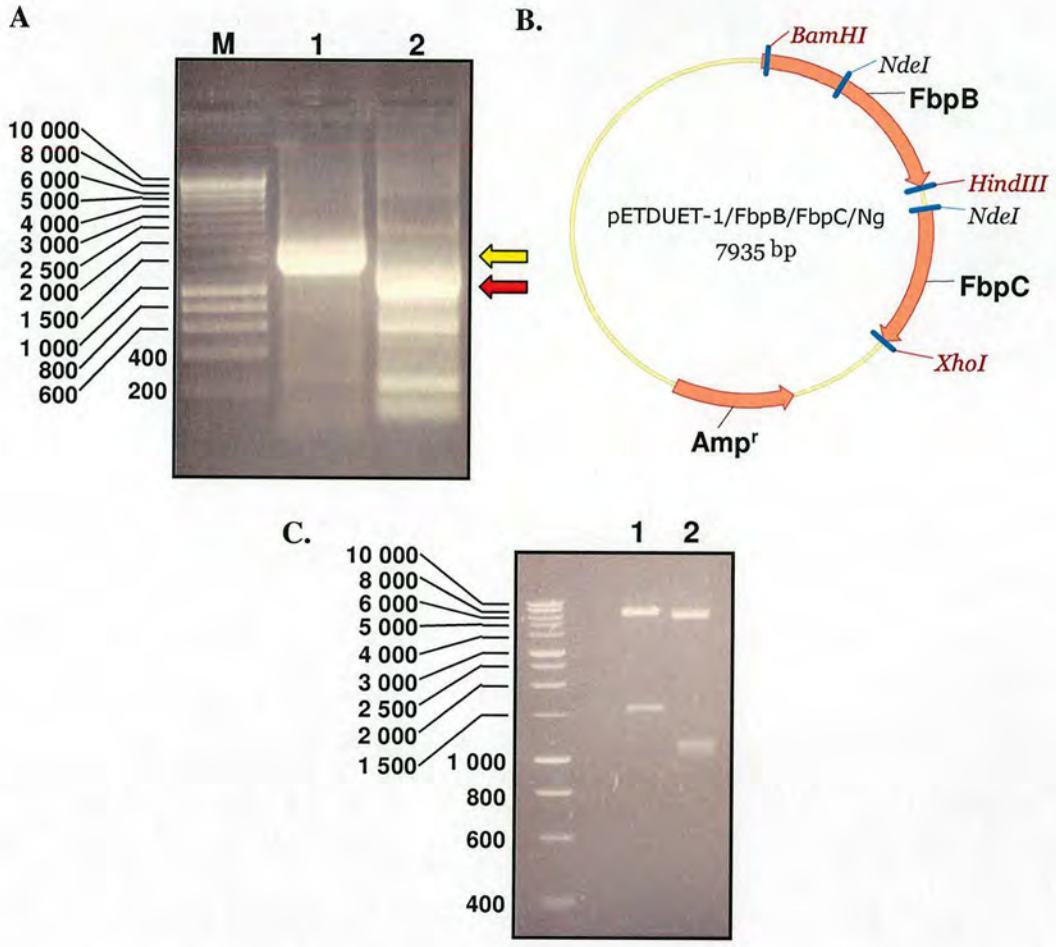

Figure 5.14. A. Agarose DNA gel showing the PCR product fro FbpB and FbpC from reaction from *N. gonorrhoeae* genomic DNA. The DNA fragment corresponding to the FbpB (lane 1, yellow arrow) and FbpC (lane 2, red arrow) genes are highlighted. **B. Vector map of pETDUET-1/FbpB/FbpC/Ng. C. Restriction analysis of pETDUET-1/FbpB/FbpC/Ng.** 1, *Bam*HI/*Hind*III digest yielding a band at ~1500 bp corresponding to FbpB. 2, *Nde*I/*Xho*I digest yielding bands at ~1050 bp corresponding to FbpC and 1150 bp corresponding to a fragment of the FbpB gene. Higher weight bands in both lanes represent the remainder of the pETDUET-1 plasmid.

pET-28a/FbpBC/Ng: Ferric-ion binding protein B and C (*FbpBC*) genes were amplified from *Neisseria gonorrhoeae* genomic DNA by PCR using the primers FbpB *Nco*I For and FbpC *Xho*I Rev. Primers were designed to incorporate an *Nco*I site at the 5' end of the FbpB gene and an *Xho*I restriction enzyme site at the and 3' end of the FbpC gene. The resulting PCR product was cloned into cloning

vector pGEM T-Easy (Promega) and the constructs verified by DNA sequencing. Plasmid containing the *FbpBC* gene insert was digested with *Nco*I and *Xho*I and the fragment corresponding to the correct insert size (~2500 bp) was ligated into pET-28a expression plasmid cut with *Nco*I and *Xho*I. This vector was chosen in order to incorporate a C-terminal hexahistidine tag on FbpC (FbpC-His_6). The ligation reaction was transformed into DH5α *E. coli* cells (Invitrogen) and the plasmid DNA purified (Qiagen mini-prep). Restriction digests confirmed the presence of the correct sized insert, and the construct containing *FbpBC* was named pET-28a/FbpBC/Ng (**Figure 5.15**).

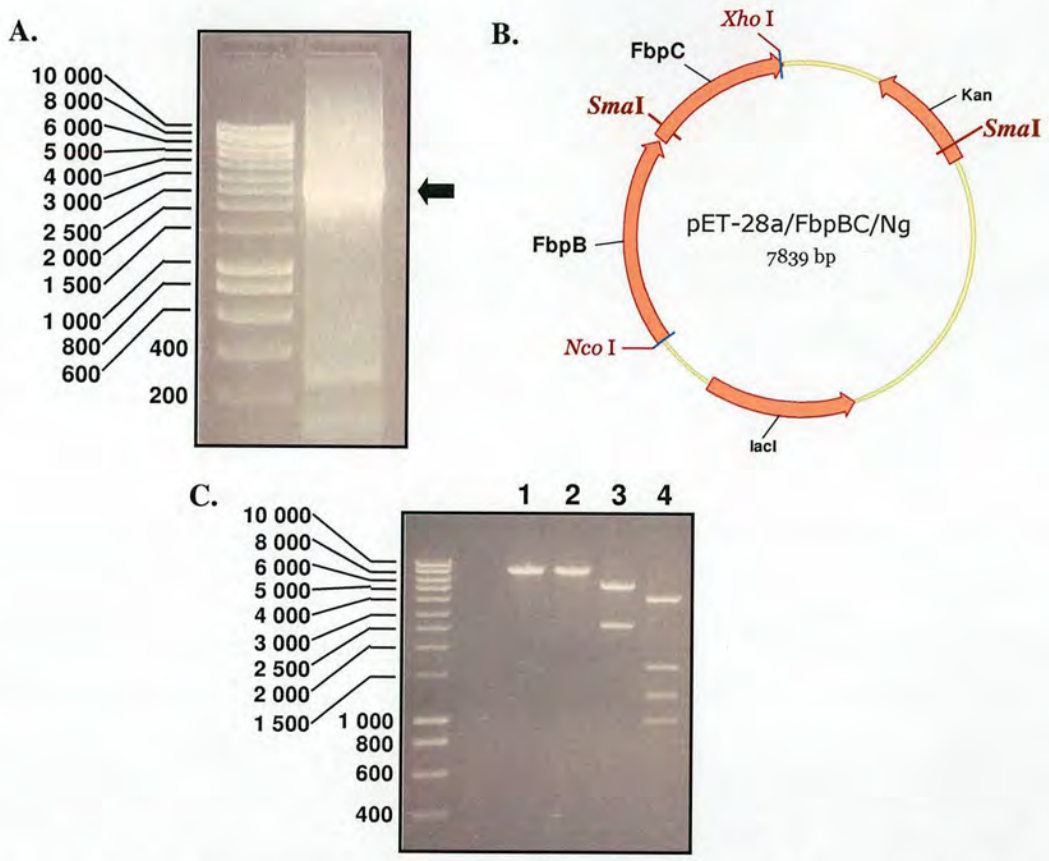

Figure 5.15. A. Agarose DNA gel showing PCR product from FbpBC reaction from *N. gonorrhoeae* genomic DNA. Band corresponding to The FbpBC fragment is highlighted (arrow). **B. Vector diagram of pET-28a/FbpBC/Ng. C. Restriction analysis of pET-28a/FbpBC/Ng.** 1, *Nco*I and 2, *Xho*I single digests yielding bands at the size of the entire plasmid (~7.8 kbp). 3, *Nco*I/*Xho*I double digest yielding a band at ~2500 bp corresponding to FbpBC. 4, *Sma*I single digest yielding bands at ~1000 bp, ~1250 bp, ~1600 bp and 4 kbp.

5.2.3 Co-Expression of *N. gonorrhoeae* FbpBC in *E. coli*

pET-28a/FbpBC/Ng and pETDuet-1/FbpB/FbpC/Ng plasmids were transformed into *E. coli* expression strain BL21(DE3) and grown on LB/kanamycin (30 μg/mL) or LB/ampicillin (100 μg/mL) agar plates, as appropriate.

Small-scale inductions in LB broth at 37 °C with 1 mM IPTG for 3 hours produced large quantities of FbpC visible by SDS-PAGE, but no visible band for FbpB for both constructs. However, Western blot analysis with an anti-C-terminal-

His_6-tag antibody (Invitrogen) of the pET-28a/FbpBC/Ng induced cells confirmed the presence of FbpC-His_6 produced from this construct. As this was the second gene in the construct with the single promotor 5' of the *FbpB* (first) gene, it was assumed that a small amount of FbpB was also expressed. This was partly confirmed when SDS-PAGE and Western blot analysis was performed on the pET/Duet-1/FbpB/FbpC/Ng induced cells. Again, there was a large band observed at the expected molecular mass of FbpC, but no visible overexpression of FbpB on SDS-PAGE. However, relatively large amounts of hexahistidine tagged protein were detected by Western blot analysis using an anti-His_6-tag antibody (Sigma). This protein was assigned as His_6-FbpB.

Large amounts of FbpC were produced from both constructs in a similar fashion to the pET-28a/FbpC/Ng plasmid. It was decided that to reduce the probability of producing insoluble protein (inclusion bodies), the induction conditions that had been optimised for producing high levels of soluble FbpC were chosen for the FbpBC constructs.

Induction at OD_{600} = 0.8 with 0.2 mM IPTG for 4-5 hours at 25 °C gave the best expression of soluble FbpC and reasonable expression of FbpB. Terrific broth was chosen as the preferred medium as this broth allowed the highest-density cell growth. Different *E. coli* expression cell lines (HMS174(DE3) and B834(DE3)) did not improve expression or solubility of the target proteins (data not shown).

5.2.4 Purification of the *N. gonorrhoeae* FbpBC Complex

The method for co-purification of the FbpBC complex relied on purifying the hexahistidine-tagged protein (His_6-FbpB or FbpC-His_6, depending on the construct), which in doing so would co-purify the corresponding protein partner.

Due to the fact that FbpB is proposed to be an inner membrane protein, the first purification stage was to purify (enrich) the inner membrane component from the *E. coli* expression cells. This removed a lot of the potentially contaminating outer membrane and periplasmic proteins that may bind nonspecifically to the chromatographic resin used in the subsequent purification steps. Enrichment of the inner membranes was achieved by first treating the FbpBC expressing cells with lysozyme followed by sonication and then by low *g* centrifugation to remove insoluble outer membrane debris. The resulting opaque supernatant contained the inner membranes. This supernatant was subjected to high *g* ultracentrifugation to pellet the mixed inner membranes, which were golden brown in colour. This pellet contained the inner membrane fraction of the cells (hence, "enriched"), and these were used for purification of the FbpBC complex.

The mixed inner membrane pellets were extracted with the non-ionic detergent *n*-dodecyl-*β*-D-maltopyranoside (DDM, Anatrace) to solubilise the transmembrane domain of the transporter (FbpB), and the extract purified using TALON Co^{2+}-affinity chromatography resin as described above. TALON resin was chosen because it binds hexahistidine tags with a higher specificity than Ni^{2+}-affinity chromatography. As membrane proteins have a higher histidine content, in general, than soluble proteins, TALON resin limits the amount of contaminating non-histidine

tagged protein binding to the media. A relatively high level of purity was obtained for biochemical analysis after just one step of affinity chromatography (**Figure 5.16**).

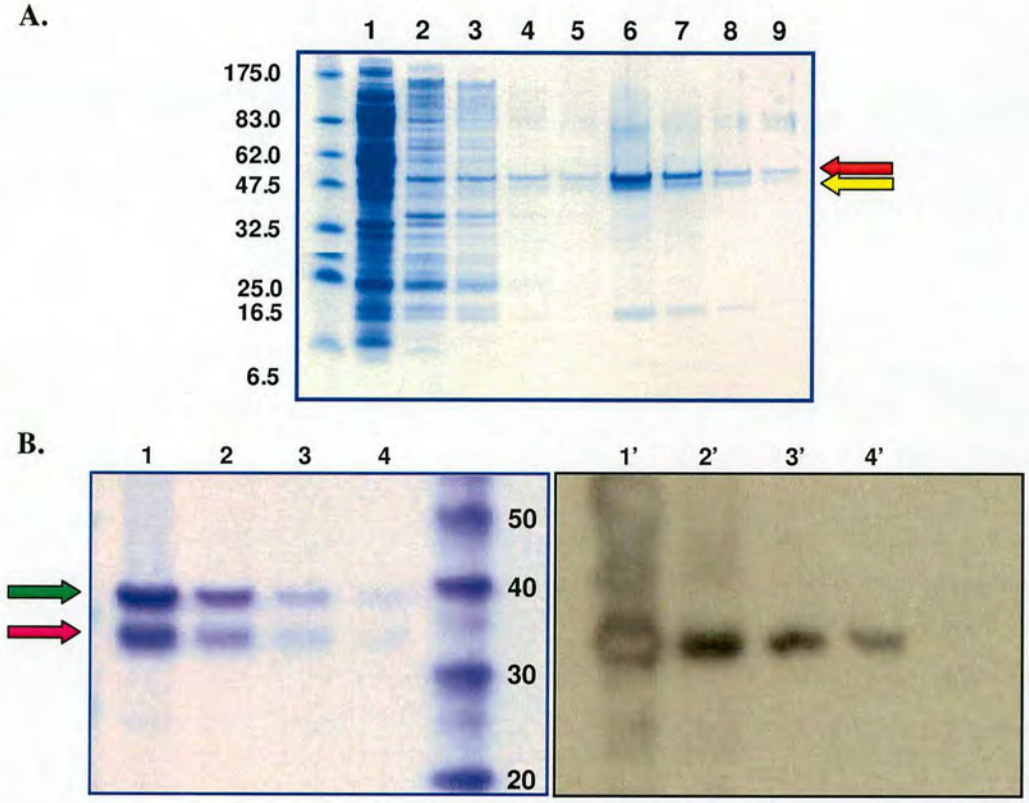

Figure 5.16. A. SDS-PAGE of TALON resin purification of FbpBC. Lanes 1-5, flow-through and wash fractions; lanes 6-9, elution fractions containing FbpB (yellow arrow) and FbpC (red arrow). **B. SDS-PAGE (left) and corresponding Western blot (right) using anti-His_6 antibody of TALON resin purification of SeMet-FbpBC.** Lanes 1-4 and 1'-4', elution fractions containing FbpBC. Note that the lower band is detected by the anti-his_6 antibody Western blot, identifying this band as His_6-FbpB (pink arrow), and verified by peptide mass fingerprinting (PMF). The upper band was identified as FbpC (green arrow) by the same technique.

5.2.5 ATPase Activity of *N. gonorrhoeae* FbpC in the FbpBC Complex

To check that the co-purified FbpC protein was a functional ATPase, the FbpBC complex was assayed in the same way as for the singly expressed FbpC protein. Results are presented in **Figure 5.17**.

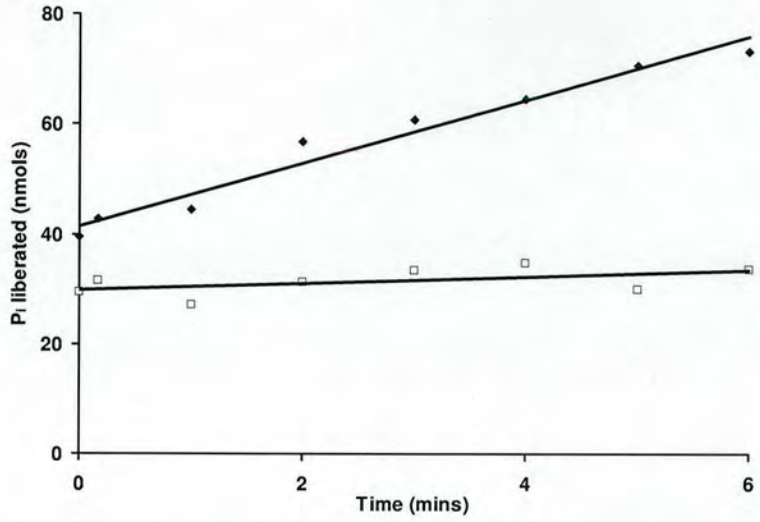

Figure 5.17. ATPase assay of FbpBC. The activity of the protein was determined to be 0.3-0.6 µmols P_i liberated/min/mg of FbpC. ◆ Assay plus $MgCl_2$, □ assay minus $MgCl_2$. Results are an average of three repeats.

The activity of FbpC in the FbpBC complex was determined to be 0.3-0.6 mg P_i liberated/min/mg FbpC. Although this value is the same as that obtained for mono-expressed FbpC-His_6, the accuracy of this value is dependent on the accurate determination of the concentration of FbpC in the FbpBC complex. This was done by measuring the total protein assayed, and dividing this value by two (assuming equal stoichiometry of FbpB:FbpC).

5.2.6 Peptide Mass Fingerprinting of *N. gonorrhoeae* His_6-FbpB

SDS-PAGE was performed on a sample of His_6-FbpB. The band thought to contain His_6-FbpB was cut-out of the gel and was subjected to in-gel tryptic digest. The peptide fragments obtained from the trypsin digest were identified as FbpB from *N. gonorrhoeae* with a probability score of 1.0. Two other *Neisseria spp* iron-permease

proteins with a very similar score were second and third best matches. The next closest match had a probability score of 5.5×10^{-9}.

The MALDI-TOF spectrum obtained for the in-gel trypsin digest of the gel band observed at ~35 kDa is shown in **Appendix 3**.

5.2.7 Discussion: FbpBC

5.2.7.1 Bioinformatic Analysis of FbpB

FbpB is proposed to be a transmembrane permease protein that forms a dimer in the cytoplasmic membrane in the active form of the ABC transporter complex. Not surprisingly for an integral membrane protein, FbpB is composed of 50% hydrophobic residues that make-up the transmembrane-spanning helices. The bioinformatic studies performed on FbpB for this study revealed that each FbpB monomer is predicted to contain 12 transmembrane helices, and thus, the active dimer complex contains 24 transmembrane helices. This is in contrast to a previously published analysis that predicted that FbpB contains 11 transmembrane helices (12). Given that the previous analysis was performed over ten years ago, and that two modern independent topology mapping programmes both yield similar results, it seems likely that the results presented in this report are more accurate. BLAST searches performed for this study revealed that the closest matches were for transmembrane domains (TMD) from other ABC transporters known to be, or proposed to be, involved in iron uptake. This supports the finding that TMD involved in the transport of similar substrates share the highest sequence homology. Interestingly, TMD from only three species were present in top 20 BLAST results:

Neisseria spp, *Haemophilus influenzae* and *Pseudomonas spp*. TMD of iron uptake ABC transporters from other Gram-negative species that may have been expected to appear, such as *Mannheimia*, *Yersinia* and *Serratia*, were found much further down the BLAST results.

5.2.7.2 Expression and Purification of FbpBC

For this study it was decided that FbpB would be best expressed as a dual clone also expressing FbpC, in an attempt to achieve good expression of the permease protein and to express and purify the TMD and NBD together. The co-expression and co-purification of the FbpBC complex was devised and optimised. Two constructs were produced and used to express the complex: one construct yielded an N-terminally hexahistidine-tagged FbpB protein, the other a C-terminally hexahistidine-tagged FbpC protein. In both systems, the histidine-tagged protein was purified by metal-affinity chromatography, and in the process co-purified the corresponding binding partner, presumably due to complex formation *in vivo*. Both components of the transporter were purified to a relatively high level of purity in a single purification step using Co^{2+}-affinity chromatography, and yields of typically 2-4 mg (0.5-1 mg/L) of each protein were achieved. As such, this is first reported description of the purification of FbpB in the literature, and hence the FbpBC complex. This is also the first report of the purification of the transmembrane domain from an iron-uptake ABC transporter. His_6-FbpB was positively identified by peptide mass fingerprinting, however, no accurate mass was determined for the complete protein by ESI-MS due to ionisation problems.

The specific activity of FbpC in the FbpBC complex was determined to be the same as for FbpC expressed from a single gene expressing plasmid.

5.3 FbpABC Association *In Vitro*

5.3.1 FbpBC Pull-Down with Biotinylated FbpA

As a proof of concept experiment before undertaking surface plasmon resonance experiments, a pull-down experiment was devised to investigate FbpABC association *in vitro*. The experiment utilised biotinylated FbpA protein (FbpA-V272C-(M-PEO_2-B)) bound to streptavidin-coated magnetic beads to pull-down the FbpBC complex from a solution containing the purified complex.

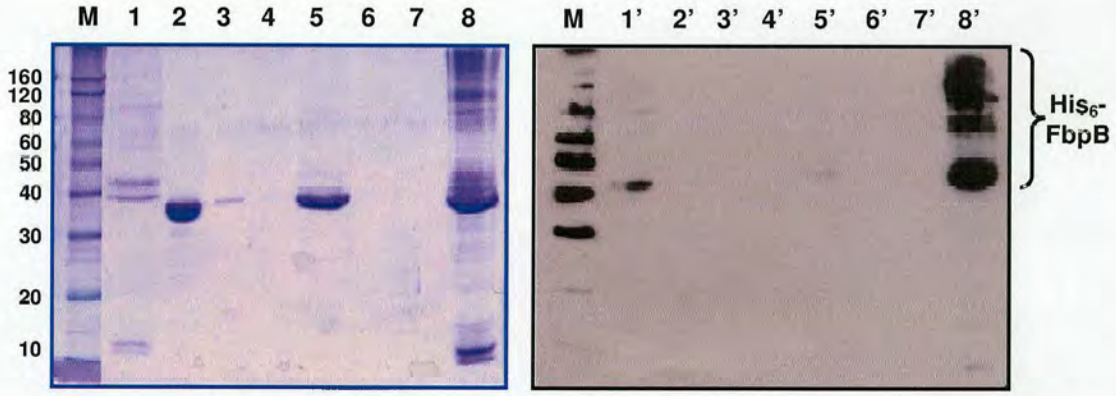

Figure 5.18. SDS-PAGE (left) and corresponding Western blot (using anti-His_6 antibody; right) of the FbpBC pull-down assay using biotinylated FbpA. Lane 1/1', purified FbpBC (positive control); lane 2/2', biotinylated FbpA flow through from streptavidin coated beads; lanes 3/3' and 4/4', wash fractions from streptavidin coated beads; lane 5/5', FbpBC flow-through from FbpA coated streptavidin beads; lanes 6/6' and 7/7', FbpBC wash fractions from FbpA coated streptavidin beads; and lane 8/8', elution fraction from streptavidin beads. Note that FbpB is present in lanes 1' and 5', and complexes of FbpB are present in the elution fractions (lane 8/8') in both the SDS-PAGE and Western blot.

The pull-down experiment of FbpBC using biotinylated FbpA revealed that FbpABC does form a complex *in vitro*. SDS-PAGE and Western blots are presented in **Figure 5.18**.

Analysis of the SDS-PAGE reveals that a large proportion of biotinylated FbpA did not bind to the magnetic streptavidin beads, most likely due to overloading of the beads (lane 2). Wash fractions after loading of biotinylated-FbpA show a small amount of residual biotinylated-FbpA present (lanes 3 and 4). The flow through fraction from FbpBC loading reveals a band at a higher mass than FbpA that is not observed on the Western blot (lane 5/5'). This band was therefore assigned as FbpC. There was no visible band for FbpB observed on the SDS-PAGE, however, the Western blot analysis did reveal a weak band above FbpC that was assigned as His_6-FbpB in the flow through fractions, but not the wash fractions (lanes 5', 6' and 7'). A large amount of protein was detected in the elution fraction by both SDS-PAGE and Western blot (lane 8/8'). Bands identifiable as FbpA and FbpC overlapping one another at a molecular mass of 34-37 kDa are only visible on the SDS-PAGE, while higher molecular mass protein bands are observed on both the SDS-PAGE and Western blots (lane 8/8'). These higher mass bands were assigned as FbpB and FbpB-containing complexes of FbpA, FbpB and FbpC. The assignment of these higher order complexes was not possible due to the fact that FbpB does not run at its predicted mass on SDS-PAGE, thus potentially yielding a false mass for any complex present.

5.3.2 Surface Plasmon Resonance of FbpBC with Biotinylated FbpA

SPR was performed to investigate whether FbpA would form a complex with FbpBC *in vitro*, and to determine the kinetics of any observed association. The method chosen to perform these experiments was to use *holo*-FbpA as the "bait" to which the purified FbpBC complex would bind when flowed over the SPR sensor chip. This was achieved by biotinylating FbpA (FbpA-V272C-(M-PEO_2-B)) to allow attachment, via the biotin moiety, to a streptavidin coated SPR sensor chip. Optimisation of loading biotinylated FbpA was first required before the experiment could be performed. As the Response Units (RU) of the sensogram output trace are measured in arbitrary units, the optimum loading of bait molecule depends on which instrument the experiments are being performed on and the bait molecule itself. For the Biocore T100, the optimum RU for the bait molecule is about 100-200. This roughly equates to about 4% coverage of the sensor chip surface. However, as each bait molecule is unique, the conditions have to be optimised for each bait molecule and experiment.

The sensogram for binding of biotinylated-FbpA (FbpA-V272C-(M-PEO_2-B) to the SPR streptavidin coated chip is shown in **Figure 5.19**. Optimum loading of the biotinylated FbpA molecule was determined to be injection of 40 nM protein for 500 s at a flow rate of 10 μL/min. This gave a loading of ~200 RU.

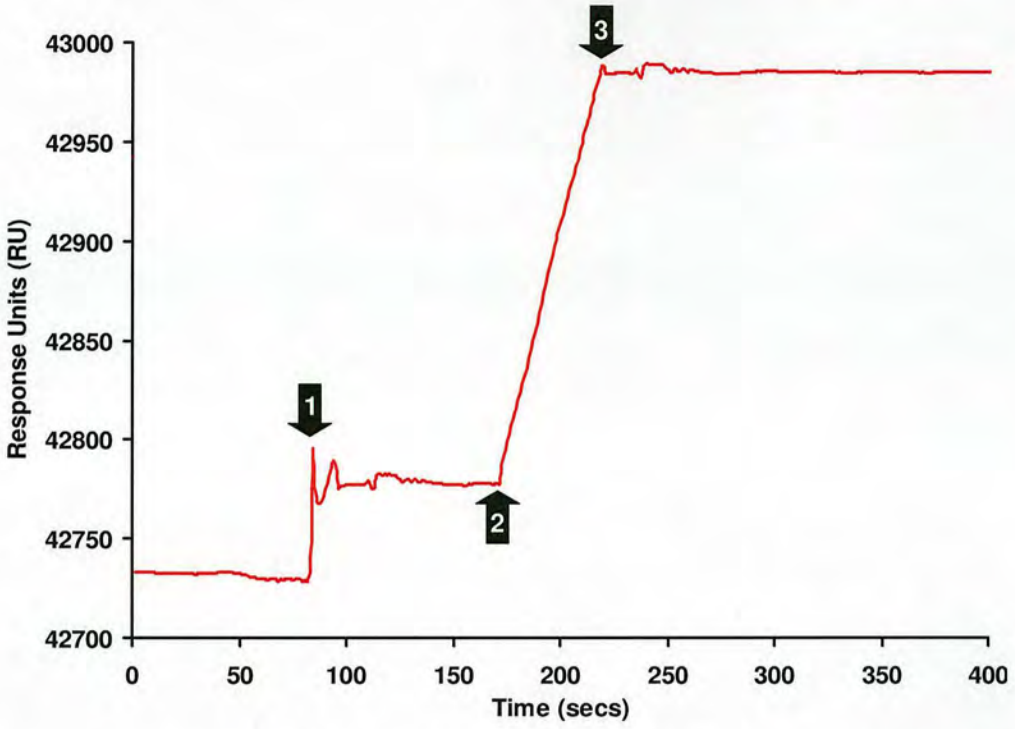

Figure 5.19. Sensogram of biotinylated-FbpA binding to streptavidin-coated SPR sensor chip. Arrow 1, buffer change artifact; arrow 2, biotinylated-FbpA injection start; arrow 3, biotinylated-FbpA injection stop.

FbpBC flow and binding conditions also had to be optimised before the kinetics experiment could be designed. This involved injection of the FbpBC complex over the FbpA loaded surface at different flow rates and for different times to achieve a response levels that would yield results that could be analysed effectively and accurately. However, it was noted during this optimisation process that the FbpABC complex was very stable. After association of the complex on the sensor chip surface, FbpBC did not readily dissociate from FbpA after injection of the FbpBC complex was ceased, and required in excess of several hours of continuous washing with buffer to dissociate less than 50% of the complex. Numerous washing conditions were tested, including high salt, low pH and high concentrations of $MgCl_2$, to induce FbpBC dissociation from FbpA, but none of

these conditions was successful for accelerating dissociation of the complex. As such, it was not possible to regenerate the sensor surface back to its "FbpA-bound only" initial conditions that would be required for accurate analysis of the data. Different buffer conditions were also investigated, but this made no difference to the dissociation time. It was decided to continue with the FbpA/FbpBC kinetics experiment, but leaving 4000 s between injections of different concentrations of FbpBC to allow partial regeneration of the sensor surface. The sensogram of the FbpABC SPR experiment is presented in **Figure 5.20**.

A.

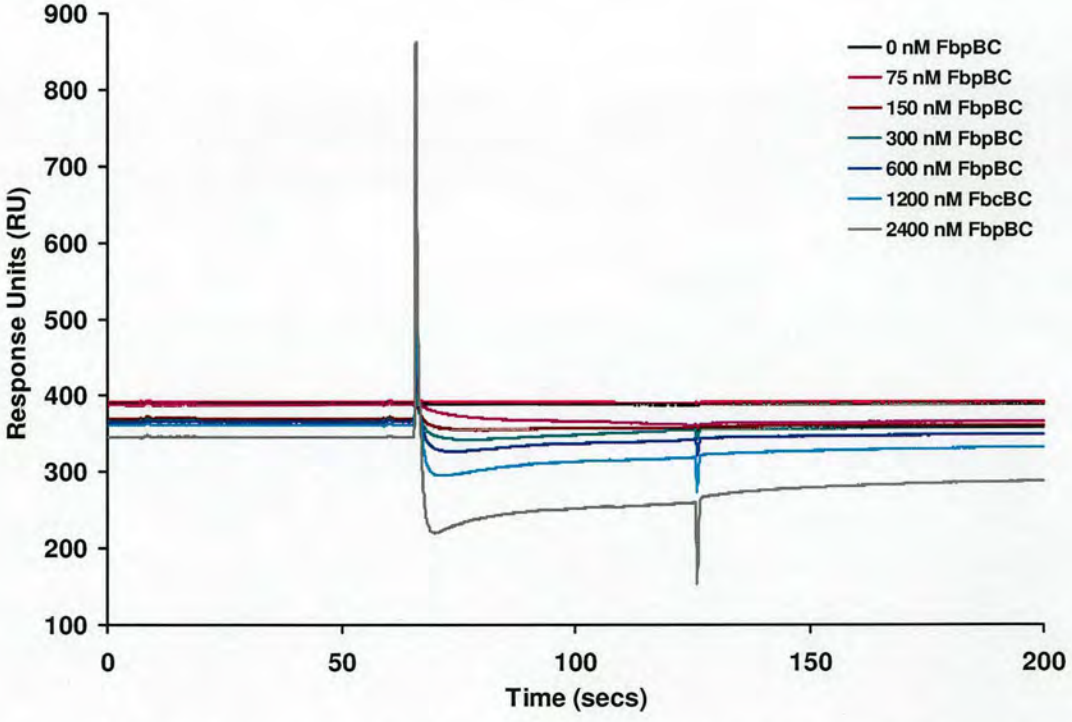

Figure 5.20. A, Sensograms of FbpBC association with biotinylated-FbpA bound to streptavidin-coated SPR sensor ship. B (next page), detail of sensogram curves. Concentrations of FbpBC are indicated in inset. Injection of FbpBC was at ~70 secs and each injection cycle was 3750 secs (only first 200 secs plotted) to allow regeneration of sensor surface (only ~50 % achieved). Due to inversion of the sensogram curves, no kinetic information about complex formation could be determined, however, concentration-dependent association was observed. Spikes at injection time-point and at ~130 secs are artifacts.

Figure 5.20 (continued). Part B. See previous page for legend.

B.

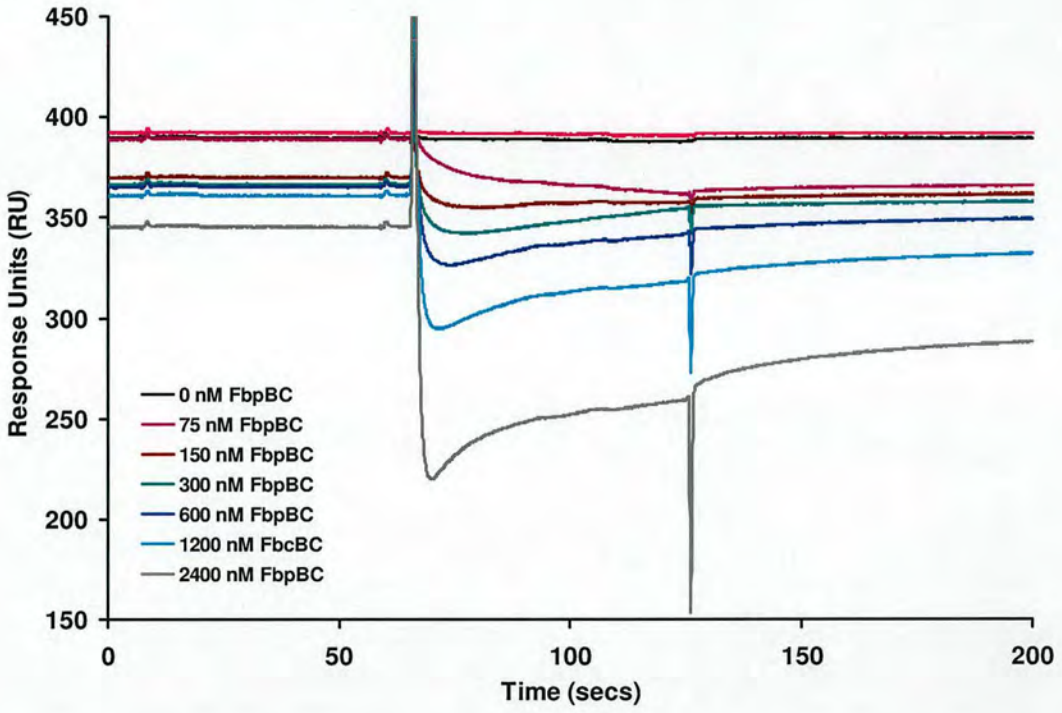

The data show that surface plasmon resonance using biotinylated FbpA attached to a streptavidin coated sensor chip to capture FbpBC was only partially successful. Although the results of the assay revealed that there was a definite concentration dependent binding of FbpBC to FbpA, large amounts of nonspecific binding of the FbpBC complex to the reference cell caused the sensogram to be inverted. This, combined with the stability of the assembled FbpABC complex, made the data impossible to analyse to obtain meaningful kinetic or affinity data.

The results do prove that the FbpABC do form a complex *in vitro* and that the complex is very stable. They also show a concentration dependent association of the three-component complex.

5.3.3 Discussion: FbpABC Association *In Vitro*

The association of the FbpABC *in vitro* was investigated by a pull-down experiment and by surface plasmon resonance (SPR).

The pull-down experiment of purified FbpBC complex by a biotinylated FbpA (FbpA-V272C-(M-PEO_2-B)) bound to streptavidin-coated magnetic beads revealed that a FbpABC complex formed *in vitro*. It was not possible, however, to determine accurately the stoichiometry of the complexes formed due to the evidence that FbpB did not run at its expected mass on SDS-PAGE or Western blot, thus yielding erroneous masses for any complexes formed. Also, the elution method from the streptavidin beads would denature all proteins bound, and could lead to unspecific protein aggregation. However, the experiment did prove that FbpBC binds to FbpA *in vitro*.

Unfortunately the SPR experiments did not provide results that could be interpreted in terms of affinity of FbpA for FbpBC, or any indication of the kinetics of complex formation. Nonspecific binding of the FbpBC complex to the reference channel caused the sensograms to be inverted, meaning that the results of any calculations based on the data were unreliable. However, there was a concentration-dependent effect in the inverted sensograms, suggesting there was FbpABC complex formation in the test channel. It was also noted during optimisation of the binding conditions before the experiment was performed that the FbpABC complex was very stable once formed. FbpBC would not readily dissociate from FbpA even when washed with high salt and low pH buffer conditions. This effect hampered the experiment as, for reliable interpretable data, it must be possible to return the sensor-

chip surface back to the starting conditions by dissociating the formed complex, and this was prohibited in the case of FbpBC by irreversible FbpABC complex formation. Future experiments could use *apo*-FbpA to investigate association of the complex, as it would be expected that no complex formation should occur.

5.4 Iron-59 Uptake Assays in Cells Expressing the *FbpABC* Operon

5.4.1 Cloning of FbpABC from *N. gonorrhoeae* Genomic DNA

Ferric-ion binding protein A, B and C (*FbpABC*) genes were amplified from *Neisseria gonorrhoeae* genomic DNA by PCR using the primers FbpA *Nco*I For and FbpC *Xho*I Rev. Primers were designed to incorporate an *Nco*I site at the 5' end of the FbpA gene and an *Xho*I restriction enzyme site at the and 3' end of the FbpC gene. The resulting PCR product was cloned into cloning vector pGEM T-Easy (Promega) and the constructs verified by DNA sequencing. Plasmid containing the *FbpABC* gene insert was digested with *Nco*I and *Xho*I and the fragment corresponding to the correct insert size (~3200 bp) was ligated into pET-28a expression plasmid cut with *Nco*I and *Xho*I. This vector was chosen to incorporate a C-terminal hexahistidine tag on FbpC for detection purposes. The ligation reaction was transformed into DH5α *E. coli* cells (Invitrogen) and the plasmid DNA purified (Qiagen mini-prep). Restriction digests confirmed the presence of the correct sized insert, and the construct containing *FbpABC* was named pET-28a/FbpABC/Ng (**Figure 5.21**).

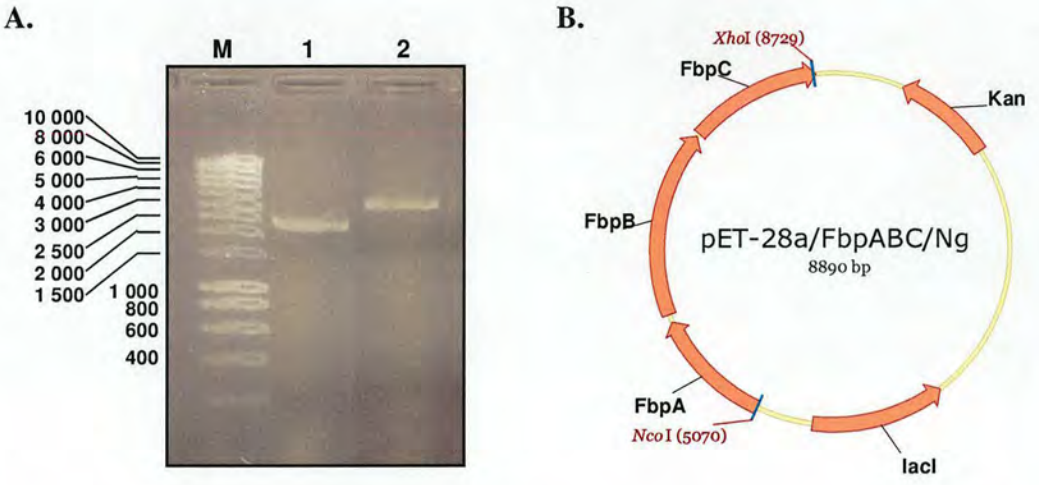

Figure 5.21. A. Agarose DNA gel of PCR products from *N. gonorrhoeae* genomic DNA. 1, FbpBC fragment and 2, FbpABC full operon used for uptake assays. **B. Plasmid map of pET-28a/FbpABC/Ng.**

Expression of the operon was checked by Western blot analysis, using an anti-C-terminal-His_6 antibody to probe for FbpC-His_6, on whole-cell extracts of mini-inductions (2 mL).

5.4.2 Iron-59 Uptake Assay

An iron-uptake was employed to elucidate if the *FbpABC* operon, when expressed in *E. coli*, would form an active iron transport complex *in vivo*. A radioactive iron assay was chosen to perform this analysis. The assay was based on a similar assay performed on the *HitABC* iron-uptake ABC transporter from *H. influenzae* by Anderson *et al* (13). In the reported work the authors used an *E. coli* cell line (H-1443) that was deficient in the siderophore enterochelin, as the host organism. The experiment for this study was performed in BL21(DE3) *E. coli* cells using two negative controls: a non-induced sample of cells transformed with the FbpABC plasmid (pETDuet-1/FbpB/FbpC/Ng), and an induced sample of cells expressing the

FbpC (pET-28a/FbpC/Ng) component of the transporter. The results of the assay are presented in **Figure 5.22**.

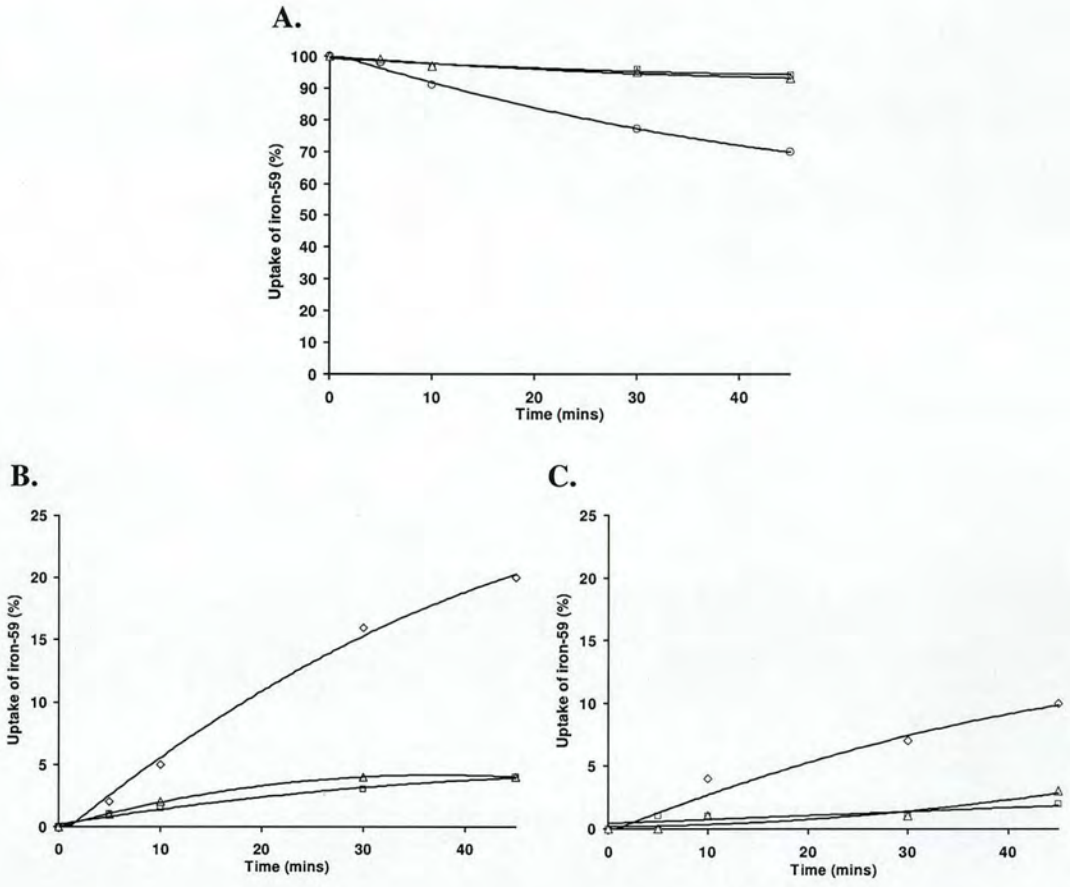

Figure 5.22. Iron-59 uptake by FbpABC expressing cells. **A**, iron-59 remaining in cell-free fraction (broth supernatant); **B**, iron-59 in periplasmic fraction; **C**, iron-59 in cytoplasmic fraction. ○ and ◇ , FbpABC-induced cells; Δ, FbpABC-non-induced cells; □, FbpC-induced cells.

The results reveal that cells expressing the FbpABC operon uptake radioactive iron-59 at a greater rate than uninduced cells containing the same plasmid, and induced cells expressing the NBD of the FbpABC transporter. The FbpABC induced cells uptake iron-59 into the periplasm and the cytoplasm, strongly suggesting that the FbpABC complex is properly functioning *in vivo*. FbpABC-expressing cells uptake ~25 times more total iron-59 than non-expressing cells, and

of this iron ~20% is present in the periplasm after 45 mins and ~10% is present in the cytoplasm after the same time. This is ~4-times more iron than is transported into the periplasm and cytoplasm of non-FbpABC-expressing cells.

5.4.3 Discussion: Iron Uptake by *FbpABC* Expressing Cells

The iron-59 uptake assays showed that a functional FbpABC complex is formed *in vivo* when the operon is expressed in *E. coli*. This supports the work performed by Anderson *et al*, although they used a different *E. coli* host organism that was deficient in the siderophore enterochelin. In this study the authors present kinetic analysis for the uptake of iron by the *HitABC* operon from *H. influenzae*, however, because the work was performed in the non-parent organism, how relevant these values are is unknown and may give a false impression of the real values (13). Expression of the genes investigated in this research varied greatly depending on the plasmid construct used and the expression/induction conditions employed. The results of this study are qualitative rather than quantitative, and reveal that the transporter is functional *in vivo*. To obtain kinetic information, studies similar to those performed on the vitamin B_{12} transporter would have to be carried out (14). In the latter case, TMD and NBD (BtuCD) were incorporated into proteoliposomes and known concentrations of radioactively-labelled substrate-loaded PBP (BtuF) were used to determine rate of uptake of the substrate. Similar experiments for FbpABC are required to allow determination of the rate of uptake of iron by this ABC transporter.

5.5 Chapter 5 References

1. Diederichs, K., Diez, J., Greller, G., Muller, C., Breed, J., Schnell, C., Vonrhein, C., Boos, W., and Welte, W. (2000) *Embo. J.* **19**, 5951-5961
2. Studier, F. W. (2005) *Protein Expr. Purif.* **41**, 207-234
3. Van Duyne, G. D., Standaert, R. F., Karplus, P. A., Schreiber, S. L., and Clardy, J. (1993) *J. Mol. Biol.* **229**, 105
4. Webb, M. R. (1992) *Proc. Natl. Acad. Sci. U S A* **89**, 4884-4887
5. Baykov, A. A., Kasho, V. N., and Avaeva, S. M. (1988) *Anal. Biochem.* **171**, 271-276
6. Chifflet, S., Torriglia, A., Chiesa, R., and Tolosa, S. (1988) *Anal. Biochem.* **168**, 1-4
7. Gonzalez-Romo, P., Sanchez-Nieto, S., and Gavilanes-Ruiz, M. (1992) *Anal. Biochem.* **200**, 235-238
8. Lau, G. H., MacGillivray, R. T., and Murphy, M. E. (2004) *J. Bacteriol.* **186**, 3266-3269
9. Nikaido, K., Liu, P. Q., and Ames, G. F. (1997) *J. Biol. Chem.* **272**, 27745-27752
10. Locher, K. P., Rees, B., Koebnik, R., Mitschler, A., Moulinier, L., Rosenbusch, J. P., and Moras, D. (1998) *Cell* **95**, 771-778
11. Hung, L. W., Wang, I. X., Nikaido, K., Liu, P. Q., Ames, G. F., and Kim, S. H. (1998) *Nature* **396**, 703-707
12. Adhikari, P., Berish, S. A., Nowalk, A. J., Veraldi, K. L., Morse, S. A., and Mietzner, T. A. (1996) *J. Bacteriol.* **178**, 2145-2149

13. Anderson, D. S., Adhikari, P., Nowalk, A. J., Chen, C. Y., and Mietzner, T. A. (2004) *J. Bacteriol.* **186**, 6220-6229

14. Borths, E. L., Poolman, B., Hvorup, R. N., Locher, K. P., and Rees, D. C. (2005) *Biochemistry* **44**, 16301-16309

Chapter 6: Concluding Remarks and Future Work

6.1 Concluding Remarks

This study is the first to re-assemble the FbpABC *in vitro* in order to elucidate complex formation of this iron transporting ABC transporter. This was facilitated by the mutation, and subsequent biotinlylation, of FbpA to allow attachment to a streptavidin-coated surface to allow the pull-down of co-expressed and purified FbpBC components. As such, this is the first report to describe the purification of the transmembrane component, FbpB, of the FbpABC transporter, and the first to prove association of all three components *in vitro*. Unfortunately, kinetic and affinity data could not be obtained for complex formation, but experimental evidence from surface plasmon resonance data suggests that the formation of the FbpABC complex is rapid and the resulting complex is very stable, and does not dissociate readily. The ATP hydrolysis activity of FbpC was comparable to that previously reported in the literature (1). No other work on iron-uptake ABC transporters has been published that focuses on complex formation *in vitro* using techniques such as surface plasmon resonance and pull-down experiments, and thus, the work undertaken and reported in this study is novel in its field.

The functionality of the FbpABC transporter was investigated by a radioactive iron-uptake assay and showed that *E. coli* cells expressing the *N. gonorrhoeae FbpABC* operon take up significantly more iron than cells not expressing the three-gene operon. Previous studies by another group have quoted values for the rate of iron uptake by the *HitABC* iron-uptake ABC transporter from *H. influenzae* in *E. coli*, but it is the opinion of this researcher that such values are invalid, as the assays performed in these studies were not performed in the parent

organism (2). True indications of the kinetics of these uptake systems can, probably, only be determined by *in vitro* experiments like those performed on the vitamin B_{12} import ABC transporter, BtuFCD, and the histidine transporter, HisQMP (3,4), or by using FbpBC expressing spheroplasts.

Wild-type and selenomethionine (SeMet)-labelled FbpC was expressed and purified in high yields in order to perform crystallographic studies at Imperial College (London), and resulted in a 2.7 Å crystal structure of FbpC. The ATP-hydrolysis activity of wild-type and SeMet-labelled FbpC was comparable to that previously reported in the literature (1). This is the first study to elucidate the structure of FbpC, and the first to report the structure of the nucleotide-binding domain from an iron-uptake ABC transporter.

In an extension of previous work performed on FbpA (5-7), the promiscuity of the iron-binding site was further investigated in this study, and demonstrated that FbpA can bind the transition metal ions ruthenium(III) and osmium(III). Investigation of the ruthenium and osmium forms of the protein by chromatography and inductively-coupled plasma optical emission spectrometry revealed that two major species of metal bound-FbpA were formed. The major species for both metals possibly contained a 4-atom clusters that may be capped with one or two phosphate ions. The possible presence of a metal cluster capped by two phosphate molecules has not previously been described for metal clusters bound to FbpA, and is thus novel. EXAFS has been performed on Ru-FbpA and analysis of the data is pending. The finding that ruthenium and osmium can bind to FbpA has not previously been reported in the literature.

6.2 Future Work

The overall trend in biology appears to be driven by the determination of the crystal structures of proteins, enzymes and complexes. Future work related to the present study will in no doubt be directed towards the elucidation of the crystal structure of the FbpABC or FbpBC complexes. However, this requirement to produce a crystal structure should not cloud the requirement for rigorous biochemical investigation of the complex, by *in vitro* iron-uptake assays and by the use of optical techniques such as surface plasmon resonance, and other such powerful analytical methods. These techniques should allow the mechanics of complex formation and stoichiometry of the complex to be determined, and may provide insight into the, still unknown, chemical mechanism of FbpABC. This will also reveal which residues are involved not only in iron translocation, but also which are involved in formation of the complex. These biochemical investigations, along with structural studies, will hopefully shed light on the, still mostly undescribed, mechanism of iron transport within the bacterial cell, and may eventually lead to the development of new chemotherapeutic agents to help combat diseases caused by bacteria.

Further investigation of FbpC will possibly reveal an additional role for this protein *in vivo*, due to the presence of the C-terminal domain that is proposed to be involved in some form of signal transduction within the bacterial cell (8). Experiments to determine the exact role of this additional domain would probably be best performed in *N. gonorrhoeae*, using FbpC C-terminal deletion mutants.

Further investigation of ruthenium and osmium binding to FbpA could be continued in the form of structural studies that may reveal novel metal clusters bound

to the protein, and metal competition assays to determine the affinity of these metals for FbpA, and to reveal if their affinities are greater than that for iron. The ability of FbpA to bind a host of metals may eventually lead to possible agents to interfere with the transport of iron with the bacterial cell, although the similarity between these bacterial periplasmic iron-binding proteins and human transferrin may mean this is not possible. However, insights into the affinity FbpA has for these exotic metals may allow researchers to determine the mechanism of iron binding and release from the protein: a process that still eludes description. Also, the promiscuous binding sites of these proteins may be utilised or engineered to allow their use in the bioremediation of hazardous metals in the environment and industry, or designed to produce novel enzymatic activity or useful biological markers (9). Further investigation of FbpA will possibly reveal new roles for this protein *in vivo*.

6.3 Chapter 6 References

1. Lau, G. H., MacGillivray, R. T., and Murphy, M. E. (2004) *J. Bacteriol.* **186**, 3266-3269
2. Anderson, D. S., Adhikari, P., Nowalk, A. J., Chen, C. Y., and Mietzner, T. A. (2004) *J. Bacteriol.* **186**, 6220-6229
3. Borths, E. L., Poolman, B., Hvorup, R. N., Locher, K. P., and Rees, D. C. (2005) *Biochemistry* **44**, 16301-16309
4. Nikaido, K., Liu, P. Q., and Ames, G. F. (1997) *J. Biol. Chem.* **272**, 27745-27752
5. Alexeev, D., Zhu, H., Guo, M., Zhong, W., Hunter, D. J., Yang, W., Campopiano, D. J., and Sadler, P. J. (2003) *Nat. Struct. Biol.* **10**, 297-302
6. Zhu, H., Alexeev, D., Hunter, D. J., Campopiano, D. J., and Sadler, P. J. (2003) *Biochem. J.* **376**, 35-41
7. Zhong, W., Alexeev, D., Harvey, I., Guo, M., Hunter, D. J., Zhu, H., Campopiano, D. J., and Sadler, P. J. (2004) *Angew. Chem. Int. Ed. Engl.* **43**, 5914-5918
8. Diederichs, K., Diez, J., Greller, G., Muller, C., Breed, J., Schnell, C., Vonrhein, C., Boos, W., and Welte, W. (2000) *Embo. J.* **19**, 5951-5961
9. Dwyer, M. A., and Hellinga, H. W. (2004) *Curr. Opin. Struct. Biol.* **14**, 495-504

Appendix 1: FbpABC Sequences

DNA sequence of the *N. gonorrhoeae FbpABC* Operon

Amino acid sequences of proteins shown above DNA sequence in colour. Key: FbpA, FbpB and FbpC.

```
                                                                    M  K  T  S  ·
  1  ATTCCGCCAC GCATTGCCCG CCGCTTCCGC CTTACGGGCG CGATGCACGG AAAAAATACA AGTCAGAACA
     TAAGGCGGTG CGTAACGGGC GGCGAAGGCG GAATGCCCGC GCTACGTGCC TTTTTTATGT TCAGTCTTGT

 71  AACAATAACC GGATCGGATA ATAACAAATT TAAAAAATAA TTATTTGCAT TTATAAAAAA GAAGGAATAC
     TTGTTATTGG CCTAGCCTAT TATTGTTTAA ATTTTTTATT AATAAACGTA AATATTTTTT CTTCCTTATG

     ·  I  R  Y  A  L  L  A  A  A  L  T  A  A  T  P  A  L  A  D  I  T  V  Y  ·
141  CTATCCGATA CGCACTGCTT GCCGCAGCCC TGACCGCCGC CACCCCCGCG CTGGCAGACA TTACCGTGTA
     GATAGGCTAT GCGTGACGAA CGGCGTCGGG ACTGGCGGCG GTGGGGGCGC GACCGTCTGT AATGGCACAT

                                                        SmaI
                                                        ~~~~~~~
     ·  N  G  Q  H  K  E  A  A  Q  A  V  A  D  A  F  T  R  A  T  G  I  K  V
211  CAACGGCCAA CACAAAGAAG CGGCACAAGC CGTTGCAGAT GCCTTTACCC GGGCTACCGG CATCAAAGTC
     GTTGCCGGTT GTGTTTCTTC GCCGTGTTCG GCAACGTCTA CGGAAATGGG CCCGATGGCC GTAGTTTCAG

     K  L  N  S  A  K  G  D  Q  L  A  G  Q  I  K  E  E  G  S  R  S  P  A  D  ·
351  AAACTCAACA GTGCCAAAGG CGACCAGCTT GCCGGCCAAA TCAAAGAAGA AGGCAGCCGA AGCCCCGCCG
     TTTGAGTTGT CACGGTTTCC GCTGGTCGAA CGGCCGGTTT AGTTTCTTCT TCCGTCGGCT TCGGGGCGGC

     ·  V  F  Y  S  E  Q  I  P  A  L  A  T  L  S  A  A  N  L  L  E  P  L  P  ·
421  ACGTATTCTA TTCCGAACAA ATCCCGGCAC TCGCCACCCT TTCCGCAGCC AACCTCCTAG AGCCCCTGCC
     TGCATAAGAT AAGGCTTGTT TAGGGCCGTG AGCGGTGGGA AAGGCGTCGG TTGGAGGATC TCGGGGACGG

     ·  A  S  T  I  N  E  T  R  G  K  G  V  P  V  A  A  K  K  D  W  V  A  L
491  CGCCTCCACC ATCAACGAAA CACGCGGCAA AGGCGTGCCG GTTGCCGCCA AAAAAGACTG GGTGGCACTG
     GCGGAGGTGG TAGTTGCTTT GTGCGCCGTT TCCGCACGGC CAACGGCGGT TTTTTCTGAC CCACCGTGAC

     S  G  R  S  R  V  V  V  Y  D  T  R  K  L  S  E  K  D  L  E  K  S  V  L  ·
561  AGCGGACGTT CGCGCGTCGT CGTTTACGAC ACCCGCAAAC TGTCTGAAAA AGATTTGGAA AAATCCGTCC
     TCGCCTGCAA GCGCGCAGCA GCAAATGCTG TGGGCGTTTG ACAGACTTTT TCTAAACCTT TTTAGGCAGG

     ·  N  Y  A  T  P  K  W  K  N  R  I  G  Y  V  P  T  S  G  A  F  L  E  Q  ·
631  TGAATTACGC CACGCCGAAA TGGAAAAACC GCATCGGTTA CGTCCCCACT TCCGGCGCGT TCTTGGAACA
     ACTTAATGCG GTGCGGCTTT ACCTTTTTGG CGTAGCCAAT GCAGGGGTGA AGGCCGCGCA AGAACCTTGT

     ·  I  V  A  I  V  K  L  K  G  E  A  A  A  L  K  W  L  K  G  L  K  E  Y
701  GATTGTCGCC ATCGTCAAAC TGAAAGGCGA AGCGGCCGCA TTGAAATGGC TCAAAGGCCT GAAAGAATAC
     CTAACAGCGG TAGCAGTTTG ACTTTCCGCT TCGCCGGCGT AACTTTACCG AGTTTCCGGA CTTTCTTATG

     G  K  P  Y  A  K  N  S  V  A  L  Q  A  V  E  N  G  E  I  D  A  A  L  I  ·
771  GGCAAGCCTT ACGCTAAAAA CTCCGTCGCC CTTCAAGCGG TTGAAAACGG CGAAATCGAT GCCGCCCTCA
     CCGTTCGGAA TGCGATTTTT GAGGCAGCGG GAAGTTCGCC AACTTTTGCC GCTTTAGCTA CGGCGGGAGT

     ·  N  N  Y  Y  W  H  A  F  A  R  E  K  G  V  Q  N  V  H  T  R  L  N  F  ·
841  TCAACAACTA CTACTGGCAC GCTTTCGCGC GTGAAAAAGG CGTACAAAAT GTCCACACCC GCCTGAATTT
     AGTTGTTGAT GATGACCGTG CGAAAGCGCG CACTTTTTCC GCATGTTTTA CAGGTGTGGG CGGACTTAAA

     ·  V  R  H  R  D  P  G  A  L  V  T  Y  S  G  A  A  V  L  K  S  S  Q  N
911  CGTCCGCCAC AGAGATCCCG GCGCACTCGT TACCTATTCC GGCGCAGCCG TGTTAAAATC CTCCCAAAAC
     GCAGGCGGTG TCTCTAGGGC CGCGTGAGCA ATGGATAAGG CCGCGTCGGC ACAATTTTAG GAGGGTTTTG

     K  D  E  A  K  K  F  V  A  F  L  A  G  K  E  G  Q  R  A  L  T  A  V  R  ·
981  AAGGATGAGG CGAAAAAATT CGTCGCCTTC CTCGCCGGCA AGGAAGGACA GCGCGCCCTG ACCGCCGTCC
     TTCCTACTCC GCTTTTTTAA GCAGCGGAAG GAGCGGCCGT TCCTTCCTGT CGCGCGGGAC TGGCGGCAGG

     ·  A  E  Y  P  L  N  P  H  V  V  S  T  F  N  L  E  P  I  A  K  L  E  A  ·
1051 GTGCCGAATA TCCTTTGAAT CCGCACGTGG TATCCACCTT CAATTTGGAA CCCATCGCCA AGTTGGAAGC
     CACGGCTTAT AGGAAACTTA GGCGTGCACC ATAGGTGGAA GTTAAACCTT GGGTAGCGGT TCAACCTTCG
```

```
     · P  Q  V  S  A  T  T  V  S  E  K  E  H  A  T  R  L  L  E  Q  A  G  M
1121 ACCCCAAGTG TCCGCCACCA CTGTTTCCGA AAAAGAACAC GCCACCCGGC TGCTTGAGCA AGCCGGTATG
     TGGGGTTCAC AGGCGGTGGT GACAAAGGCT TTTTCTTGTG CGGTGGGCCG ACGAACTCGT TCGGCCATAC

     K
                                                                  M  K  N
1191 AAATAAGCCG TTTTCGGATT GTCAAACGGG CGGACATTTA TACTGTCCGC CCGTTTTGCC GATGAAAAAC
     TTTATTCGGC AAAAGCCTAA CAGTTTGCCC GCCTGTAAAT ATGACAGGCG GGCAAAACGG CTACTTTTTG

      T  M  S  P  K  K  I  P  I  W  L  T  G  L  I  L  L  I  A  L  P  L  T  L  ·
1261 ACTATGTCTC CTAAAAAAAT ACCCATTTGG CTTACCGGCC TCATCCTACT GATCGCCCTG CCGCTTACCC
     TGATACAGAG GATTTTTTTA TGGGTAAACC GAATGGCCGG AGTAGGATGA CTAGCGGGAC GGCGAATGGG

     · P  F  L  Y  V  A  M  R  S  W  Q  V  G  I  N  R  A  V  E  L  L  F  R  ·
1331 TGCCTTTTTT ATATGTCGCT ATGCGTTCGT GGCAGGTCGG CATCAACCGC GCCGTCGAAC TGTTGTTCCG
     ACGGAAAAAA TATACAGCGA TACGCAAGCA CCGTCCAGCC GTAGTTGGCG CGGCAGCTTG ACAACAAGGC

     · P  R  M  W  D  L  L  S  N  T  L  T  M  M  A  G  V  T  L  I  S  I  V
1401 CCCGCGTATG TGGGATTTGC TCTCCAACAC CTTGACGATG ATGGCGGGCG TTACCCTGAT TTCCATTGTT
     GGGCGCATAC ACCCTAAACG AGAGGTTGTG GAACTGCTAC TACCGCCCGC AATGGGACTA AAGGTAACAA

      L  G  I  A  C  A  L  L  F  Q  R  Y  R  F  F  G  K  T  F  F  Q  T  A  I  ·
1471 TTGGGCATTG CCTGCGCCCT TTTGTTCCAA CGTTACCGCT TCTTCGGCAA AACCTTTTTT CAGACGGCAA
     AACCCGTAAC GGACGCGGGA AAACAAGGTT GCAATGGCGA AGAAGCCGTT TTGGAAAAAA GTCTGCCGTT

     · T  L  P  L  C  I  P  A  F  V  S  C  F  T  W  I  S  L  T  F  R  V  E  ·
1541 TCACCCTGCC TTTGTGCATC CCCGCATTTG TCAGCTGTTT CACCTGGATC AGCCTGACCT TCCGCGTCGA
     AGTGGGACGG AAACACGTAG GGGCGTAAAC AGTCGACAAA GTGGACCTAG TCGGACTGGA AGGCGCAGCT

     · G  F  W  G  T  V  M  I  M  S  L  S  S  F  P  L  A  Y  L  P  V  E  A
1611 AGGATTTTGG GGGACAGTGA TGATTATGAG CCTGTCCTCG TTTCCGCTCG CCTACCTGCC CGTCGAGGCG
     TCCTAAAACC CCCTGTCACT ACTAATACTC GGACAGGAGC AAAGGCGAGC GGATGGACGG GCAGCTCCGC

      A  L  K  R  I  S  L  S  Y  E  E  V  S  L  S  L  G  K  S  R  L  Q  T  F  ·
1681 GCACTCAAAC GCATCAGCCT GTCTTACGAA GAAGTCAGCC TGTCCTTGGG CAAAAGCCGC CTGCAAACCT
     CGTGAGTTTG CGTAGTCGGA CAGAATGCTT CTTCAGTCGG ACAGGAACCC GTTTTCGGCG GACGTTTGGA

                                                                  NdeI
                                                                  ~~~~~
     · F  S  A  I  L  P  Q  L  K  P  A  I  G  S  S  V  L  L  I  A  L  H  M  ·
1751 TTTTTTCCGC CATCCTCCCA CAGCTCAAAC CCGCCATCGG CAGCAGCGTG TTACTGATCG CCCTGCATAT
     AAAAAAGGCG GTAGGAGGGT GTCGAGTTTG GGCGGTAGCC GTCGTCGCAC AATGACTAGC GGGACGTATA

     ~
     · L  V  E  F  G  A  V  S  I  L  N  Y  P  T  F  T  T  A  I  F  Q  E  Y
1821 GCTGGTCGAA TTTGGCGCGG TATCCATTTT GAACTACCCC ACTTTTACCA CTGCCATTTT CCAAGAATAC
     CGACCAGCTT AAACCGCGCC ATAGGTAAAA CTTGATGGGG TGAAAATGGT GACGGTAAAA GGTTCTTATG

      E  M  S  Y  N  N  N  T  A  A  L  L  S  A  V  L  T  A  V  C  G  I  V  V  ·
1891 GAAATGTCCT ACAACAACAA TACCGCCGCC CTGCTTTCCG CTGTTTTGAC GGCGGTGTGC GGCATCGTCG
     CTTTACAGGA TGTTGTTGTT ATGGCGGCGG GACGAAAGGC GACAAAACTG CCGCCACACG CCGTAGCAGC

     · F  G  E  S  I  F  R  G  K  A  K  I  Y  H  S  G  K  G  V  A  R  P  Y  ·
1961 TATTTGGAGA AAGCATATTT CGCGGCAAAG CCAAGATTTA CCACAGCGGC AAAGGCGTTG CCCGTCCTTA
     ATAAACCTCT TTCGTATAAA GCGCCGTTTC GGTTCTAAAT GGTGTCGCCG TTTCCGCAAC GGGCAGGAAT

     · P  V  K  T  L  K  L  P  G  Q  I  G  A  I  V  F  L  S  S  L  L  I  L
2031 TCCCGTCAAA ACCCTCAAAC TGCCCGGTCA GATCGGCGCG ATTGTTTTTT TAAGCAGCTT GTTGATTTTG
     AGGGCAGTTT TGGGAGTTTG ACGGGCCAGT CTAGCCGCGC TAACAAAAAA ATTCGTCGAA CAACTAAAAC

      G  I  I  I  P  F  G  V  L  I  H  W  M  M  V  G  T  S  G  T  F  A  L  V  ·
2101 GGCATTATTA TCCCCTTTGG CGTATTGATA CATTGGATGA TGGTCGGCAC TTCCGGCACA TTCGCGCTCG
     CCGTAATAAT AGGGGAAACC GCATAACTAT GTAACCTACT ACCAGCCGTG AAGGCCGTGT AAGCGCGAGC

     · S  V  F  D  A  F  I  R  S  L  S  V  S  A  L  G  A  I  L  T  I  L  C  ·
2171 TATCCGTATT TGATGCCTTT ATCCGTTCCT TAAGCGTATC GGCTTTAGGT GCGATTTTGA CTATATTATG
     ATAGGCATAA ACTACGGAAA TAGGCAAGGA ATTCGCATAG CCGAAATCCA CGCTAAAACT GATATAATAC

     · A  L  P  L  V  W  A  S  V  R  Y  R  N  F  L  T  V  W  I  D  R  L  P
2241 TGCCTTGCCC CTTGTTTGGG CATCGGTTCG CTATCGCAAT TTTTTAACCG TTTGGATAGA CAGGCTGCCG
     ACGGAACGGG GAACAAACCC GTAGCCAAGC GATAGCGTTA AAAAATTGGC AAACCTATCT GTCCGACGGC
```

```
      F  L  L  H  A  V  P  G  L  V  I  A  L  S  L  V  Y  F  S  I  N  Y  T  P ·
2311  TTTTTACTGC ACGCCGTCCC CGGTTTGGTT ATCGCCCTAT CCTTGGTTTA TTTCAGCATC AACTACACCC
      AAAAATGACG TGCGGCAGGG GCCAAACCAA TAGCGGGATA GGAACCAAAT AAAGTCGTAG TTGATGTGGG

      ·  A  V  Y  Q  T  F  I  V  V  I  L  A  Y  F  M  L  Y  L  P  M  A  Q  T ·
2381  CTGCCGTTTA CCAAACCTTT ATCGTCGTCA TCCTTGCCTA TTTCATGCTT TACCTGCCGA TGGCGCAAAC
      GACGGCAAAT GGTTTGGAAA TAGCAGCAGT AGGAACGGAT AAAGTACGAA ATGGACGGCT ACCGCGTTTG

      ·  T  L  R  T  S  L  E  Q  L  P  K  G  M  E  Q  V  G  A  T  L  G  R  G
2451  CACCCTGAGG ACTTCCTTGG AACAACTCCC CAAAGGGATG GAACAGGTCG GCGCAACATT GGGGCGCGGA
      GTGGGACTCC TGAAGGAACC TTGTTGAGGG GTTTCCCTAC CTTGTCCAGC CGCGTTGTAA CCCCGCGCCT

      H  F  F  I  F  R  T  L  V  L  P  S  I  L  P  G  I  T  A  A  F  A  L  V ·
2521  CACTTCTTTA TTTTCAGGAC GTTGGTACTG CCGTCCATCC TGCCCGGCAT TACCGCCGCA TTCGCACTCG
      GTGAAGAAAT AAAAGTCCTG CAACCATGAC GGCAGGTAGG ACGGGCCGTA ATGGCGGCGT AAGCGTGAGC

      ·  F  L  K  L  M  K  E  L  T  A  T  L  L  L  T  A  D  D  V  H  T  L  S ·
2591  TCTTCCTCAA GCTGATGAAA GAGTTGACCG CCACCCTGCT GCTGACCGCC GACGATGTCC ACACGCTCTC
      AGAAGGAGTT CGACTACTTT CTCAACTGGC GGTGGGACGA CGACTGGCGG CTGCTACAGG TGTGCGAGAG

      ·  T  A  V  W  E  Y  T  S  D  A  Q  Y  A  A  A  T  P  Y  A  L  M  L  V
2661  CACCGCCGTT TGGGAATACA CATCGGACGC ACAATACGCC GCCGCCACCC CTTACGCGCT GATGCTGGTA
      GTGGCGGCAA ACCCTTATGT GTAGCCTGCG TGTTATGCGG CGGCGGTGGG GAATGCGCGA CTACGACCAT

      L  F  S  G  I  P  V  F  L  L  K  K  Y  A  F  K
2731  TTATTTTCCG GCATACCCGT ATTCCTGCTG AAGAAATACG CCTTCAAATA ACAGCTTGAG GAAGCACCGC
      AATAAAAGGC CGTATGGGCA TAAGGACGAC TTCTTTATGC GGAAGTTTAT TGTCGAACTC CTTCGTGGCG

        M  T  A  A  L  H  I  G  H  L  S  K  S  F  Q  N  T  P  V  L  N  D  I
2801  TATGACCGCC GCCCTGCACA TCGGACACCT GTCCAAAAGT TTTCAAAACA CCCCGGTTTT AAACGACATT
      ATACTGGCGG CGGGACGTGT AGCCTGTGGA CAGGTTTTCA AAAGTTTTGT GGGGCCAAAA TTTGCTGTAA

                      SmaI
                      ~~~~~~~
      S  L  S  L  D  P  G  E  I  L  F  I  I  G  A  S  G  C  G  K  T  T  L  L ·
2871  TCGCTCAGCC TCGACCCGGG CGAAATTCTC TTTATCATCG GCGCGTCCGG CTGCGGCAAA ACCACCCTTT
      AGCGAGTCGG AGCTGGGCCC GCTTTAAGAG AAATAGTAGC CGCGCAGGCC GACGCCGTTT TGGTGGGAAA

      ·  R  C  L  A  G  F  E  Q  P  D  S  G  E  I  S  L  S  G  K  T  I  F  S ·
2941  TACGCTGCCT TGCCGGTTTC GAACAACCCG ATTCCGGCGA AATTTCGCTT TCCGGCAAAA CCATCTTCTC
      ATGCGACGGA ACGGCCAAAG CTTGTTGGGC TAAGGCCGCT TTAAAGCGAA AGGCCGTTTT GGTAGAAGAG

      ·  K  N  T  N  L  P  V  R  E  R  R  L  G  Y  L  V  Q  E  G  V  L  F  P
3011  GAAAAATACC AACCTTCCCG TCCGCGAACG CCGTTTGGGT TACCTCGTAC AGGAAGGCGT GCTGTTCCCC
      CTTTTTATGG TTGGAAGGGC AGGCGCTTGC GGCAAACCCA ATGGAGCATG TCCTTCCGCA CGACAAGGGG

    H  L  T  V  Y  R  N  I  A  Y  G  L  G  N  G  K  G  R  T  A  Q  E  R  Q ·
3081  CACCTGACCG TTTACCGCAA TATCGCCTAC GGTCTCGGCA ACGGCAAAGG CAGGACGGCG CAAGAGCGAC
      GTGGACTGGC AAATGGCGTT ATAGCGGATG CCAGAGCCGT TGCCGTTTCC GTCCTGCCGC GTTCTCGCTG

      ·  R  I  E  A  M  L  E  L  T  G  I  S  E  L  A  G  R  Y  P  H  E  L  S ·
3151  AGCGCATCGA AGCCATGTTG GAATTGACCG GCATTTCCGA ACTTGCCGGA CGCTATCCGC ACGAACTTTC
      TCGCGTAGCT TCGGTACAAC CTTAACTGGC CGTAAAGGCT TGAACGGCCT GCGATAGGCG TGCTTGAAAG

      ·  G  G  Q  Q  Q  R  V  A  L  A  R  A  L  A  P  D  P  E  L  I  L  L  D
3221  GGGCGGACAA CAACAGCGCG TCGCCCTCGC CCGCGCCCTC GCCCCCGACC CCGAACTGAT TTTGTTGGAC
      CCCGCCTGTT GTTGTCGCGC AGCGGGAGCG GGCGCGGGAG CGGGGGCTGG GGCTTGACTA AAACAACCTG

    E  P  F  S  A  L  D  E  Q  L  R  R  Q  I  R  E  D  M  I  A  A  L  R  A ·
3291  GAACCCTTCA GCGCGCTGGA CGAACAGTTG CGCCGCCAGA TTCGCGAAGA CATGATTGCC GCCCTGCGCG
      CTTGGGAAGT CGCGCGACCT GCTTGTCAAC GCGGCGGTCT AAGCGCTTCT GTACTAACGG CGGGACGCGC

      ·  N  G  K  S  A  V  F  V  S  H  D  R  E  E  A  L  Q  Y  A  D  R  I  A ·
3361  CCAACGGCAA ATCCGCCGTT TTTGTCAGCC ACGACCGCGA AGAAGCCCTG CAATACGCCG ACCGGATTGC
      GGTTGCCGTT TAGGCGGCAA AAACAGTCGG TGCTGGCGCT TCTTCGGGAC GTTATGCGGC TGGCCTAACG

      ·  V  M  K  Q  G  R  I  L  Q  T  A  S  P  H  E  L  Y  R  Q  P  A  D  L
3431  CGTGATGAAA CAGGGGCGCA TCCTCCAAAC CGCAAGCCCT CACGAATTGT ACCGACAACC TGCCGACCTT
      GCACTACTTT GTCCCCGCGT AGGAGGTTTG GCGTTCGGGA GTGCTTAACA TGGCTGTTGG ACGGCTGGAA
```

```
    D  A  A  L  F  I  G  E  G  I  V  F  P  A  A  L  N  A  D  G  T  A  D  C ·
3501 GATGCCGCCC TGTTTATCGG CGAAGGCATC GTGTTCCCCG CCGCGCTCAA CGCCGACGGC ACCGCCGATT
     CTACGGCGGG ACAAATAGCC GCTTCCGTAG CACAAGGGGC GGCGCGAGTT GCGGCTGCCG TGGCGGCTAA

    ·  R  L  G  R  L  P  V  Q  S  G  A  P  A  G  T  R  G  T  L  L  I  R  P ·
3571 GCAGATTGGG CCGCCTGCCC GTCCAAAGCG GCGCACCCGC AGGCACGCGC GGTACACTGC TCATCCGTCC
     CGTCTAACCC GGCGGACGGG CAGGTTTCGC CGCGTGGGCG TCCGTGCGCG CCATGTGACG AGTAGGCAGG

    · E  Q  F  S  L  H  P  H  S  A  P  A  A  S  I  H  A  V  V  L  K  T  T
3641 GGAACAGTTC AGCCTTCACC CCCATTCCGC ACCCGCCGCC TCCATTCACG CCGTGGTTCT CAAAACCACG
     CCTTGTCAAG TCGGAAGTGG GGGTAAGGCG TGGGCGGCGG AGGTAAGTGC GGCACCAAGA GTTTTGGTGC

   P  K  A  R  H  T  E  I  S  L  R  A  G  Q  T  V  L  T  L  N  L  P  S  A ·
3711 CCCAAAGCGC GGCATACCGA AATCAGCCTC AGGGCCGGAC AAACCGTCCT CACGCTCAAC CTCCCTTCCG
     GGGTTTCGCG CCGTATGGCT TTAGTCGGAG TCCCGGCCTG TTTGGCAGGA GTGCGAGTTG GAGGGAAGGC

    · P  T  L  S  D  G  I  S  A  V  L  H  L  D  G  P  A  L  F  F  P  G  N ·
3781 CCCCCACCCT GTCAGACGGC ATTTCCGCCG TCCTCCATTT GGACGGTCCC GCCCTGTTCT TCCCCGGAAA
     GGGGGTGGGA CAGTCTGCCG TAAAGGCGGC AGGAGGTAAA CCTGCCAGGG CGGGACAAGA AGGGGCCTTT

    · T  L
3851 TACCCTCTGA AAGGCGGCAG CATCCACAAG CCTGCGGATA TTTATCTTGT TGGAAACAGA ATTTGTTTGC
     ATGGGAGACT TTCCGCCGTC GTAGGTGTTC GGACGCCTAT AAATAGAACA ACCTTTGTCT TAAACAAACG

                                                                          NdeI
                                                                          ~~~~~
3921 TATATTCAAC CTGCGCGCCC CAAGCCAAAC ACGGCACGCA CGGCACGCAG GCAGCCGTTT CTGCCCATAT
     ATATAAGTTG GACGCGCGGG GTTCGGTTTG TGCCGTGCGT GCCGTGCGTC CGTCGGCAAA GACGGGTATA

                    NdeI
~                   ~~~~~~~
3991 GCCGCCCCTT CCAACCACAT ATGCCGCACA CCGCAGCATA CGAAAGGATA TATTATGGCA AAAGTACTCG
     CGGCGGGGAA GGTTGGTGTA TACGGCGTGT GGCGTCGTAT GCTTTCCTAT ATAATACCGT TTTCATGAGC
```

Bioinformatic Analysis of FbpABC

	Gene size	Protein size (mature protein)	Pedicted mass (mature protein)	Predicted pI (mature protein)
FbpA	993 bp	331 aa (309 aa)	35 837 kDa (33 637 kDa)	9.60 (9.52)
FbpB	1527 bp	509 aa	56 310 kDa	9.67
FbpC	1056 bp	352 aa	37 900 kDa	6.91

Amino acid sequence of FbpA from *N. gonorrhoeae* (red residues indicate the signal peptide of the pre-protein that is cleaved during translocation of the mature protein into the periplasm):

```
  1  MKTSIRYALL AAALTAATPA LADITVYNGQ HKEAAQAVAD AFTRATGIKV
 51  KLNSAKGDQL AGQIKEEGSR SPADVFYSEQ IPALATLSAA NLLEPLPAST
101  INETRGKGVP VAAKKDWVAL SGRSRVVVYD TRKLSEKDLE KSVLNYATPK
151  WKNRIGYVPT SGAFLEQIVA IVKLKGEAAA LKWLKGLKEY GKPYAKNSVA
201  LQAVENGEID AALINNYYWH AFAREKGVQN VHTRLNFVRH RDPGALVTYS
251  GAAVLKSSQN KDEAKKFVAF LAGKEGQRAL TAVRAEYPLN PHVVSTFNLE
301  PIAKLEAPQV SATTVSEKEH ATRLLEQAGM K
```

Amino acid sequence of FbpB from *N. gonorrhoeae*:

```
  1  MKNTMSPKKI PIWLTGLILL IALPLTLPFL YVAMRSWQVG INRAVELLFR
 51  PRMWDLLSNT LTMMAGVTLI SIVLGIACAL LFQRYRFFGK TFFQTAITLP
101  LCIPAFVSCF TWISLTFRVE GFWGTVMIMS LSSFPLAYLP VEAALKRISL
151  SYEEVSLSLG KSRLQTFFSA ILPQLKPAIG SSVLLIALHM LVEFGAVSIL
201  NYPTFTTAIF QEYEMSYNNN TAALLSAVLT AVCGIVVFGE SIFRGKAKIY
251  HSGKGVARPY PVKTLKLPGQ IGAIVFLSSL LILGIIIPFG VLIHWMMVGT
301  SGTFALVSVF DAFIRSLSVS ALGAILTILC ALPLVWASVR YRNFLTVWID
351  RLPFLLHAVP GLVIALSLVY FSINYTPAVY QTFIVVILAY FMLYLPMAQT
401  TLRTSLEQLP KGMEQVGATL GRGHFFIFRT LVLPSILPGI TAAFALVFLK
451  LMKELTATLL LTADDVHTLS TAVWEYTSDA QYAAATPYAL MLVLFSGIPV
501  FLLKKYAFK
```

Amino acid sequence of FbpC from *N. gonorrhoeae*:

```
  1  MTAALHIGHL SKSFQNTPVL NDISLSLDPG EILFIIGASG CGKTTLLRCL
 51  AGFEQPDSGE ISLSGKTIFS KNTNLPVRER RLGYLVQEGV LFPHLTVYRN
101  IAYGLGNGKG RTAQERQRIE AMLELTGISE LAGRYPHELS GGQQQRVALA
151  RALAPDPELI LLDEPFSALD EQLRRQIRED MIAALRANGK SAVFVSHDRE
201  EALQYADRIA VMKQGRILQT ASPHELYRQP ADLDAALFIG EGIVFPAALN
251  ADGTADCRLG RLPVQSGAPA GTRGTLLIRP EQFSLHPHSA PAASIHAVVL
301  KTTPKARHTE ISLRAGQTVL TLNLPSAPTL SDGISAVLHL DGPALFFPGN
351  TL
```

Appendix 2: Mass Spectra: FbpA

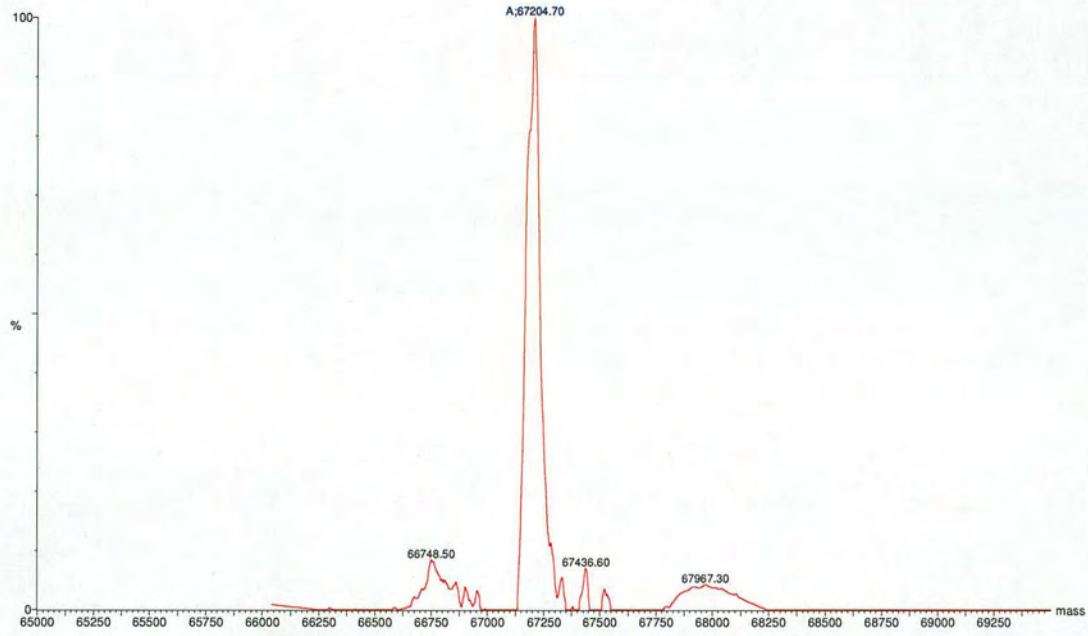

1. FbpA-R48C: dimer mass 67 198 ± 11.4 Da (theoretical mass 67 176 Da)

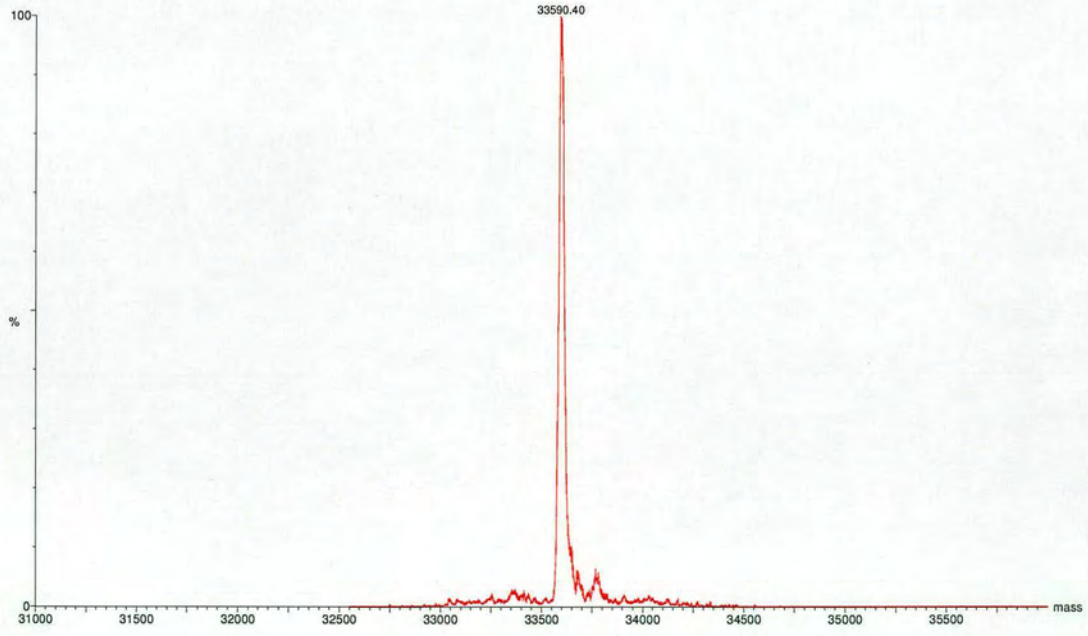

2. FbpA-R48C: reduced mass 33 585 ± 5.0 Da (theoretical mass 33 588 Da)

3. FbpA-R48C: as purified masses 33 585 ± 5.0 Da, 33 706 ± 4.9 Da (cysteinylation) and 33 886 ± 4.9 Da (glutathiolylation) (theoretical mass of FbpA-R48C 33 588 Da)

4. FbpA-R48C-IAA: reduced mass 33 640 ± 2.3 Da(theoretical mass 33 645 Da)

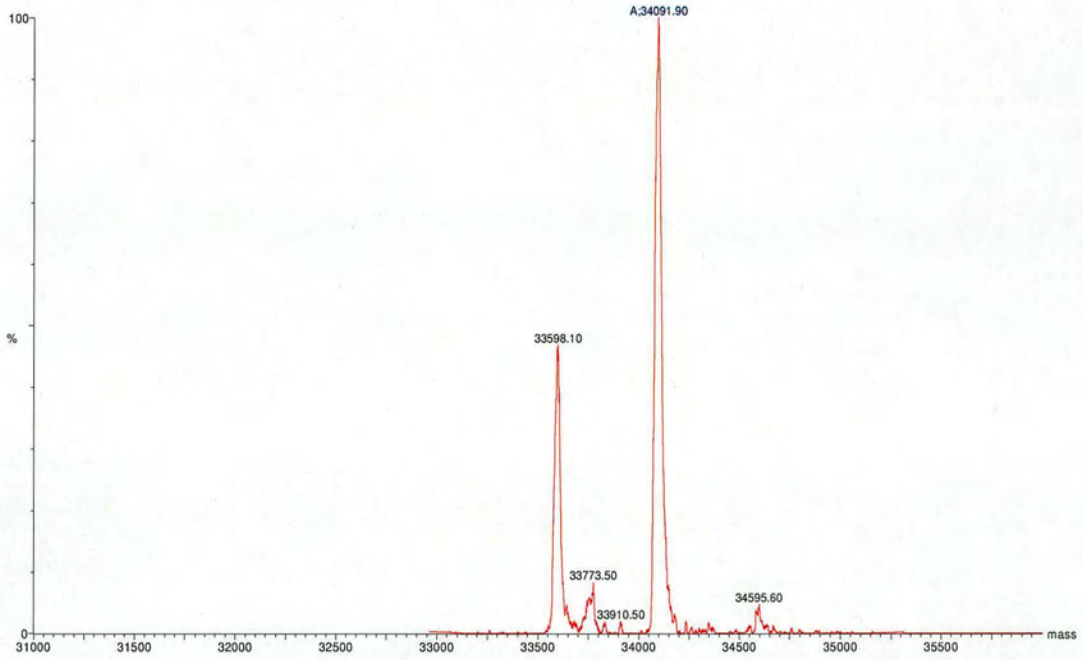

5. FbpA-R48C-AMS: modified mass 33 094 ± 5.9 Da (theoretical mass 34 078 Da)

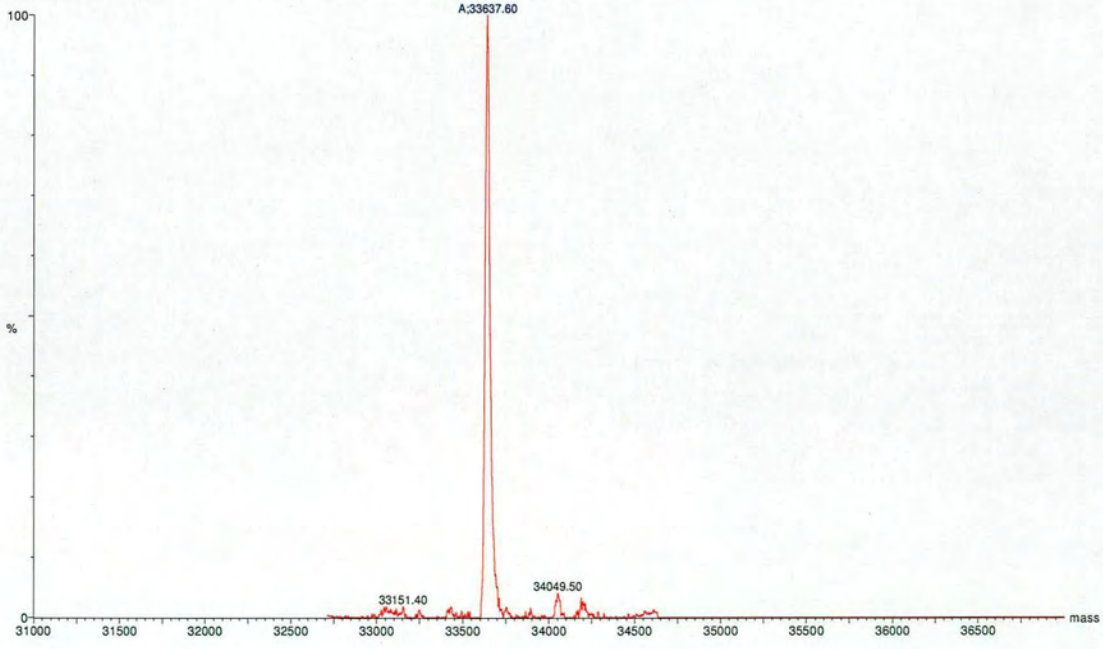

6. FbpA-V272C: reduced mass 33 640.86 ± 2.3 Da (theoretical mass 33 643 Da)

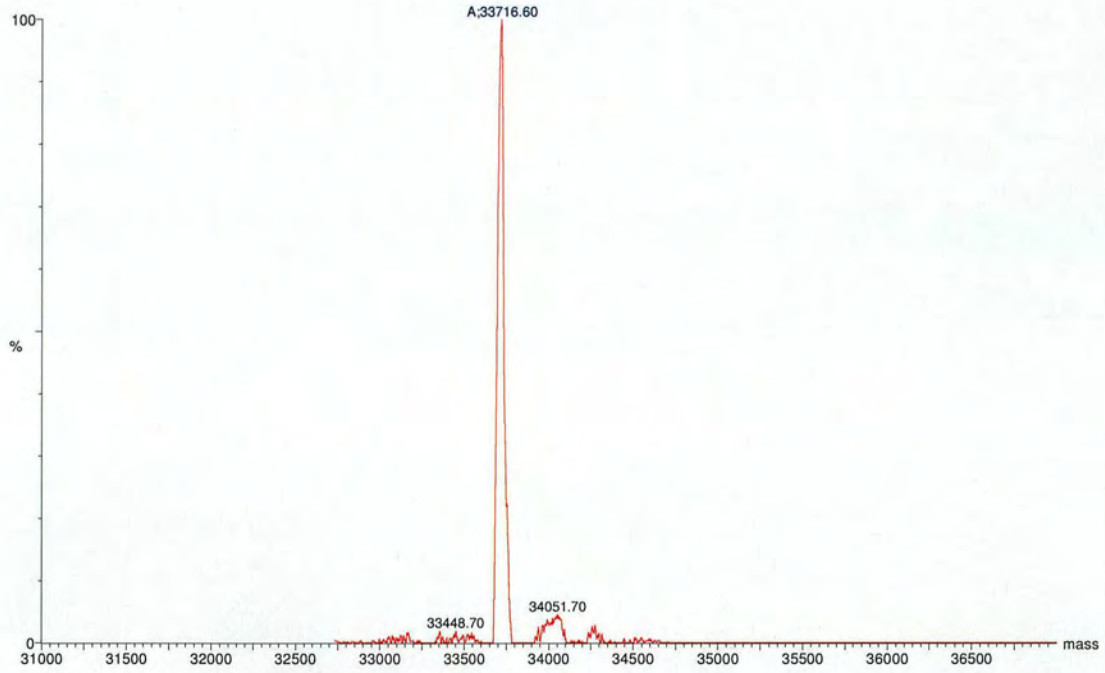

7. FbpA-V272C-IAA : reduced mass 33 707 ± 6.7 Da (theoretical mass 33 700 Da)

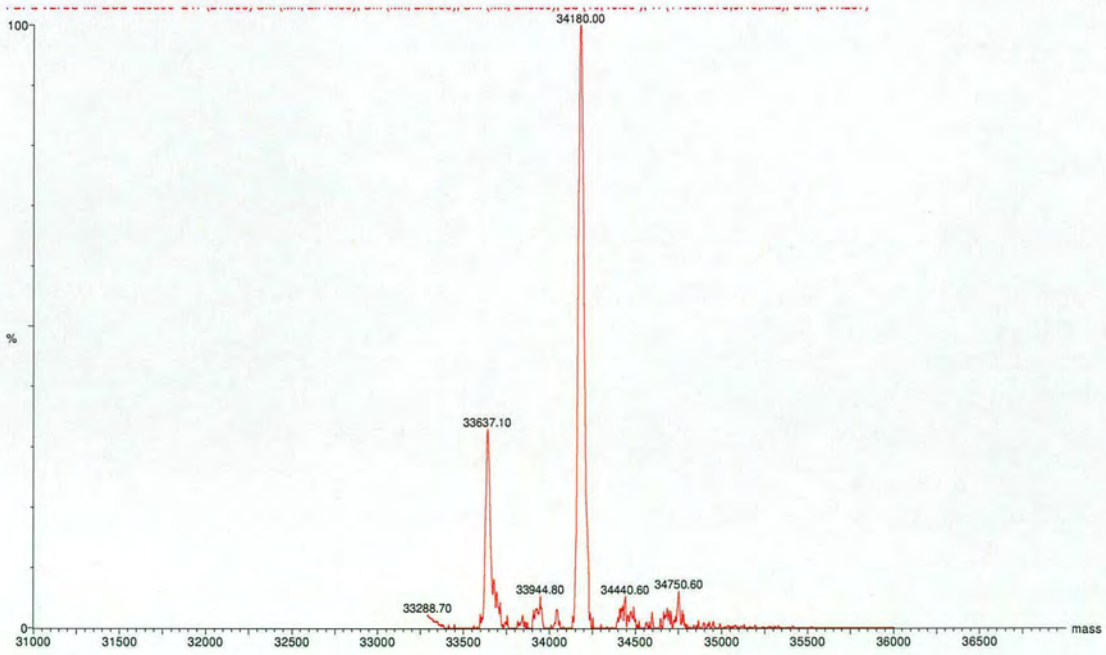

8. FbpA-V272C-(M-PEO_2-B) : reduced mass 33 640.86 ± 2.3 Da (theoretical mass 33 643 Da)

Appendix 3: Peptide Mass Fingerprinting: FbpBC

Trypsin digest of FbpC

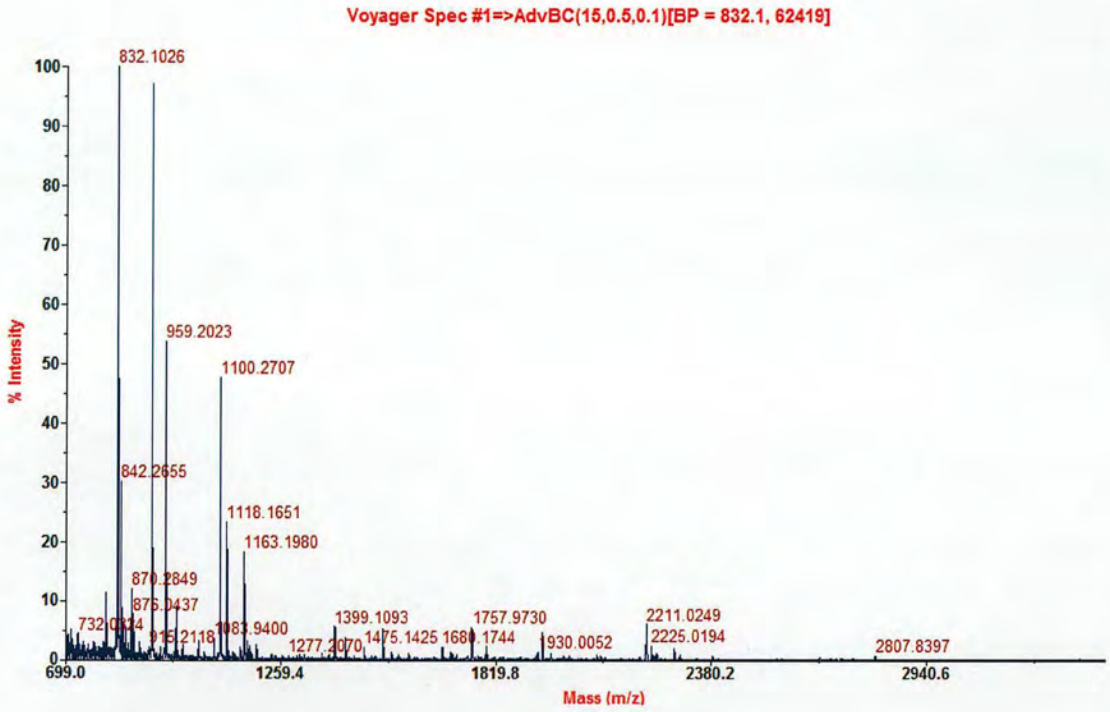

Hits table for the above trypsin digest:

	MOWSE Score	#/56(%) Masses Matched	Protein MW (Da)/pI	Accession #	Species	Protein Name
1	2.126e+06	12 (21)	37858/7.2	Q50966	NEIGO	Ferric cations import ATP-binding protein fbpC (EC 3.6.3.30)
2	90.4	4 (7)	15429/9.1	Q9R352	NEIME	Regulatory protein PilA (Fragment)
3	65.0	6 (10)	71680/5.4	Q9S368	NEIGO	Putative ATP-binding protein
4	65.0	7 (12)	71732/5.4	Q9S359	NEIME	Putative ATP-binding protein
5	64.9	7 (12)	71789/5.4	Q9S360	NEIME	Putative ATP-binding protein
6	57.7	5 (8)	87705/9.5	O87626	NEIFL	Penicillin-binding protein 1A (PBP-1a) (PBP1a)
7	44.0	4 (7)	32042/5.9	Q8KS36	NEIME	Outer membrane protein (Fragment)

Trypsin digest of FbpB

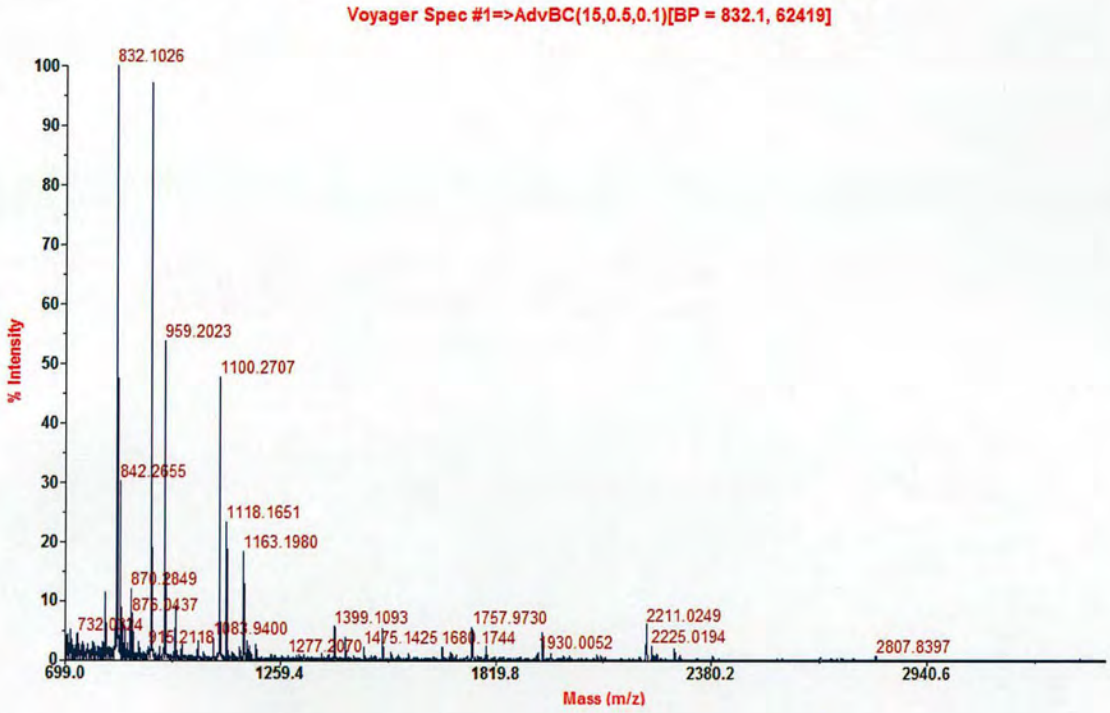

Hits table for the above trypsin digest:

Rank	Probability	Est'd Z	Protein Information and Sequence Analyse Tools (T)	pI	kDa
+1	1.0e+000	2.17	T gi|1098688|gb|AAB63560.1| FbpB	10.1	56.70
2	5.5e-009	-	T gi|5731350|gb|AAC32391.2| transcriptional activator NtrC [Herbaspirillum seropedicae]	6.1	54.71
3	2.1e-010	-	T gi|13235527|emb|CAC33654.1| DNA ligase [Rickettsia montanensis]	7.8	54.98
+4	1.2e-011	-	T gi|16272750|ref|NP_438969.1| phosphoenolpyruvate carboxykinase [Haemophilus influenzae Rd KW20]	5.4	59.61